DISSERTATION

# Breakline Modelling from Airborne Laser Scanner Data

ausgeführt zum Zwecke der Erlangung des akademischen Grades eines Doktors der
technischen Wissenschaften unter Leitung von

O.Univ.Prof. Dipl.-Ing. Dr.techn. Karl Kraus
Institut für Photogrammetrie und Fernerkundung (E122),
Technische Universität Wien

eingereicht an der Technische Universität Wien
Fakultät für Mathematik und Geoinformation

von

Dipl.-Ing. Christian Briese
Flurgasse 53
A-7011 Siegendorf
Matr.Nr.: 9526144

Wien, im Oktober 2004 . . . . . . . . . . . . . . . . . .

# Abstract

Airborne laser scanning (ALS) allows a very detailed sampling of the landscape within a more or less automated recording procedure. For the representation of the models computed on the basis of the acquired irregular distributed point cloud mostly raster resp. grid models or triangulated irregular networks (TINs) are in use, which only implicitly store breakline information. However, for a high quality surface description the explicit storage of breaklines within the data structure of these models is necessary. Therefore, a 3D vector representation of the breaklines is essential.

This thesis introduces a basic modelling concept, which allows the formulation of 3D breaklines not only from ALS data but also from any kind of point cloud data. In order to fulfil the needs for the modelling of breaklines on the basis of unclassified ALS data the basic concept is step-by-step extended. The resulting modelling framework is based on a pairwise intersection of robustly estimated local surface elements along the breaklines. It allows a modelling with the help of original unclassified ALS point clouds even in wooded areas. For this modelling procedure a 2D approximation of the breaklines is required. For the practical application of this method a higher automatisation is needed. Therefore, a further part of the work concentrates on methods, which allow to reduce the effort for the determination of these initial values. For this aim the semi-automatic concept of breakline growing is presented and further fully automatic methods for the breakline extraction are shortly presented.

Practical examples demonstrate the results of the introduced methods. Next to the modelling of breaklines the process of data reduction of the final resulting hybrid surface models is considered and practically shown with the help of an example. In order to stress the general validity of the basic breakline modelling concept further examples using image matching data from the Mars surface and terrestrial laser scanner data are presented. Additionally to the topographic applications, a small example demonstrates the capability of the method for building edge extraction.

Furthermore, the current status of research in the area of sensor design, surface modelling, and breakline modelling is outlined. A further part of the work provides a detailed look at the ALS data acquisition process by an analysis of the capabilities of the range determination techniques. Additionally, the sampling resolution of current ALS systems is analysed under the consideration of the laser footprint. A final section summarises the methods and provides an outlook into future research work.

# Kurzfassung

Das flugzeuggetragene Laserscanning (Airborne Laser Scanning, ALS) ermöglicht eine äußerst dichte großflächige Abtastung der Landschaftsoberfläche aufgrund des hohen Automatisierungsgrades. Auf Basis der aufgenommenen Punktwolke werden in der Folge Rastermodelle, Gittermodelle oder Triangulationen erstellt, die Bruchkanteninformation nur implizit beinhalten. Zur Ableitung hochqualitativer Oberflächenmodelle ist es hingegen notwendig diese Bruchkanteninformation explizit in der Modellierung zu berücksichtigen und anschließend in die Datenstruktur des resultierenden Oberflächenmodells zu integrieren. Daher ist eine explizite Modellierung der Bruchkanten auf Basis einer 3D Vektor Repräsentation notwendig.

Der Schwerpunkt dieser Arbeit liegt in der Entwicklung von Methoden zur Ableitung von Bruchkanten aus Laser-Scanner-Daten. Am Anfang dieser Überlegungen steht eine Methode, die die Beschreibung von Bruchkanten auf Basis von umgebenden Punkten unabhängig von der Datenerfassungsmethode ermöglicht. Schrittweise wird dieses Basiskonzept verfeinert, um schlussendlich die Beschreibung der Bruchkanten auf Basis von unklassifizierten zufällig verteilten ALS-Punkten durchzuführen. Die aus dieser Erweiterung resultierende Methode beschreibt Bruchkanten als Schnittlinie von robust bestimmten analytischen Flächenpaaren, die auf Basis der Punkte in der Nähe der Bruchkante bestimmt werden. Durch die automatische robuste Elimination der Nicht-Bodenpunkte im Zuge der Flächenbestimmung wird eine Modellierung der Bruchkanten in bewaldeten Gebieten ermöglicht. Dieser Algorithmus benötigt zur Bestimmung der 3D Kante eine 2D Näherung der gesamten Bruchkante. Daher werden im Folgenden Strategien bzw. Lösungen angeführt, die eine stärkere Automatisierung der Bruchkantenbestimmung ermöglichen und so die Praxistauglichkeit erheblich erhöhen. Neben dem semi-automatischen Wachsen der Kanten, werden auch einige Ansätze zur Vollautomatisierung vorgestellt.

Ein Abschnitt mit praktischen Beispielen demonstriert die Anwendbarkeit der entwickelten Methoden und geht neben der reinen Modellierung auch auf die Integration der Kanten in die Oberflächenmodellierung und auf die anschließende Datenreduktion ein. Um die vielseitigen Anwendungen der Methode zu präsentieren, folgen Beispiele aus der automatischen Bildzuordnung der Marsoberfläche (image matching) und aus dem Bereich des terrestrischen Laserscannings (TLS). Zusätzlich zu den topographischen Anwendungen wird ein kleines Beispiel der Gebäudekantenmodellierung auf Basis von TLS-Daten vorgestellt.

Neben dem Schwerpunkt der Bruchkantenmodellierung widmet sich ein Teil der Arbeit dem aktuellen Stand der Forschung im Bereich ALS, Oberflächenmodellierung und Bruchkantenmodellierung, während sich ein weiterer Abschnitt mit der ALS-Datenaufnahme genauer auseinandersetzt. Neben einer genaueren Betrachtung der Methoden zur Entfernungsbestimmung wird das Abtastverhalten der ALS-Sensoren unter der Berücksichtigung der Größe des Abtastflecks untersucht. Abschließend werden, neben einem Ausblick auf zukünftige Forschungsaktivitäten, die Methoden und Ergebnisse zusammengefasst.

# Contents

# Chapter 1

# Introduction

Automatic data recording systems have revolutionised the area of topographic surveying as well as close range object acquisition in the last years. Next to digital methods in photogrammetry (e.g. image matching techniques), the development of *laser scanning* (LS, also often referred as *LiDAR* (Light Detection and Ranging)) for three-dimensional (3D) data acquisition led to developments of highly automated all-digital processing chains up to the final products.

In contrast to the "classical" manual data acquisition methods, like terrestrial surveying and analytical photogrammetry for surface determination, these new automatic recording methods allow a very dense sampling of the object resp. area of interest resulting in a huge amount of unstructured data within a short time. Subsequently, the extraction of relevant features for certain applications (e.g. the terrain surface or building models) based on this data is necessary. In order to extract the information fully or at least semi-automatically from the unstructured point cloud a certain knowledge base including information about the object and the sensing process is essential. This preferable automatic task of feature resp. object extraction is oppositional to the "classical" methods in surveying, where the object interpretation, abstraction, and the topology network are gathered manually during the data acquisition by a human interpreter. Within the paper of Ackermann and Kraus 2004 this basic distinction between the data acquisition techniques is mentioned. The authors distinguish between the following two opposite philosophies of (topographic) acquisition systems:

- For one group of capturing methods an efficient terrain capturing is sought by *gathering as few points resp. data as possible* – just enough to fulfil the accuracy requirements. This directly implies an intelligent information resp. data selection process having in mind the special quality requirements for a certain application.

- In contrast to the first group, the opposite philosophy is to *gather as much information as possible* and build afterwards the model to the individual needs on the basis of a lot of (potentially redundant) information.

The first principle was mainly applied in the past using manual data recording procedures, where the cost per point was high. In the last years Ackermann and Kraus 2004 recognise a trend to the second group due to the availability of automatic data recording systems, where the cost per point is very low. The advantage of data recording following the second philosophy is that the data is not categorically collected for a certain use. Wider application fields

can be defined afterwards on the basis of the same data just using different processing chains. Additionally, it should be mentioned that the use of automated methods for data acquisition and modelling (as far as possible) allows to reduce the subjective influence of an individual operator, who performs a selection, abstraction, and attribution process based on the individual knowledge. Furthermore, it should be stressed that it is very important to document all performed acquisition and processing steps. Supplementary to the pure result of the processing chain a well documented quality description should be provided for further analysing resp. processing steps.

Especially *airborne laser scanning* (ALS) has altered topographic data capturing in the last few years. ALS allows a very dense sampling of the landscape with the help of high frequent range and angle observations along a flight path. Next to its high degree of automatisation and cost effective manner another advantage of laser scanning is the active sensor. It allows operation independent of (solar) illumination and permits data extraction unattached from daylight (Kraus 2004). Due to its capability of penetrating the forest canopy (through small openings in the vegetation) even in densely wooded areas, it distinguishes itself in the derivation of *digital terrain models* (DTMs). The transformation of the point cloud into a global co-ordinate system is performed by direct georeferencing with the help of additional observations of a *position and orientation system* (POS) co-registered to the local scanner co-ordinate system (Wehr and Lohr 1999). The main research and application fields of ALS are currently in the area of DTM generation (especially for hydrologic applications), city modelling, infrastructure mapping (e.g. power lines), and the determination of forest stand parameters resp. models (cf. (Axelsson 2000), (Brenner 2000), (Rottensteiner and Briese 2003), (Melzer and Briese 2004), (Pyysalo and Hyyppä 2002) and (Wack et al. 2003)).

As mentioned before, one of the main applications of ALS is the determination of topographic surface models. For the representation of these models generated from ALS data or other automated data acquisition techniques (e.g. image matching techniques (Gülch 1994)) mostly *raster* resp. *grid models* or *triangulated irregular networks* (TINs) are in use. In general, these models are only computed on the basis of an irregular distributed point cloud. Therefore, they do only implicitly store breakline information. The quality of the breakline description within these models depends, next to the original point sampling interval, on the size of the stored raster resp. grid or triangle cells. In contrast to these models without an explicit breakline description, it is essential for high quality surface models (e.g. for hydrological applications) to store breakline information explicitly in the data structure. For this aim a 3D vector description of breaklines is necessary. Based on this description an integration of relevant breaklines into a constrained triangulation process or into a hybrid grid data structure (Kraus 2000) can be performed (cf. 2.2). Additionally, breaklines are very important for the task of data reduction, because they help to describe surface discontinuities even in models with big raster resp. grid or triangle cells. Next to the fundamental role of breaklines for the final surface models the explicit description of these discontinuity lines is very important for the generation of DTMs from ALS data. For the determination of a DTM a classification of the acquired point cloud into terrain and off-terrain points is required. For this aim a lot of different algorithms were developed (cf. section 2.2). An international filtertest (Sithole and Vosselman 2003) shows deficits of all methods used by the participants in the areas of surface discontinuities even when the algorithms have some spatial rules to avoid misclassification next to breaklines. To cope with this problem an integration of explicitly modelled breaklines during the whole DTM generation procedure is essential. However, this makes a prior modelling of breaklines, based on the original unclassified ALS points, necessary.

2

This thesis focuses on the subject of breakline modelling from ALS data considering special data characteristics. The basic concept allows the description of breaklines from any kind of point cloud data. Therefore, the development of the method can be seen in a more general framework (cf. chapter 4).

In the following chapter 2 the current status of research in sensor design, surface modelling and breakline modelling is summarised. Chapter 3 focuses on the ALS sampling process. Subsequently, new suggestions for the modelling of breaklines from unstructured point cloud data are presented. After a general presentation of the basic concept the chapter focuses on the handling of ALS data and threats special cases like the consideration of off-terrain points. Further extensions to the basis concept (e.g. consideration of additional observations within the modelling procedure) conclude this chapter. Furthermore, chapter 5 concentrates on developments for the automatisation of the modelling procedure. For this task the concept of breakline growing is presented (cf. 5.1 and 5.2). Additionally, a fully automatic procedure (cf. 5.3) is introduced. The following chapter presents some representative real data examples and demonstrates the pros and cons of the methods. The generality of the presented method is demonstrated with terrestrial laser scanner (TLS) data and a point cloud from image matching. Next to the modelling process the capability of data reduction is demonstrated. The final chapter 7 summarises the presented methods and gives an outlook into further research work.

# Chapter 2

# Status of Research

As it has been already mentioned in the introduction, ALS is a rather new rapidly growing technology (cf. (Flood 2001)). Improvements and extensions of the data recording systems as well as of the postprocessing algorithms can be found within a very short update rate. The design of the method was largely technology driven. Next to the expansions in the range measurement techniques using lasers, Ackermann 1999 points out the importance of developments of precise kinematic positioning of airborne platforms using the differential Global Positioning System (GPS) and inertial attitude determination by inertial measurement units (IMUs) for accurate direct georeferencing. Furthermore, the increasing computer power played an important role, allowing the storage and processing of such huge amount of data.

The research in the area of ALS focuses on different subjects bearing in mind different applications. However, it can be subdivided into three key areas:

- Sensor design

- Sensor calibration and georeferencing

- Automated object extraction resp. modelling

Due to the wide area of ALS research this section focuses on the work in respect to the modelling of breaklines. The first section deals with the available sensors and gives a short outlook into future sensor developments. It highlights the system parameters, which have to be considered during the modelling process. The next section focuses on the topic of surface modelling. Finally, the status of research concerning the main issue within this thesis – the breakline modelling from ALS data – is summarised.

Within this thesis the area of sensor calibration, georeferencing and adjustment of observations leading to a homogenous point cloud in a project co-ordinate system is not treated, because it would go beyond the scope of this thesis. However, the following small list of publications should give a reference to the current activities within this research area (cf. (Filin and Vosselman 2004), (Kager 2004), (Katzenbeisser 2003), (Schenk 2001) and (Vosselman and Maas 2001)). Continuative literature for further applications of ALS data within the area of automated object extraction and modelling was already mentioned in chapter 1.

## 2.1 Sensor Design

This section gives a short summary on the characteristics of current available ALS sensors and presents an example of an ALS point cloud, which is the basic data source for the surface and breakline modelling procedure. The characterisation of the point cloud will be continued in section 3, where the question: "What can be sensed?" will be answered by an analysis of the range estimation technique and the scan pattern on the sampled surface.

In general, a laser scanner can be seen as an active sensor system providing range measurements by electromagnetic waves in different directions to backscattering surfaces. The principle of laser scanning can be used on different platforms. This allows to tell airborne (ALS), satellite (SLS) and terrestrial (TLS) laser scanning apart. In contrast to other data acquisition systems "laser scanning is not capable of any direct pointing to a particular object or object feature" (Ackermann 1999). The resulting bi-directional sampling pattern in object space depends next to the individual surface on the relative position of the laser beam in respect to the illuminated surface, the system design of the deflection unit (which guides the laser beam through the object space), and the range measurement rate.

For the range measurement two different methods have to be distinguished. On the one hand the *pulse measurement* method estimates the distance to the backscattering object with the help of the travelling time of short laser pulses, whereas on the other hand the *phase difference measurement* uses a continuous waveform for the determination of the object distance (cf. (Wehr and Lohr 1999)). Furthermore, laser scanning can be classified into static or kinematic data acquisition. The laser scanner mounted on an airplane or satellite operates in kinematic mode, whereas TLS can be used either in static (e.g. mounted on a tripod) or kinematic (mounted on vehicles, e.g. for tunnel or city modelling data acquisition) applications. During the airborne data recording the sensor is moved along the flight path. The movement of the plane resp. helicopter and the 2D deflection unit, which deflects the laser beam across the flight path, leads to a strip wise observation of the illuminated terrain surface. As aforementioned the time dependent position and orientation of the laser sensor can be observed with the help of a synchronised POS usually consisting of a GPS and an IMU (Wehr and Lohr 1999).

The characteristics of typical present airborne systems are summarised in table 2.1. Nowadays, all commercial available ALS sensor systems use the pulse measurement principle. The parameters, which describe the characteristics of an ALS system, are broken apart into the following key elements:

- Range measurement unit

- Deflection unit

- Position and Orientation System

The *range measurement unit* is responsible for the emission of the laser beam as well as for the processing of the received echo. One of the main parameters is the pulse repetition rate, which corresponds to the number of emitted laser pulses per second (or in other more practical words: the maximal number of points per second neglecting the capability of range estimation to multiple backscattering surfaces). Additionally, the footprint size at a certain flying height depending on the beam divergence of the laser beam and the pulse duration (cf. 3.1) is important. The further parameters within the range measurement characteristics correspond to

| Range measurement unit | |
| --- | --- |
| Specification | Typical value |
| Operating Attitude resp. maximal distance | 100-6000m |
| Wavelength | $0.8\mu$m to $1.56\mu$m |
| Pulse Duration | 5ns-10ns resp. . 1.5m-3m |
| Beam Divergence | 0.2mrad-2mrad |
| Footprint | 0.2m-2m |
| Pulse Repetition Rate | 5kHz-100kHz |
| Multiple Returns | 2-5 |
| Intensity | Yes |
| **Deflection unit** | |
| Specification | Typical value |
| Field of View | 14°-75° |
| Scan Rate | 25Hz-650Hz |
| Scan Pattern | Zigzag, parallel, elliptical, sinusoidal |
| **Position and Orientation System** | |
| Specification | Typical value |
| GPS Frequency | 1Hz-2Hz |
| INS Frequency | 50Hz-200Hz |
| **Accuracy at a typical flying height of 1000m over ground** | |
| Elevation | 0.1m-0.2m |
| Planimetric | 0.5m-1m |

***Table 2.1:*** *Characteristics of typical commercial ALS systems.*

the echo processing (maximal number of detectable echoes per pulse (Multiple Returns), the storage of the echo intensity corresponding to a certain range) and the maximal operating altitude limited by the maximal determinable distance. State-of-the-art commercial ALS sensors typically measure first and last pulse [1], while others allow to store up to five ranges to different reference points. Additionally, it has to be mentioned that current systems record the intensity of the received echo. This information is only very rarely used, because the recorded intensity values are very noisy and additionally, a lot of systematic effects can be recognised due to the fact that these intensities are not calibrated (e.g. the angle of deflection and reflection or the varying power of the emitted laser beam are not considered within current systems).

The parameters related to the *Deflection unit* describe the illuminated area across the flight path. On the basis of the field of view, the scan rate, the design of the deflection unit, the pulse repetition rate, and the flying speed the point density on the surface at a certain distance to the ALS sensor can be computed. The design of the deflection unit (e.g. oscillating mirror, rotating polygon, fiber cells) yields to a certain scan pattern on the terrain surface (cf. (Wehr and Lohr 1999)).

The accuracy of the delivered point cloud in a certain global co-ordinate system is strongly influenced – next to precision of the range and angle observations of the ALS sensor – by the

---

[1] Along the travel path of the emitted laser beam different objects might be illuminated by one emitted laser beam (cf. section 3.1, e.g. in the case of illuminated trees on the terrain surface). Then the term "first pulse" corresponds to the range estimation to the first illuminated object surface within the travel path (in the previous example the tree crown), whereas the term "last pulse" corresponds to the backscattering echo from the furthermost object (in the previous example the terrain surface).
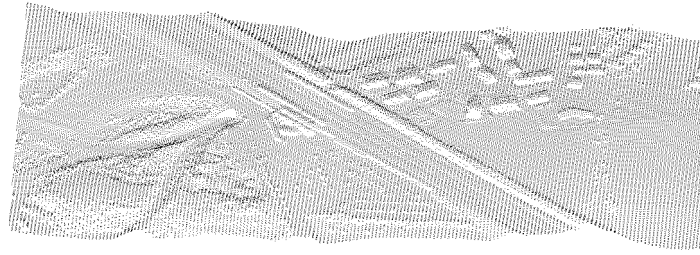
**Figure 2.1:** *Point cloud (point distance on the terrain surface: approx. 2m) of one ALS strip (strip width: approx. 430m, OEEPE (now EuroSDR) test data set Vaihingen, cf. (Briese et al. 2004)).*

accuracy and quality of the *Position and Orientation System* (Katzenbeisser 2003). One important characteristic point next to the accuracy measures concerning the POS, is the frequency of the POS in determining the position and the orientation of the ALS sensor (cf. table 2.1).

Within the research area of sensor design one can recognise that a lot of parameters of the sensors were improved in the last years (e.g. smaller beam divergence, higher operation altitude, pulse repetition rate, and higher frequency and accuracy of the POS). These enhancements led to the determination of more dense and accurate data and allowed to expand the application fields. The next step of future ALS sensor systems lies in the development of sensors, which allow to digitise the full received echo (*full-waveform* ALS) with a very high frequency (Wagner et al. 2004). This additionally high amount of data will provide further information about the sensed object. The research in this area is just at the beginning, but in the future e.g. one can think of applying range detectors in the post-processing mode adapted to the needs of a certain application or of the determination of additionally quality information for the reliability of the computed distance to the object (Wagner et al. 2004). The US National Aeronautics and Space Administration (NASA) has already developed and operated waveform digitising ALS, allowing a sampling rate of the echo of 500 mega-samples per second (this corresponds to a range sampling interval of 0.3m). The potential for vegetation and topographic mapping was presented by Blair et al. 1999. Within the commercial section, such full-waveform ALS sensors were just developed by the companies Riegl and Optech (cf. (Riegl 2004a) and (Optech 2004)). The first full-waveform ALS pilot projects have already started. Another, to a certain degree oppositional, trend in ALS is the design of laser beams with smaller and smaller beam divergence (tendency to "single mode" echoes). With these sensors the number of multiple returns will be reduced due to the smaller footprint. Since the information per echo decreases, the derivation of further information of the sensed object, leading to a classification of the data, is only possible in relation to adjacent backscattering surfaces. An interesting aspect for future system design may eventually be the combination of narrow and wide (storing the full-waveform) beams in order to use the advantage of both. A first step into this direction can be seen in the development of the new Optech ALTM 3100 sensor offering a dual beam divergence (0.3mrad or 0.8mrad) in order to set the footprint to the individual needs (e.g. a bigger footprint increases the possibility to hit small linear features like power lines to a high degree) (Optech 2004). Having in mind the new developments, it will be very important to understand the physical process of backscattering, echo detection and intensity estimation in the future. This will allow to determine further information about the sensed surfaces, which can hopefully be very useful in further processing chains.

Finally, an unstructured ALS point cloud in the project co-ordinate system – the typical output

of an ALS data acquisition mission – of a part of one ALS strip is presented in figure 2.1. This is the basic data source for the upcoming modelling or feature extraction steps.

## 2.2 Surface Modelling

In general, a model can be seen as an imitation or emulation of a certain phenomenon (cf. (Merriam-Webster 2004)). Usually, models are used as miniature representations of phenomena focussing on the necessary aspects (for a certain application) and are in order to reduce the complexity of subsequent analysis steps not just a further identical instance (one-to-one copy). Within the area of natural sciences a mathematical description of a certain phenomenon with the help of functional models is widely used in different application fields.

Within this thesis the main focus lies on methods for the determination and representation of topographic surface models. The aim of the surface modelling techniques is to describe a continuous object surface (e.g. the terrain surface) with the help of mathematical models. The challenging task for the algorithms for surface model reconstruction is the generation of a continuous approximation of the object surface based on a set of discrete (due to the limits of data acquisition) observations. An additionally important problem is the persistent storage of these models. A lot of different methods have been developed in the past to solve these problems. The following paragraphs shortly summarise the state of the basic concepts for the topographic surface modelling. Further details and references can be found in the literature (e.g. (Ackermann and Kraus 2004), (Heitzinger 1999), (Kraus 2000), (Pfeifer 2002), (Thurston 2003)).

For the determination as well as for the persistent storage of digital topographic surface models different concepts do exist. One of the basic differences in modelling corresponds to the way of handling the input data. Whereas one group of methods usually uses the input data directly as modelling frame and does concentrate on the determination of the absent topology (*topological modelling*), other methods formulate the surface with the help of a certain more or less complex mathematical description (*functional modelling*). Furthermore, one has to distinguish 3D from so-called commonly used 2.5D [2] solutions.

**Topological Modelling**

Within the area of topological modelling the surface is described with the help of the original measured data and additionally determined topological information. The input data consists of a set of points and eventually of a set of previously – during data capture – defined resp. observed topological information (e.g. manually measured breaklines).

The surface description, which is in this case based on the determination of the topology, is generated with the help of a set of (geometric) rules. The previous introduced topological information has to be preserved (breaklines) using constraints within the evaluations of the rules, as long as this does not lead to inconsistency. This results in a graph, where the definition of neighbourhood is performed by edges connecting adjacent surface points, which describe the

---

[2]The group of 2.5D algorithms resp. data structures describes the surfaces with the help of a graph of a bivariate function, leading to the limitation that just one value is valid for the 2D parameter domain. Usually the parameter domain of 2.5D solutions is the ground plane, the height information belonging to a certain point defined by his planar co-ordinates is restricted to just one attribute value. Certain surface features like overhangs and caves can not be described with the help of 2.5D modelling techniques (cf. (Pfeifer 2002)).

topographic surface. However, it has to be mentioned that these topological relations themselves do not define a surface. A further interpolation rule defining the determination of the surface in between the given original data, is necessary.

A very widely used topological method for surface description is the TIN (also called triangulation), which describes the surface with a set of adjacent planar triangles. For the determination of the topology a lot of different algorithms do exist (e.g. Delaunay triangulation (Kraus 2000), greedy triangulation (Dickerson et al. 1997), etc. ). The TIN is not limited to the field of topographic mapping nor to a 2.5D description. With the use of advanced methods for the topology determination a 3D surface description (e.g. based on a tetrahedralisation including a certain knowledge base) is possible (cf. (Heitzinger 1999)). Further methods in relation to topographic mapping are shortly described in Pfeifer 2002). For the storage of TINs a lot of different data formats are in use.

### Functional Modelling

Methods using the functional modelling principle describe the surface with the help of certain functions determined on the basis of the original observed data. This mathematical formulation is usually performed by 2.5D algorithms, which describe the surface with the help of a bivariate function, leading to the limitation that just one value is valid for the parameter domain. Once the surface is functionally described, the model has to be stored persistently. One way of storing would be to save the resulting function defined over a certain parameter domain. The other commonly used way is to discretise the function by evaluating it at certain parameter values. For this aim raster or grid data structures are usually used. The advantage of the discretisation lies in the facilitated possibility of exportation into commonly used data exchange formats. The functional modelling techniques can be broken apart into interpolation and approximation methods. Interpolation methods use functions running exactly through the original data, whereas approximation methods use functions, which just approximate the data, allowing to compute smooth surfaces by removing (filtering) measurement errors by the use of overdetermined systems. The most commonly used methods are *moving least squares* (Lancaster and Salkauskas 1986), *finite elements* (Hoschek and Lasser 1993), and the statistical based *kriging* (Journel and Huijbregts 1978) similar to the *least squares interpolation (also referred as linear prediction)* (cf. (Kraus and Mikhail 1972) and (Kraus 1998)).

Topological resp. functional methods have their individual advantages for certain data acquisition techniques and applications. In the case of very dense and highly redundant data (like in ALS) the functional modelling using a highly overdetermined functional modelling procedure (e.g. used by least squares interpolation or kriging) must be favoured, because it allows to eliminate measurement errors (filtering) and additionally provides quality control due to the solution of overdetermined equation systems within an adjustment procedure (cf. (Ackermann and Kraus 2004)). In contrast to the advantages of functional modelling, topological methods like the TIN must be favoured if the original measured data should be preserved, which is e.g. often important within tacheometric data acquisition (Ackermann and Kraus 2004). Functional methods operate in general in 2.5D, but for TINs certain solutions for 3D modelling are already available. Another advantage of TINs concerning 3D modelling is that the only thing that must be changed in order to perform a 3D modelling is the method for the topology determination, whereas the data structure of the model can usually remain unchanged. Furthermore, the integration of breaklines as constraints within the modelling procedure can easily be realised by the use of TINs, whereas the effort of breakline integration within the modelling and storage within functional modelling techniques is higher (cf. (Kraus 2000)).
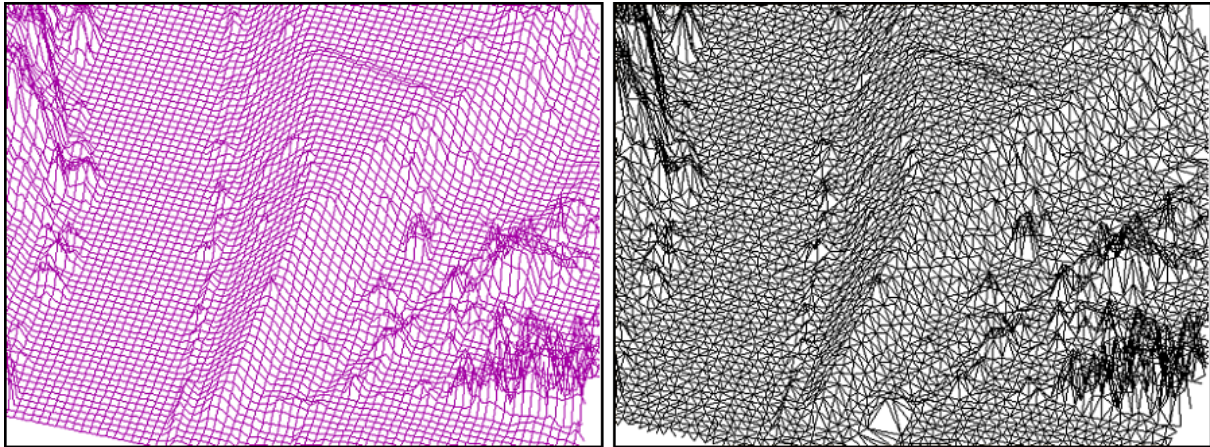
*Figure 2.2:* *Surface representation: Grid (on the left) and TIN model (on the right) computed on the basis of the same ALS point cloud. The breakline information is only implicitly stored within these models (cf. chapter 1).*

The most common data structures within the area of surface modelling are raster, grid and TIN representations (cf. figure 2.2). Whereas raster models describe the height over the complete cell (mostly squares) in an area based way, grid models store the height information in a vector based structure at discrete grid points, which are connected by grid edges. At large they are regular distributed and the distance between the grid points is constant. The grid data structure is commonly used in software packages operating on the basis of functional modelling techniques. In practise the terms grid and raster are mixed very often due to the fact that grid models with regular squared surface cells can be stored in a similar way as squared raster models. An extension of the grid structure is the hybrid grid model, which additionally allows to integrate irregularly distributed vector information (e.g. breaklines) into the grid data structure (Kraus 2000). The TIN data structure was already mentioned in the previous paragraphs (in the practical application linear interpolation is used in between the stored points). It can be seen as an extension to the vector based grid data structure allowing an irregular distribution of the descriptive points (with the loss of storage advantages of regular distributed points) by the use of (typically planar) triangles as smallest surface elements. In general, the data structures are usually strongly linked to the modelling techniques, but due to the wide spread of different software packages a transformation from one data structure to another is essential.

Nowadays 2.5D surface models are a very important basic data source within spatial information systems, but there will be the need of a full 3D description of the landscape in order to fulfil the needs of more and more complex spatial analysis methods in the future. A concept for 3D topographic surface modelling is presented within the thesis of Pfeifer 2002. To meet the requirements of high quality 3D topographic modelling Pfeifer 2002 presents solutions for the determination of filtered smooth local surface patches on the basis of a 3D triangulation of the original data. It can be seen as a *combination of topological and functional modelling* and allows gaining the advantages of both (cf. (Pfeifer 2002)).

**Surface Modelling based on ALS data**

As mentioned before, the determination of DTMs is one of the most common tasks using ALS data. However, for this aim one has to bear in mind that the points recorded by ALS systems may lie on different backscattering surface objects. On the one hand this is the terrain surface, but on the other hand echoes from other objects are recorded. Nowadays, the LS sensing

10

process itself is not capable to distinguish these different backscattering objects. Therefore, it is necessary to separate the terrain and off-terrain points in a post-processing step in order to derive a model describing the terrain surface. For this task a lot of different classification resp. filter algorithms were already developed (cf. (Axelsson 2000), (Kraus and Pfeifer 1998), (Vosselman 2000), etc.). A short summary of published algorithms and an international comparison of the results of different filter methods can be found within the publication Sithole and Vosselman 2003.

Next to the generation of DTMs other types of surface models play a decisive role for further applications. For example, the *digital surface model* (DSM) describing the uppermost topographic surface seen from the bird-eye's view (usually computed on the basis of all acquired ALS data) is interesting for visibility or for the propagation of electromagnetic waves studies. Furthermore, a very commonly used conception is the normalised digital surface model (nDSM), which is usually defined as a model describing the height of objects (e.g. houses) in respect to the terrain surface. This model is often used as basic data for the analysis of vegetation or building heights resp. models. It can be computed by subtracting the DTM from the DSM. The list of different models can be easily extended – there is a long catalogue of further different models, which are in use (e.g. crown models) –, but the problem is that often a general valid definition and determination procedure is not given (cf. (Pfeifer 2004)). However, even the definition of the DTM is not always clear, e.g. the question if bridges really belong to the DTM is always critical.

## 2.3   Breakline Modelling

Current available surface modelling techniques based on ALS data store breakline information only implicitly in the data structure (cf. chapter 1 and figure 2.2). However, in order to describe genuine topographic surfaces with a high quality for e.g. hydrological applications, the additional consideration of explicitly described structure elements (e.g. breaklines and peaks) is essential independent of the used surface modelling technique. These structures have to be used within the modelling procedure (e.g. constraints within a TIN and/or separation lines between two smooth functionally described surface patches) and must be integrated within the data structure of the stored models (Kraus 2000). For this aim an explicit vector based description of the breaklines is essential. Additionally, as mentioned in the introduction, breaklines play an important part in the process of data reduction of the final surface models. An overview on the developments in the area of breakline determination from ALS data follows in the next paragraphs.

Up to now breaklines are usually digitised manually by the measurement of relevant (for a certain application) points along one line. The selection of the important lines and the way the line is discretised is up to the individual human interpreter. With the development of ALS and image matching techniques ideas of automatic breakline determination based on the delivered point cloud data arose.

Up to now the international research in the area of breakline extraction from ALS data has concentrated on the development of methods for the fully automated 2D detection of breaklines in so-called range images. The range images – a 2.5D raster representation of the surface – are used in order to apply image processing techniques. These methods for ALS data lean ajar algorithms developed for the extraction of breaklines on the basis of photogrammetric data (cf.

(Weidner 1994) and (Wild and Krzystek 1996)). In the following, the basic concept of one of these methods is presented. Most of the developed methods share their fundamental ideas. Further algorithms built-on ALS data are mentioned at the end of this section.

Brügelmann 2000 presents a full processing chain starting from an ALS range image leading to smooth vector breaklines. Within this method the first and essential step is the extraction of edge pixels in the range image. This is performed with the help of a raster based method using a hypothesis testing method presented by Förstner 1998. This method of second derivatives and hypothesis testing treats breakline detection in range images on the same principle as finding edges in intensity images. The basic idea is that edge pixels are borders of homogeneous regions and that therefore the following two basic properties for edge pixels should be valid:

- The homogeneity measure on edge pixels should differ significantly from the one determined in homogeneous regions.

- The homogeneity measure should be locally maximal across the edge.

In order to derive this homogeneity measure for range images Förstner 1998 starts with the calculation of the gradient image $\mathbf{g} = \nabla d = (d_c, d_r)^\top$, with c = column and r = row, as a two-channel image. Whereas for intensity images the squared gradient magnitude is often used as homogeneity measure, Förstner 1998 recommends to use the multi-channel extension applied to the gradient image. This leads to a homogeneity measure called *quadratic variation* $h_2 = \kappa_1^2 + \kappa_2^2$ closely related to the second derivatives based on the two principal curvatures $\kappa_1$ and $\kappa_2$ describing the maximum and minimum normal curvature at every pixel. Considering noise variances $\sigma_{n_{cc}}$, $\sigma_{n_{cr}}$, and $\sigma_{n_{rr}}$ leads to the following $\chi_3^2$-distributed test statistics $z_2 = \frac{d_{cc}^2}{\sigma_{n_{cc}}^2} + \frac{d_{cr}^2}{\sigma_{n_{cr}}^2} + \frac{d_{rr}^2}{\sigma_{n_{rr}}^2}$, which can be used within a hypothesis test (cf. (Förstner 1998)) for the determination of significant edge pixels. As mentioned before, the result of this process are pixels marked with the attribute *edge pixel*. To generate the 2D position of the breakline within the broad regions of edge pixels Brügelmann 2000 applies a thinning operation after a non-maxima-suppression taking into account the direction of the maximum curvature. Then, a further raster to vector conversion allows to generate 2D vector breaklines. Within this step Brügelmann 2000 performs some smoothing using a 2D cubic polynomial splining method in order to perform a certain generalisation and elimination of zigzag effects caused by the original raster data structure. After the 2D determination of the breaklines Brügelmann 2000 finally extracts the height of the breaklines from a slightly smoothed vegetation free DTM at the planimetric position of the 2D vector breaklines leading to a 3D vector representation. Furthermore, Brügelmann 2000 compares the results of the breakline modelling procedure to photogrammetric measured breaklines. The quantitative (2D) assessment of the extracted breaklines in comparison to the manually digitised lines showed that the distances between both vector data sets lead to a mean distance of 0.59m. 35% of the computed distances were smaller than 0.25m, 80% were smaller than 1m. Brügelmann 2000 concludes that the automatically extracted breaklines hold a comparable 2D precision of the photogrammetric ones, because the differences are in the order of magnitude of the precision of the photogrammetric breaklines.

Next to this interesting approach, a lot of further algorithms within the area of edge based segmentation techniques based on raster ALS surface models, which share the basic aims of the presented algorithm from Förstner 1998 and Brügelmann 2000, were developed. All have in common to use image processing techniques in order to extract 2D breakline pixels, which have to be refined in further steps. For example Gomes-Pereira and Wicherson 1999 use the first
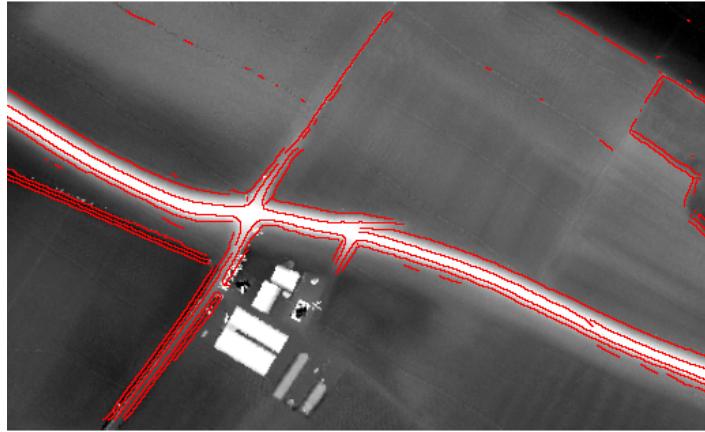
***Figure 2.3:*** *Part of the result of the breakline modelling technique presented by Brügelmann 2000.*

derivatives to identify edge pixels on the border between regions with different slopes whereas Gomes-Pereira and Janssen 1999 use the Laplacian operator for the detection of breaklines. Sui 2002 uses gradient images, whereas in Rieger et al. 1999 a method for the breakline extraction based on a slope model is presented. A different semi-automated approach for the 2D breakline modelling based on snakes was introduced within the thesis of Kerschner 2003. In contrast to the other publications this procedure starts with a rough approximation of the planimetric position of the breakline. Then the breakline is refined within an iterative process with the help of snakes, guided by locally determined main curvature values (estimated by differential geometry) on the basis of a grid surface model (cf. (Kerschner 2003)).

Summarising the current status of research in the area of breakline modelling, it can be seen in the literature that published experiments show quite interesting results for 2D extraction. Especially vegetation free breaklines on dikes can be extracted quite well (cf. (Brügelmann 2000)) in 2D. However, certain breaklines are usually only partly detected. A problem of all these raster based approaches is that they all operate only in 2D and just interpolate the height from a more or less smoothed DTM, which can be eventually affected by classification resp. filter errors caused by the DTM generation process. The height of the breakline is computed totally independent of the determination of the 2D position. Therefore, a determination process allowing the estimation of breaklines in 3D has to be preferred.

A basic concept allowing a 3D refinement of approximately 2D detected or just manually roughly measured breaklines was already published in Briese et al. 2002 and Kraus and Pfeifer 2001. First tests were performed within the master thesis Brzank 2001. Extensions to this basic idea allowing the modelling of breaklines on the basis of unclassified original ALS point clouds are presented within this thesis (cf. chapter 4). Some of the basic ideas were already published in Briese 2004. The determination of the breaklines based on the unclassified ALS data prior to the DTM generation on the basis of the original ALS data should guarantee that all information, without any errors from potentially earlier processing steps, is available within the breakline modelling procedure and should allow to support subsequent necessary filter and classification processes (cf. chapter 1), which are essential for the DTM generation based on ALS data.

# Chapter 3

# The Airborne Laser Scanning (ALS) Sampling Process

An in-depth understanding of the data acquisition process is essential to estimate the level of detail that can be resolved from a scanned point cloud in order to develop applicable modelling or feature extraction techniques. Therefore, this chapter provides a closer look at the ALS sampling process, which leads to a discretisation of natural topographic surfaces (cf. figure 3.1). For this aim, in the case of LS data, it is on the one hand necessary to analyse the range measurement determination and on the other hand the resulting scan pattern must be studied to get a better impression of "What can be sensed i.e. observed by current ALS systems".

In general, the quality of a certain observation can be characterised by the terms resolution, precision, and accuracy. Whereas the resolution describes the smallest observable and storable difference of an observation, the precision and accuracy express the quality of the determined observations with the help of statistical methods (usually the standard deviation, assuming a normal distribution of the probability density function of the observed quantity, is used). The precision (also referred as inner accuracy) describes the quality of an observation in respect to observations of the same population (conformity within a set of observations of the same random variable), while the accuracy states the quality in respect to independently determined values (e.g. to a set of control points) resp. to the "true" value (cf. (Mikhail 1976)). In practice, these terms, describing some aspects of the quality of a certain measurement process, are unfortunately mixed very often.

The intention of this chapter is not a detailed quantitative determination of these quality measures, which are mostly sensor and project dependent, though the following two subsections try to highlight general problems that have to be considered within the ALS sampling process. The first section concentrates on problems and limitations of current ALS range determination systems, whereas the focus of the second section lies in the analysis of the scan pattern. For this aim a resolution measure for the sampling process, which was originally published in Lichti 2004 intended for TLS data, is presented. This measure can be used in a similar way for ALS data, which is demonstrated with the help of practical examples. Furthermore, these sections especially consider the sampling of discontinuity areas.

14
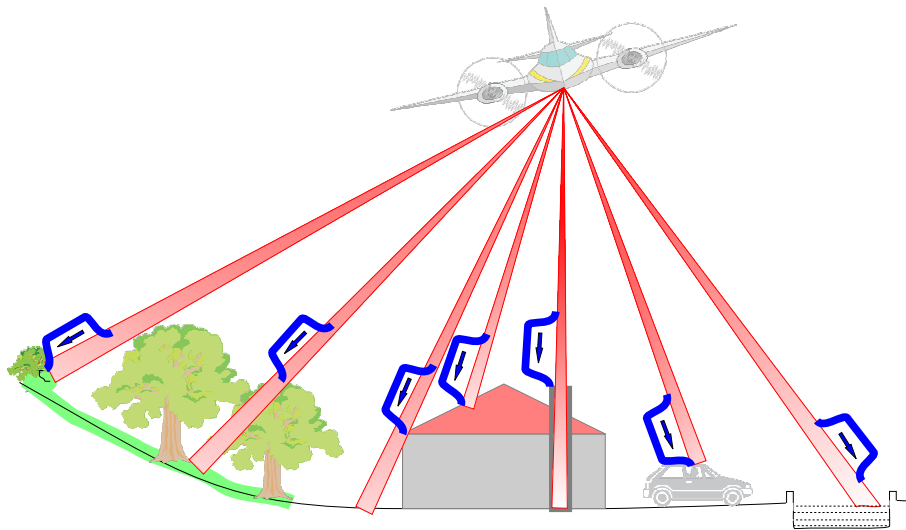
**Figure 3.1:** *The ALS sampling process. The emitted laser beams interact along their travel path with different objects with different backscattering properties. (Kraus 2004)*

## 3.1 Range Determination

As mentioned in section 2.1 current ALS sensors use the pulse measurement principle for the determination of the range to an illuminated object surface. For the analysis of the capability of the range determination methods used in current commercial ALS sensors, it is on the one hand interesting to get an idea about the precision of the determined range and on the other hand the ability of resolving more than one object along the line of sight resp. the travel path of the laser beam is important.

Looking at the data sheets of ALS system providers, it can be recognised that different quality measures are in use. The quality information concerning the range measurement ability is usually very short and mostly one just gets the information about the minimum and maximum determinable range and the resolution of the range determination. For example the data sheet of the Falcon II ALS from the company TopoSys GmbH lists a range coverage of 1600m and a range resolution of 1.95cm (TopoSys 2004). Furthermore, usually the final accuracy of the ALS point cloud at well defined surfaces at a certain flying height is provided.

First commercial ALS sensors have offered to distinguish between the *first* and *last* pulse and have allowed to store just one range. Advanced systems are capable of recording more than one range, even if the distance between the objects is smaller than the beam duration. Nowadays, no detailed information about used methods and no quality description providing information about the ability to resolve to objects or detailed precision analysis, is offered to the subsequent data processors. The following paragraphs provide a more detailed look at the properties and problems within the area of range estimation.

One very important thing that must be considered using LS data, is the fact that the emitted laser beam has a certain spatial dimension. In the case of the emission of laser pulses this spatial dimension can be characterised by the beam divergence and the pulse duration resp. length, which can be seen for a few pulses in figure 3.1 in a schematic way. This leads to the fact that the distance to the sampled "point" on the illuminated backscattering surface corresponds
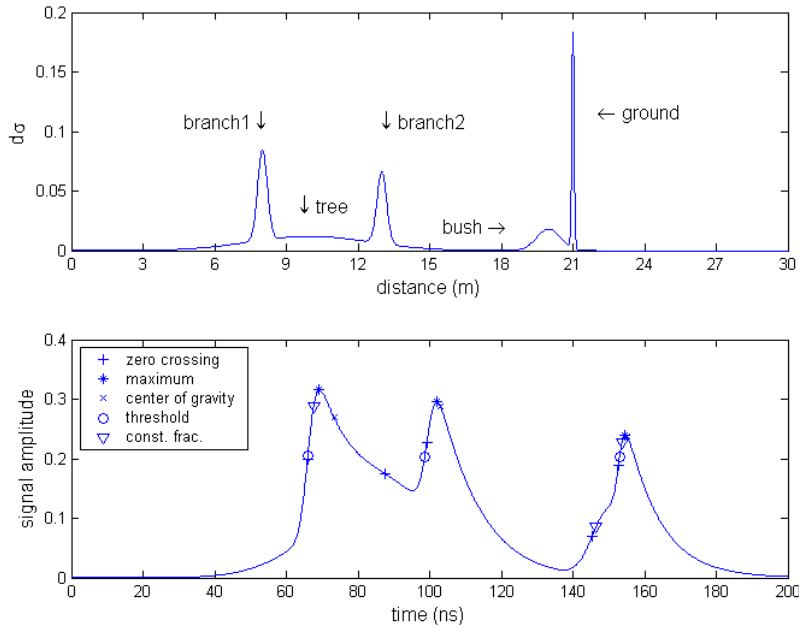
***Figure 3.2:*** *Synthetic example of a complex echo from different backscattering objects. The objects (tree with branches, bush and terrain) are described by the effective scattering cross section (upper part). The resulting echo (lower part) that can be received by the ALS sensor is the result of the superimposition of the individual backscattering echoes of the different objects. The legend in the lower picture indicates the different results of different echo detection techniques used for the range determination. (Wagner et al. 2004)*

to a certain illuminated small surface area called *footprint*, which is illuminated for a certain time period (corresponding to the pulse duration, typically about 5ns-10ns resp. 1.5m-3m, cf. table 2.1). The big task for the range determination is the computation of the "true" object distance. For this mission it is necessary to define a reference point within the footprint and a reference time within the pulse duration. This point is typically defined on the one hand as the centre of the emitted laser beam (based on the conception that this corresponds to the direction of the main energy of the emitted laser beam) and on the other hand the reference time within the pulse duration is usually defined as the rising edge of the pulse. However, current commercial system providers do not offer any detailed information concerning their pulse detection algorithm.

Furthermore, one has to bear in mind that the received echo can be rather complex, if several objects within the travel path of the laser pulse generate individual backscatter pulses (cf. (Briese 2000), (Jutzi and Stilla 2004), (Katzenbeisser 2004), and (Wagner et al. 2004)). Therefore, it is important to consider that the pulse duration is the limiting factor of the total separation of two echoes from different surfaces. This total separation is only possible, if the distance (measured along the travel path of the laser beam) of the two backscattering object surfaces is bigger than the half of the pulse duration (cf. (Briese 2000) and (Katzenbeisser 2004)).

Figure 3.2 presents one synthetic example, which demonstrates the complex task of range estimation in areas of multiple backscattering surfaces. In order to estimate the range, there is a need of a method, which allows to detect the rising edge. These detection methods are used to set the reference point at the emitted beam at the time of the pulse emission and additionally the same method (having in mind that in the ideal case the shape of the echo remains

unchanged) is applied to the received echo. In the ideal case of a planar target area, which is normal to the beam travel path, the shape of the received echoes is unaffected, whereas in all other cases the shape of the echo (e.g. the rising of the leading edge) changes.

In order to reduce the influence of the echo shape a lot of different echo detectors can be considered, but what can be seen in the paper Wagner et al. 2004 is that an ideal detector for all common cases does not exist. All algorithms tested on synthetic examples, presented in the previous mentioned publication, for the determination of the rising edge, showed significant systematic range errors on certain synthetic topographic objects (even for the case of a tilted roof the range values vary by 0.4m for a laser footprint of 1m). Furthermore, due to the overlay of individual echoes from different surfaces, certain object surfaces could not be resolved, e.g. it was not always possible to separate echoes from low vegetation and the terrain surface. Fortunately, one commonly used method for echo detection, the constant fraction method, reduces the influence of tilted surfaces to a very high degree, so that the systematic effect concerning the range determination on ALS data on embankments or tilted roofs is usually low.

Having in mind the problems with echo detection and the missing information about the practical realisation, it is difficult to answer the question of the precision and the capability of resolving two different objects correctly in a general way. Both factors may vary strongly within an ALS project area depending on the illuminated objects and the influence especially of low vegetation, which diversifies with the growth of the vegetation, is difficult to estimate (cf. (Pfeifer et al. 2003), (Wagner 2004)). Systems allowing the digitisation of the whole returned echo (cf. section 2.1) might provide further information in the future.

Nowadays, we just have the chance to estimate the quality of ALS systems based on independently acquired control information. These studies show that the accuracy of the height information acquired from a typical flying height of 1000m is in the decimetre level, whereas the precision on well defined surfaces is in the order of few centimetres (Kraus 2000). The influence especially of low vegetation leading to an accuracy reduction of the final surface models in vegetated areas was already proven e.g. in Briese et al. 2001 and Pfeifer et al. 2003. Due to these experiences one has to have in mind that the precision resp. the accuracy in vegetated areas is influenced by the effect of the echo overlaying, which is very critical for the range estimation and can lead to systematic range errors.

In the area of breaklines the problem of echo overlaying is always present, because as soon as the footprint illuminates both surfaces on the left and right of the breakline the varying distances within this small surface element lead to systematic distance measurement errors due to the fact that a certain averaging is performed. Therefore, it must be noted that the measurements very close to breaklines (at a distance in the order of the footprint diameter) are not the best candidates for the description of the breaklines. Furthermore, it has to be mentioned that linear features, like power lines, are affected by positional errors due to the fact that the measurement system always assigns the determined range to the centre of the laser beam (cf. previous paragraphs, (Lichti 2004), (Melzer and Briese 2004), and (Jutzi and Stilla 2004)).

## 3.2 Scan Pattern

As mentioned in the previous chapter, the pulse repetition rate, the scan rate, the field of view (depending on the flying height), the design of the deflection unit, and the flying speed lead
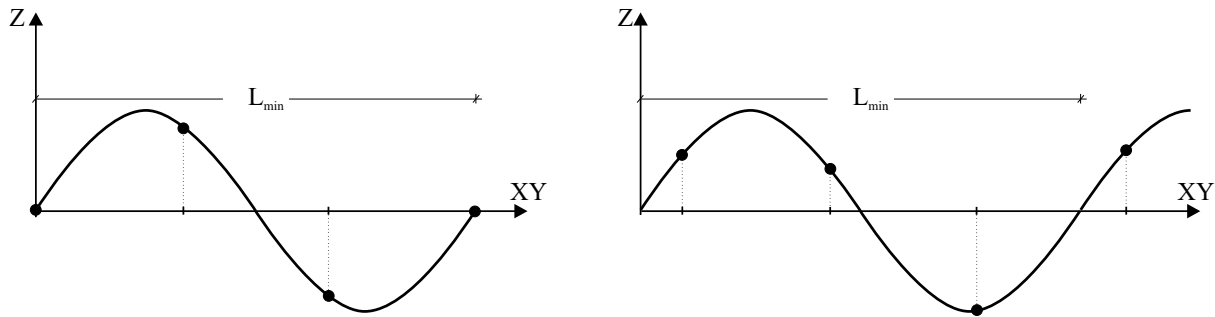
***Figure 3.3:*** *Minimum wavelength $L_{min}$ of a surface model and two arrangements of recorded point cloud data for its reconstruction (black dots), with the sampling resolution $\Delta$. (Kraus 2004)*

to a scan pattern with a certain point spacing on the object surface. The following paragraphs concentrate on the details that can be resolved with the help of a certain scan pattern under the consideration of a certain beam width.

In general, based on the point cloud resolution the minimum wavelength $L_{min}$ that can be reconstructed can be determined with the help of the sampling theorem. Referring to this proposition the sampling resolution $\Delta$ must be smaller than half of the wavelength of $L_{min}$ [1]. Kraus 2004 recommends to use a sampling resolution of $3\Delta$ in order to consider positional errors in ALS data. Figure 3.3 presents two examples demonstrating the reconstruction ability of a surface with the help of this demand.

However, in order to study the resolution of the ALS sampling process, it is not enough to look at the angular sampling interval resp. on the point distance on the sampled surface. A scan with the same angular resolution but with different beam widths leads due to the averaging effect of the footprint size (overlapping echoes, cf. 3.1) to a different discretisation of the sampled surface. Therefore, next to the sampling interval, one has to consider the influence of the laser beam width for the determination of the resolution of the delivered point cloud data (cf. (Lichti 2004)). Subsequently, with a resolution measure considering both effects the above presented sampling theorem can be consulted to answer the question of the minimum determinable surface wavelength $L_{min}$. Lichti 2004 has presented a method for the determination of such a resolution measure, called effective instantaneous field of view (EIFOV), for TLS data. This method, which can be used in a similar way for ALS data, allows to consider both previous mentioned factors in order to determine a resolution measure for LS data. In the following the method presented by Lichti 2004 is summarised and its application to ALS data is discussed with the help of practical examples.

The determination of the sampling resolution in Lichti 2004 is based on a bi-variate representation of the discretised sampled surface $\rho_s$ in the polar domain (with the range $\rho$ and the angles $\theta, \alpha$) assuming a constant angular increment resp. grid ($\Delta_\theta$, $\Delta_\alpha$). On this basis the sampled surface $\rho_s$ can be described with the use of the Dirac delta function[2]:

---

[1] If the equation $L_{min} = 2\Delta$ is exactly satisfied (then $1/\Delta$ is the so-called *Nyquist Frequency*), a reconstruction would be prevented in the case of three points with the same height amplitude resp. value (Kraus 2004).

[2] In contrast to the presented equations within the paper of Lichti 2004 the equations are here extended in order to consider unequal angular sampling intervals.

$$\rho_s(\theta, \alpha) = \sum_{m=-\infty}^{\infty} \sum_{n=-\infty}^{\infty} \rho_c(m\Delta_\theta, n\Delta_\alpha)\delta(\theta - m\Delta_\theta, \alpha - n\Delta_\alpha) \tag{3.1}$$

The use of constant angular sampling increments is valid for static TLS systems over the whole observed scene, whereas for ALS systems operating in kinematic mode (cf. section 2.1) this is not exactly valid (e.g. the flying speed influences the increment in flight direction). However, in order to reduce the complexity a e.g. mean increment for $\Delta_\theta$ and $\Delta_\alpha$ can be used. It has to be mentioned that this sampled representation is due to its dependency on the object phase not shift invariant. Leaving ajar to similar problems in digital imaging systems (cf. (Park et al. 1984)), Lichti 2004 introduces the concept of the average system point spread function (PSF), which allows to model randomly located point sources under the assumption that the independent variables are uniformly distributed on the sampling interval. On the basis of this thought the modulation transfer function (MTF) analysis can be applied to model the sampling process of LS systems. Furthermore, the same concept can be used for the angular sampling interval as well as for the consideration of the beam divergence (Lichti 2004):

– In the case of the angular sampling interval the average PSF concept is used for the modelling of the random angular phase shifts of the scanned scene. Subsequently, the average PSF, which can be determined by averaging within the sampling grid (assuming a uniform probability distribution), allows the determination of the corresponding average MTF by the modulus of the average PSF's 2D Fourier transform. This leads to the following product of sinc-functions describing the angular sampling process without the consideration of the footprint:

$$AMTF_s(\mu, \nu) = \left| \frac{\sin(\pi\Delta_\theta\mu)}{\pi\Delta_\theta\mu} \frac{\sin(\pi\Delta_\alpha\nu)}{\pi\Delta_\alpha\nu} \right| \tag{3.2}$$

where $\mu$ and $\nu$ are the spatial frequency variables of the observed surface [3].

– In order to describe the beam width Lichti 2004 assumes an uniform probability of governing the angular position of the range measurement [4] and a circular footprint with the diameter $\delta$. This leads to the following AMTF:

$$AMTF_b(\mu, \nu) = \left| \frac{2J_1(\pi\delta\sqrt{\mu^2 + \nu^2})}{\pi\delta\sqrt{\mu^2 + \nu^2}} \right| \tag{3.3}$$

where $J_1$ is the first order Bessel function of the first kind.

The combined $AMTF_{sb}$, which describes both factors considering a rectangular angular grid and a circular footprint, can be determined as the product of the individual AMTFs (Lichti 2004):

---

[3]This formulation is restricted to analysis in the direction of the co-ordinate axes of $\mu$ and $\nu$, which are – due to simplicity – parallel to the angle grid.

[4]This assumption does not consider any physical properties of the laser beam (e.g. the irradiance distribution within the footprint) and any dependency of the range determination techniques (cf. section 3.1))

$$AMTF_{sb}(\mu, \nu) = AMTF_s AMTF_b \qquad (3.4)$$

However, the interpretation of the $AMTF_{sb}$ by analysing the frequency domain of the sampled surface is for an untrained person a difficult task. Therefore, the determination of one value in spatial domain, which describes the system capabilities, has to be preferred for practical applications. Therefore, Lichti 2004 presents a measure called effective instantaneous field of view (EIFOV) for the analysis of the sampling resolution. For the determination of the EIFOV the definition of a certain cut-off frequency $\mu_c$ is necessary:

$$EIFOV = \frac{1}{2\mu_c} \qquad (3.5)$$

at which the $AMTF_{sb}$ equals a certain threshold, $A$:

$$AMTF_{sb} \mid_{\mu=\mu_c} = A \qquad (3.6)$$

In the literature different solutions for the specification of the cut-off frequency can be found (cf. (Lichti 2004), (Kraus and Schneider 1988)). Lichti 2004 proposes to use $A = 2/\pi$ in order to enforce the condition that EIFOV = $\Delta$ for $\Delta \gg \delta$ (i.e. for a small footprint in respect to the angular grid the cut-off frequency equals the Nyquist Frequency). In the following the practical results of the method applied to two ALS systems are presented.

### 3.2.1  The resolution of the angular sampling process for two ALS systems

For the analysis of the angular sampling process the system characteristics of the Falcon II ALS from the company TopoSys ((Löffler 2003) and (TopoSys 2004)) and the ALTM 3100 designed by the company Optech (Optech 2004) were chosen. Whereas the TopoSys ALS (fibre scanner) has a significant difference in the angular sampling grid in-flight and across the flight direction and a relatively large beam width of 1mrad, the angular grid of the Optech scanner is considered to be constant (which is true – according to the Optech system specification – for 96% of the ALS strip width) offering a dual beam divergence of 0.3mrad and 0.8mrad [5]. Figure 3.4 presents the $AMTF_{sb}$ for a typical flying height of approx. 1000m and an approx. flying speed of 70m/s of these two ALS systems. In this example the $AMTF_{sb}$ is split on the one hand according to the different angular grid for the TopoSys scanner and on the other hand the dual beam divergence of the Optech scanner leads to two different functions for the ALS system. Furthermore, the sampling interval, the beam width and the EIFOV are reduced to linear units. The parameters for the determination of the $AMTF_s b$ can be found in the table 3.1 [6].

---

[5]The Optech ALTM 3100 system offers the possibility of a varying pulse repetition rate, field of view, ... allowing to adapt it to the individual needs. For this example a typical point spacing of 1m on the ground surface was chosen, although the systems allows a denser sampling at the flying height of 1000m.

[6]The analysis of the $AMTF_{sb}$ within this thesis is restricted to the main axis of the co-ordinate system describing the frequency domain of the sampled surface with parallel angular sampling grids. However, the scanner of the
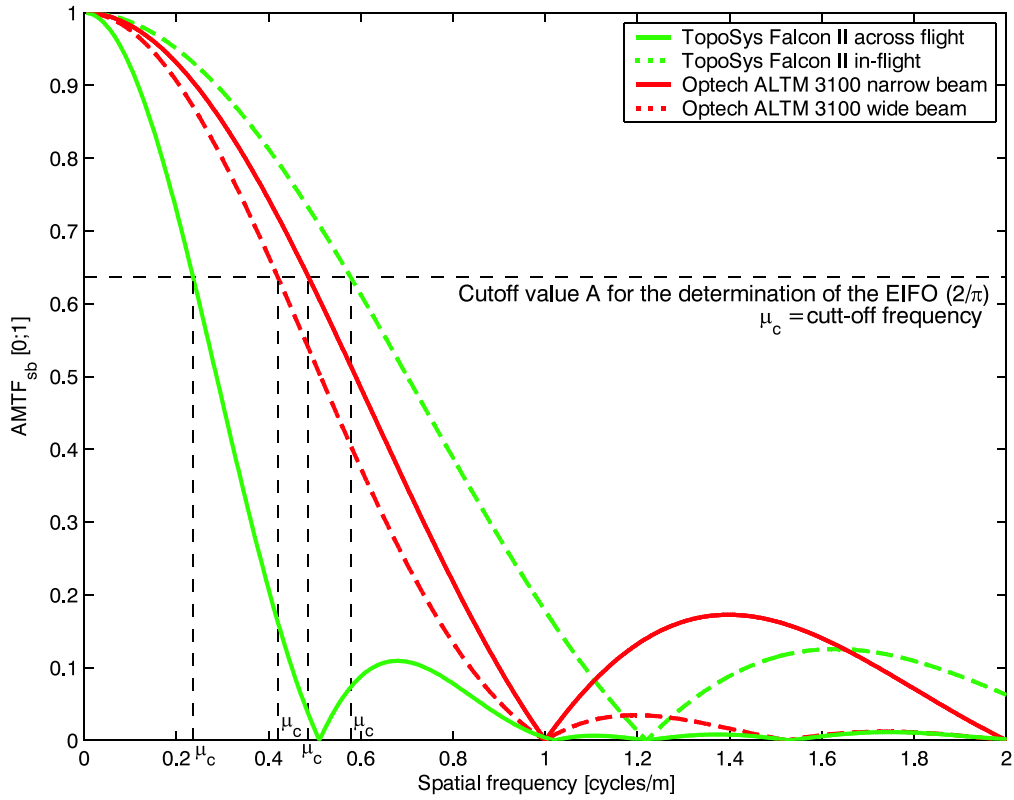
***Figure 3.4:*** *AMTF$_{sb}$ for two ALS systems.*

| ALS Sensor | $\Delta$[m] | $\delta/2$[m] | EIFOV [m] |
|---|---|---|---|
| TopoSys Falcon II across flight sampling | 1.96 | 1.00 | 2.12 |
| TopoSys Falcon II in-flight sampling | 0.11 | 1.00 | 0.87 |
| Optech ALTM 3100 narrow beam | 1.00 | 0.30 | 1.03 |
| Optech ALTM 3100 wide beam | 1.00 | 0.80 | 1.19 |

***Table 3.1:*** *Determined EIFOV [m] for two ALS systems with the point distance on the sampled surface $\Delta$ and the beam diameter on the sampled surface $\delta$ at a flying height of approx. 1000m and a flying speed of approx. 70m/s (cf. (Löffler 2003), and (Optech 2004)).*

Furthermore, the results of the EIFOV computation with the cut-off frequency $\mu_C$ with $A = 2/\pi$ for these two systems can be found on the one hand in table 3.1 and on the other hand $\mu_c$ and $A$ are visualised in the figure 3.4. What can be seen in the table is – similar to the TLS examples presented in Lichti 2004 – that a big footprint in respect to the angular grid reduces the sampling resolution to a high degree, e.g. the angular sampling resolution described by the EIFOV of the TopoSys scanner in-flight direction (0.87m) is 7.9 times higher than point distance (0.11m) in this direction. This fact indicates that neighboured points are highly correlated due to the overlapping footprints on the sampled surface, which leads on the one hand to an increase of accuracy of the range measurement, if this redundant information is used within an overdetermined modelling procedure, but on the other hand it demonstrates that a high point density does not necessarily lead to a more detailed surface sampling due to the limitations provoked by the footprint size. The dual beam example based on the Optech scanner demonstrates that the resulting EIFOV is hardly affected by the footprint size as long as the footprint is smaller than the angular sampling grid (cf. table 3.1), because for an decreasing footprint the EIFOV tends towards the sampling distance on the surface.

At the end it must be mentioned that the concept of the EIFOV is just one way, which allows the characterisation of the angular surface sampling of LS systems, but despite of some simplifications (e.g. neglecting the irradiance distribution within the footprint) it allows an objective and user friendly characterisation of different ALS systems, which is important in order to choose the adequate sensor system under the consideration of certain flight parameters (e.g. flying height) for a certain application. Furthermore, the results of the AMTF modelling resp. the EIFOV are an interesting measure for the determination of the minimum reconstructable wavelength $L_{min}$ according to the sampling theorem. For example $L_{min}$, computed under the terms of the recommendations of Kraus 2004 ($L_{min} = 3\Delta$), of the TopoSys ALS in-flight direction is, based on the EIFOV measure approx. 2.6m, whereas neglecting the footprint size by the use of the average point distance instead of the EIFOV would lead to the obvious (having in mind the beam width of 1mrad) too small $L_{min}$ of approx. 0.3m.

### 3.2.2 The sampling of surface discontinuities

Within this section of surface sampling it has to be mentioned that dense sampling does not substitute the modelling of surface structures like breaklines (cf. chapter 1, and (Kraus 2004)). In the following the influence of the sampling resolution on the detection and modelling of breaklines is shortly discussed.

In order to detect and model the breaklines on the basis of the observed ALS point cloud, it is necessary to reconstruct the surface to the left and right of the discontinuity line having in mind the sampling theorem. However, in the case of planar surfaces next to the breakline the demand of the sampling theorem can be reduced to the following equation (cf. (Kraus 2004)):

$$B_{min} = 2\Delta \tag{3.7}$$

company TopoSys allows a relative high frequent oscillation of the sensor (*swing mode*) within the airplane, which leads to an oscillating scan pattern on the sampled surface and therefore to an improved sampling of linear features (cf. (TopoSys 2004)). This swing mode is not considered within these computations.
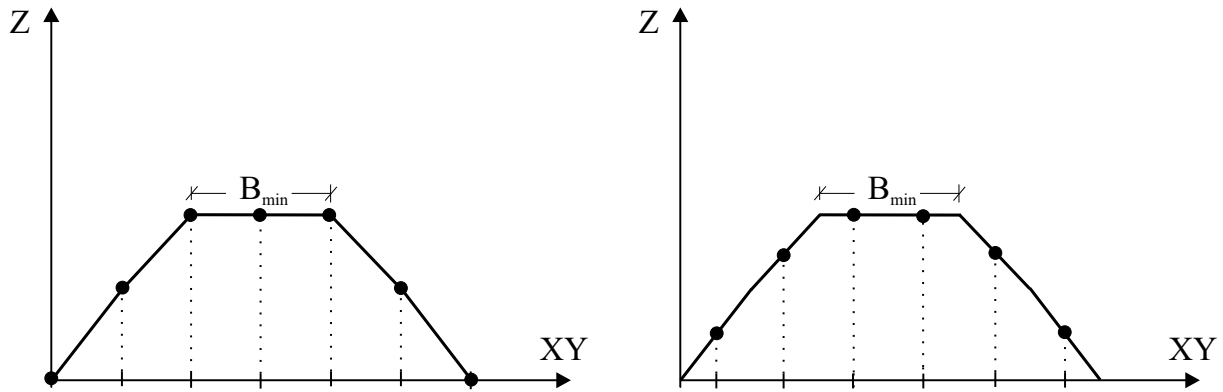
***Figure 3.5:*** *Minimal crest $B_{min}$, which is necessary for the modelling of the breaklines on a dike. Two different arrangements of recorded point cloud data for the reconstruction (black dots), with the sampling resolution $\Delta$ are displayed. (Kraus 2004)*

where $B_{min}$ is the minimal extend of the surface (measured normally to the breakline direction) on one side of the breakline, which is necessary for the detection and modelling of breaklines. This statement is illustrated in figure 3.5. The calculation of the minimum necessary sampling resolution $\Delta$ for the modelling of a certain discontinuity area can be performed with the above presented concept based on the $AMTF_{sb}$. For example, the crest of the dike must be wider than 4.2m in the case of the previous mentioned TopoSys ALS (neglecting its oscillation capability (cf. footnote 6)), if the breakline direction is parallel to the flight path.

# Chapter 4

# Breakline Modelling

The importance of explicitly described structure elements for high quality surface modelling and for the storage of these models including the advantages for data reduction were mentioned in the previous chapters. Especially breaklines, which can geometrically be defined as lines along of them the tangent planes of the surface show a discontinuity (the surface has $C^0$ continuity, but not $C^1$ continuity), are very important for the geomorphology of terrain models. Therefore, the main focus of this thesis is the development of a modelling framework, which allows to determine an explicit description of breaklines on the basis of ALS data and further available information.

Next to breaklines, further structure information like formlines and special points like peaks are in use for the description of topographic surfaces (cf. (Kraus 2000)), but usually there does not exist a common valid definition. Whereas peaks are in general defined as the highest points within a certain local area enforcing a horizontal surface tangent, the definition of formlines is not so clear (cf. (Pfeifer 2002)). Nonetheless, one possible definition based on the surface curvature, which states that along the formline the normal curvature in the direction of the formline is zero or at least very small compared to the curvature in the other directions, can be used. However, this thesis is limited to the modelling of breaklines, but eventually some of its ideas are interesting for the determination of other structure information.

The basic aims of the breakline modelling from ALS data are the following:

- The 3D co-ordinates of the breakline should be determined within one step.

- The modelling of the breaklines should be possible on the basis of the original irregular distributed point cloud data in order to use all available information unadulterated.

- The previous point necessitates the consideration of off-terrain points (e.g. in the case of overgrown breaklines) within the modelling procedure due to the exclusion of other preprocessing steps.

- The method should allow to use further information resp. observations next to the point cloud data.

- An objective classification into relevant and unrelevant breaklines should be possible.

- The degree of automatisation should be as high as possible.

– The process should deliver accuracy information to allow a determination of the 3D modelling quality.

In the following section the basic principles of the breakline modelling method are presented. Afterwards, the modelling based on plane pairs in 2.5D as well as in 3D including a small ALS example is demonstrated. Subsequently, the method will be extended step-by-step in order to cope with specific ALS problems (off-terrain points are considered in section 4.3). Furthermore, the integration of additional information sources (e.g. image data) is considered in section 4.4. The result of the modelling process is a detailed description of the breakline. In order to reduce the high amount of data, one section concentrates on the data reduction of the modelled breaklines according to an user defined approximation accuracy. The final section of this chapter gives an outlook into future research work.

It must be stressed that the basic modelling concept presented in this chapter is a semi-automatic breakline modelling procedure for which a rough 2D approximation of the breakline is necessary (cf. the following section 4.1). Concepts, which allow to overcome resp. help to reduce this limitation, follow in chapter 5.

Furthermore, it has to be mentioned that the modelling of the breaklines should start after the complete georeferencing process of the ALS data in order to exclude systematic errors caused by strip discrepancies. However, the breakline information could be an important further input for the georeferencing process, especially for the correction of planar errors between overlapping ALS strips (cf. (Kager 2004)). Therefore, one can think of the determination of the breaklines prior the adjustment, independent for each ALS strip. However, it has to be considered that after the strip adjustment the breakline determination has to be repeated, if the adjustment process itself does not allow the additional determination of breaklines based on the original unclassified ALS data within the same step.

## 4.1 Basic Modelling Concept

This section treats the explicit modelling of breaklines from irregular distributed point cloud data in a general way (regarding the data acquisition process), and it is based on the following considerations:

Basically, it is assumed that the given point cloud data, except at the positions of breaklines, describes smooth surfaces (in terms of the sampling interval, cf. section 3.2). This basic assumption is necessary for the use of interpolation or approximation methods to reconstruct the surface between the observed data, but furthermore this legitimates – up to a certain degree – also extrapolation. Therefore, one can think of grouping the point cloud into two groups, each group including the points on either side of the breakline, and subsequently reconstruct the surface on each side independently. This leads to two surface descriptions, which are valid for one side only. Moreover, the intersection of these two modelled surfaces is – under the assumption of the validity of extrapolation – a model of the breakline itself.

This means that a model of the surface is fitted to the data in the vicinity of the breakline. So the breakline model is formulated in the following way: A breakline is the intersection of two smooth surfaces, each surface interpolating the points on either side. This concept can be used in general for the explicit description of breaklines on the basis of point cloud data.
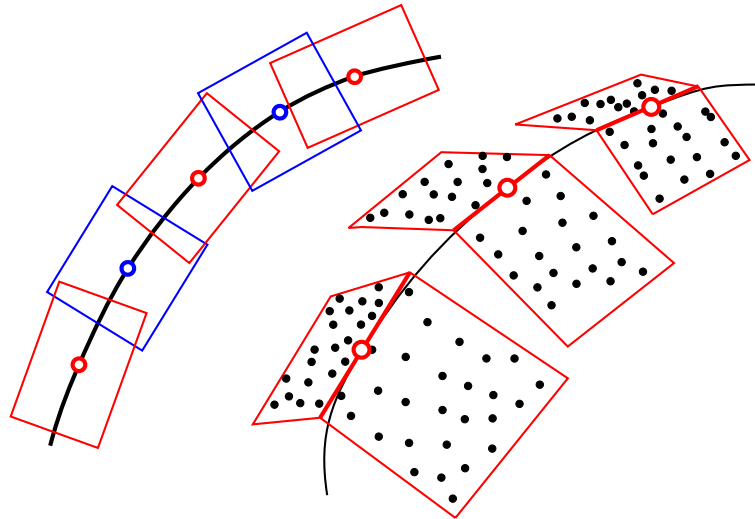
***Figure 4.1:*** *Basic concept for the description of breaklines with the help of intersecting patch pairs determined on the basis of surrounding point cloud data. Left: Ground view of overlapping patch pairs; Right: Perspective view of a reduced number of patch pairs (overlapping pairs are removed) with their point cloud support (cf. (Kraus and Pfeifer 2001) and (Briese et al. 2002)).*

However, it must be mentioned that this formulation of the breaklines is limited to the intersection of two surfaces. In order to describe intersections or crossings of the breaklines the basic concept has to be extended.

The previous paragraph describes the modelling of a breakline conceptually on the basis of a global approach. In general, global algorithms have the capability to produce more homogeneous results than local approaches considering a small neighbourhood only. However, having in mind the big amount of data from ALS systems, global approaches lead even for simple tasks to a very high computational effort. Therefore, local approaches have to be preferred. A further advantage of local approaches is that not the entire process is affected by a small local change in the input data.

Considering these thoughts leads to a breakline modelling concept, which uses small continuously overlapping surface patch pairs supported by the point cloud data in a certain neighbourhood of the breakline (cf. figure 4.1). Analytic surfaces, which can be determined with the help of an adjustment procedure on the basis of the respective point cloud data, can be used for modelling the surface patch pairs.

However, by looking at the processing sequence of the breakline determination *one can recognise that there is somehow a circular argument involved*: On the one hand the aim is to reconstruct the structure line, but on the other hand the structure line is essential for grouping the points into the classes "Left" and "Right".

Though, the previous mentioned circular argument can be broken due to the fact that for grouping the complete knowledge of the breakline is not necessary:

– Firstly, in the case of ALS data the problem of splitting the data in two groups can be simplified to a 2D problem, where the breakline needs to be defined in the ground plane only. However, this leads to a reduction of the model to 2.5D, but this simplification is

also possible in the TLS case by looking at the point cloud from one TLS position in the 2D angular domain (cf. section 6.3). The separation of the points can be performed in the 2D space, whereas the subsequent modelling of the two intersecting surfaces can be performed in 3D space.

– Furthermore, the problem can be reduced by the use of a known approximation of the breakline instead of the complete breakline (e.g. in the 2D parameter space), which can be subsequently refined in an iterative process using the above mentioned breakline modelling framework.

So, if a 2D approximation is known, the modelling can be performed straight on automatically by a step-by-step refinement of the determined 3D line.

However, the still open problem is that it cannot be expected that these approximations are available in the forefront. Therefore this concept needs an additionally prior step allowing to obtain this essential information. For the determination of this approximations different methods can be considered. In general, we can distinguish manual from so-called semi-automatic approaches with user assistance, and fully automatic solutions. One can think of the usage of one of the raster based methods for 2D breakline extraction already presented in section 2.3, for example. In certain landscapes the use of water shed analysis can be considered (cf. (Kraus and Pfeifer 2001)). Finally, it should be mentioned that the rough approximation can also be determined on the basis of already available 2D data sources or it can be manually digitised (2D) in a fast way in a visualisation of the surface determined on the basis of the available point cloud data (e.g. a shading). These and further algorithms for the determination of the approximations will be the topic of the following chapter 5.

In contrast to the other methods presented in section 2.3 this method allows a simultaneous modelling of all three co-ordinates within one process. Furthermore, the original irregular distributed data points themselves are the input for the breakline modelling procedure, because it is not restricted to a raster data structure. Besides, further information about the object surface in the vicinity of the breakline can be used for the reconstruction, and an analysis of the accuracy of the intersection line is possible by the use of adequate functional surface modelling techniques.

This basic concept can be seen as the foundation of subsequent extensions, which allow to fulfil the goals of the breakline modelling procedure mentioned at the beginning of this chapter. The following sections provide a deeper look into the practical realisation and into the concepts of the necessary extensions. As mentioned before, the determination of the approximate breakline is discussed in the next chapter.

## 4.2   Modelling based on Plane Pairs

This section presents the modelling of breaklines with the help of intersecting plane pairs. These plane pairs describe the surface in the vicinity of the breaklines on the basis of the previous mentioned basic concept. Furthermore, it is assumed that an approximation of the breakline is available. Therefore, the input for the modelling procedure is on the one hand the 2D
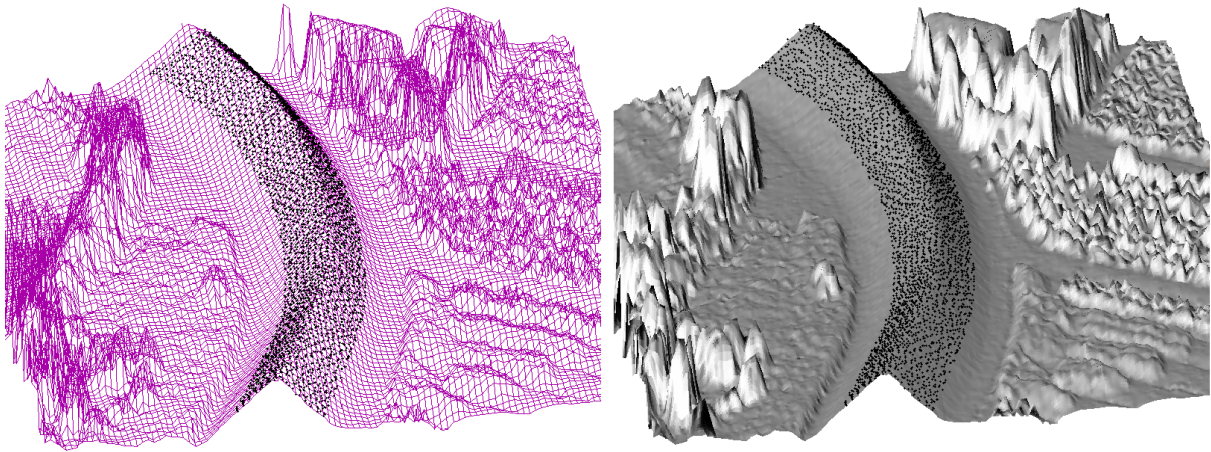
***Figure 4.2:*** *Surface model (Left: Grid representation; Right: Shading of the grid model) together with the ALS point cloud (black dots) in the vicinity of a breakline.*

approximation and on the other hand the ALS point cloud data. Figure 4.2 presents a typical ALS point cloud within a buffer zone around the breakline[1].

Planes have the advantage that only a few parameters have to be determined and the intersection of the surface elements is straight forward. Furthermore, it can be argued that, seen from a geometrically point of view, the intersecting plane pairs should represent approximations of the tangent plane on the surfaces in the vicinity of the breaklines.

However, if the delivered point cloud would be free of measurement errors and the approximative breakline would correctly split the point cloud into two groups, it would be enough to take the nearest three points (measured in the orthogonal direction to the breakline) within one patch and determine the plane pair through these points. Though, we have to consider measurement errors and approximation errors of the breakline. Therefore, a wider neighbourhood around the breakline must be chosen for the determination of the plane pair (cf. figure 4.2) under the consideration of the sampling capabilities using e.g. the EIFOV measure (cf. section 3.2) and the approximation accuracy of the breaklines.

In order to reduce the influence of points with an increasing orthogonal distance to the breakline a *weight function* can be used. This weight function (in the following example a function composed of bell curves) can be parameterised in a way that points near the breakline get a high weight, whereas the weight of points far away from the breakline declines. Additionally, points with a certain distance to the breakline should have no resp. a reduced influence to the run of the surface patches ,and therefore, their weight should also be very low. This considers the thoughts of the previous chapters, where it was mentioned that the points very close to the breakline (where the footprint of the ALS sensor illuminates both surface pairs) are affected by distance measurement errors (cf. chapter 3). An example of such a weight function, which has to be set due to the ALS system and project characteristics is presented in figure 4.3. This weight function reduces the weight of points in a small buffer zone around the breakline itself due to the previous mentioned ALS properties.

---

[1]The practical examples of this chapter were obtained within a test project initiated by the German Federal Agency for Hydrology ("Bundesanstalt für Gewässerkunde").
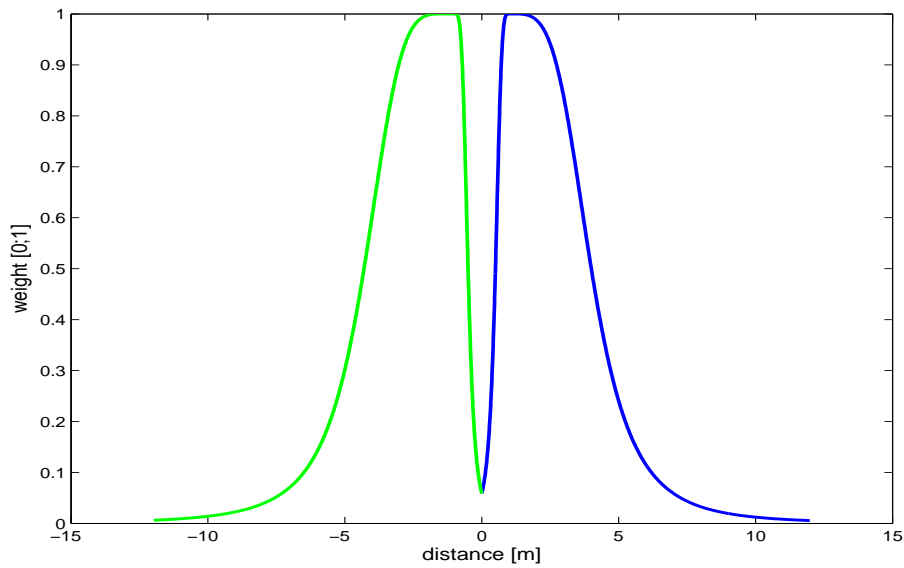
**Figure 4.3:** *Weight function composed of four bell curves, which defines an individual weight for each point depending on the distance to the breakline; Green (negative distance values): Weight function for points belonging to the support of the left surface patch; Blue (positive distance values): Weight function for points of the right surface patch; Additionally, points in a small buffer zone (in this figure ±1m) around the breakline (distance zero) get a lower weight due to distance measurement errors in the vicinity of breaklines (cf. chapter 3).*
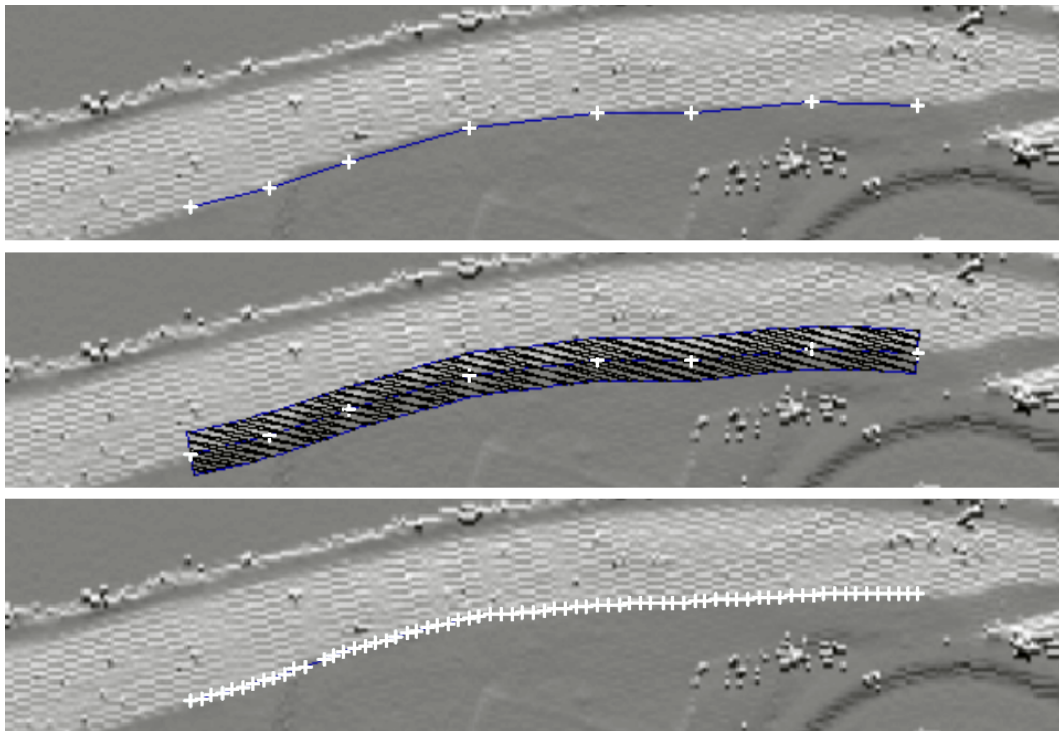


**Figure 4.4:** *Work flow (beginning at the top) of 3D modelling based on a 2D approximation of the breakline demonstrated on a practical example. The middle part shows the buffer zone around the breakline approximation and the ALS point cloud (black dots) inside this area. In the lowest picture the refined breakline is presented.*

Now a closer look to the practical realisation is presented (cf. also figure 4.4). For the modelling procedure the following steps have to be performed:

- In the fist step it is necessary to determine the buffer zone around the breakline on the basis of the approximation of the breakline. In the following, all ALS points within this buffer zone should support the subsequent modelling procedure (cf. the middle part of figure 4.4).

- After the selection of the ALS data (within the practical examples of this thesis a topographical database was used for this task in order to allow a fast access to the point cloud data of an ALS project) the point cloud has to be sorted according to the stationing in respect to the approximation of the breakline. For data selection, the original breakline has to be set to the left and to the right in order to compute the buffer zone. Within practical tests it turned out that the best solutions are provided with the help of parallel curves on the basis of an Akima interpolation (cf. (Kraus 2000)) of the approximation of the breakline.

- With the calculated stationing the selection of the point cloud for the modelling of the surface patches is possible. Therefore, the next step is the determination of the surface pairs within an adjustment procedure.

- Based on the result of the adjustment of all patch pairs, a refined breakline can be computed by the determination of one representative point within one patch. Furthermore, the tangent of the breakline can be calculated (in the case of plane pairs it is just the intersection line of the surface patches).

The aim of the modelling procedure is to refine the breakline within an iterative procedure by a step-by-step regrouping of the ALS point cloud. Therefore, based on the results of the last step the upper procedure can be repeated in order to refine the breakline until there is not a significant change in the results anymore (in order to increase the performance the reexportation of the ALS point cloud can be skipped if the resulting breakline does not differ too much from the original approximation of the breakline). In figure 4.4 the size of the surface patches was 5m (along the breakline) by 10m (across the breakline direction). The overlap between neighbouring patches was 50 percent.

As mentioned before, as a result of the modelling procedure one representative point on the intersection line in the centre of the patch and the direction of the intersection line (tangent of the breakline) are stored per patch pair. An additional interesting result is the intersection angle between the surface patches along the entire breakline, which allows a further analysis. Due to the fact that the surface elements are determined within an adjustment procedure, precision measures for the estimation of the unknowns (plane parameters resp. surface normal) can be computed. Further quality parameters (e.g. the accuracy of the intersection line) can be estimated by the use of error propagation.

A lot of extensions to this basic processing work flow can be considered. Some of them are essential for modelling the original ALS data (e.g. Robust Modelling), whereas others can contribute to more stable and reliable results. In the following sections a few extensions are mentioned. However, in the following subsections a more detailed look on the planar patch determination procedure is performed. In general, we must distinguish a 3D determination process from a 2.5D computation.

### 4.2.1 3D Plane

For the determination of an adjusting plane based on a 3D point cloud a straight forward solution based on an eigenvalue problem does exist (cf. e.g. (Pfeifer 2002)). This solution allows to determine a plane in 3D without any approximate values. Basically, a plane $\tau$ can be described in Hesse's form with the normal vector $\mathbf{n}$ and the constant $c$. In the following, the basic steps for the determination of the plane, which minimises the sum of the squares of the weighted orthogonal distances of the points in respect to the plane, are summarised:

In the first step it is necessary to reduce the co-ordinates of all $n$ given points $\mathbf{P_i} = \begin{pmatrix} x_i & y_i & z_i \end{pmatrix}^T$ by the co-ordinates of the weighted COG:

$$\overline{\mathbf{P_i}} = \mathbf{P_i} - \mathbf{COG} = \begin{pmatrix} \overline{x_i} & \overline{y_i} & \overline{z_i} \end{pmatrix}^T \tag{4.1}$$

This allows to reduce the problem to the determination of the normal vector $\mathbf{n}$, because the adjusting plane contains the origin (COG) of this local co-ordinate system.

Subsequently, the adjusting plane can be determined by the following eigenvalue system (cf. (Pfeifer 2002)):

$$(\mathbf{A}^T \mathbf{W} \mathbf{A} - \lambda \mathbf{E})\mathbf{n} = 0 \tag{4.2}$$

where

$\mathbf{A} = \begin{pmatrix} \overline{x_1} & \overline{y_1} & \overline{z_1} \\ \vdots & \vdots & \vdots \\ \overline{x_n} & \overline{y_n} & \overline{z_n} \end{pmatrix}$, the weight matrix $\mathbf{W} = diag(w_i)$, which allows to set an individual weight $w_i$ for each point, and the (3,3) unit matrix $\mathbf{E}$. The three eigenvectors $\mathbf{n_1}, \mathbf{n_2}$, and $\mathbf{n_3}$ with their respective eigenvalues $\lambda_1, \lambda_2$, and $\lambda_3$ are the solutions of the system. Considering the fact that we are interested in a solution, which minimises the squared discrepancies, the adjusting plane determined on the basis of the smallest eigenvalue is the solution of the adjustment. The following example demonstrates an interesting approach for the determination of the plane on the previous mentioned adjustment procedure.

Figure 4.5 presents a practical application of the presented adjustment procedure. The distance of the acquired point cloud in respect to an adjusting plane was analysed in order to study the precision of the range determination unit of a TLS of the company Riegl (LMS-Z420i). Within this test a sigma of the range measurement unit of approx. 7mm could be determined. Furthermore, the determined histogram, which displays the differences of approx. 190000 points, showed no significant systematic effects.

The previous example demonstrates the practical use of the adjustment procedure for the determination of resolution measures. However, one has to bear in mind that the discrepancies determined within this adjustment setup are measured in orthogonal direction to the determined plane.

Having in mind these advantages one can think of the determination of the 3D breakline based on two independently determined planes with the help of this full 3D solution. In fact this is
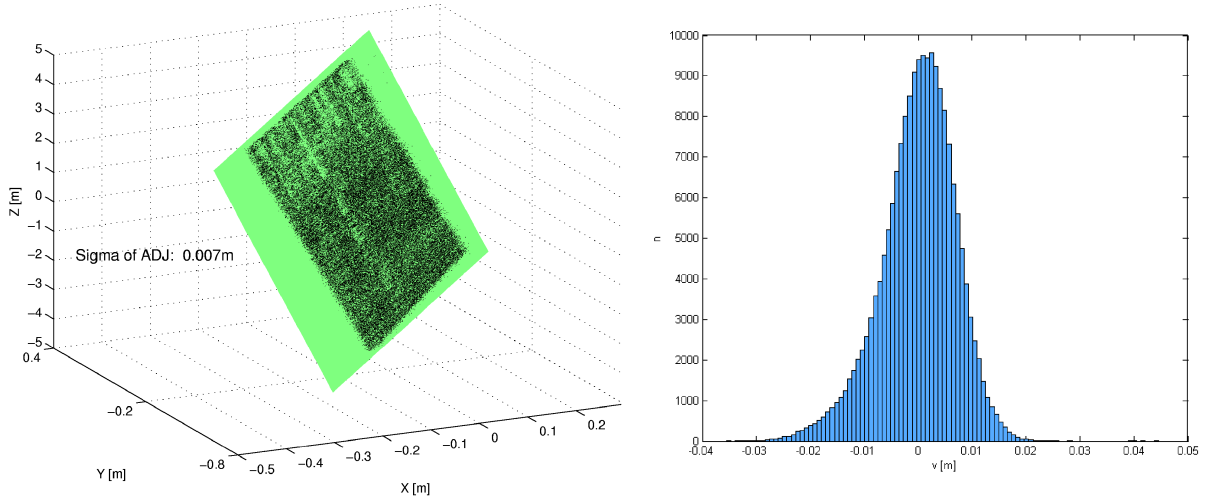
***Figure 4.5:*** *3D Plane adjustment of TLS data of a planar object surface (Riegl LMS-Z420i (Riegl 2004b)); Left: Adjusted plane and TLS point cloud; Right: Histogram of the residuals.*

a very interesting way to determine the two surface patches, but, furthermore, especially for the use with ALS data, a 2.5D formulation of the patches has to be considered (cf. the next subsection), as well.
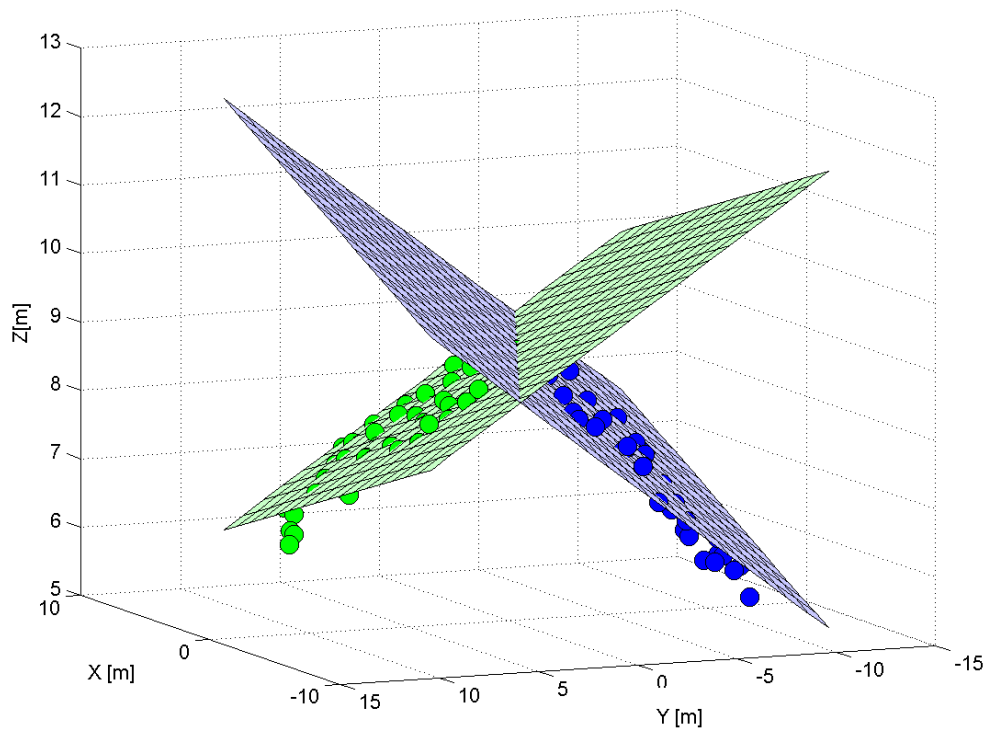
### 4.2.2 2.5D Plane Pair

In contrast to the 3D solution, the 2.5D solution uses a 2D parametrisation of the surface. For the use of ALS data it is useful to choose the ground plane as parameter domain. This leads to an adjustment system where the height values (z-values) at a certain position have to be determined. In contrast to the previous procedure, the residuals are measured orthogonal to the parameter domain, what means that the residuals are measured in z-direction (in the case of the use of the ground plane as parameter domain).

In order to estimate the plane pair, both surfaces (left and right, subscripts $_l$ and $_r$) can be determined within the following adjustment procedure:

$$
\begin{aligned}
r_{i,l} &= +\underline{a_l}X_{i,l} &+\underline{b_l}Y_{i,l} &+\underline{c_l} & &-Z_{i,l} \\
r_{i,r} &= & &+\underline{a_r}X_{i,r} &+\underline{b_r}Y_{i,r} &+\underline{c_r} &-Z_{i,r}
\end{aligned}
\tag{4.3}
$$

where the points $P_{i,l}(X_{i,l}, Y_{i,l}, Z_{i,l})$ resp. $P_{i,r}(X_{i,r}, Y_{i,r}, Z_{i,r})$ are assigned either to the left or right surface. On the basis of these equations the corresponding plane parameters $a$, $b$, and $c$ can be determined by minimising the quadratic residuals $r_i$.

Figure 4.6 presents a practical example of the adjustment of one patch pair (10m by 10m) on the basis of ALS data in the vicinity of a breakline. The sigma of the adjustment was 0.06m. Points near the breakline got a higher weight than points with a higher orthogonal distance. Furthermore, a footprint size of 0.5m was considered (cf. section 4.2).

***Figure 4.6:*** *2.5D plane pair of one patch (10m by 10m) determined from ALS data (green resp. blue circles); Sigma of adjustment: 0.06m.*

Summarising the properties of the two different surface techniques it must be mentioned that each of them has its individual advantage. The big difference of the both lies on the one hand in the generality of the 3D method and on the other hand in the way the residuals are measured. In the case of ALS data the 2.5D method is usually sufficient due to the data acquisition technique. Furthermore, it allows the determination of the off-terrain points (e.g. points on the vegetation) with the help of an analysis of the height values in z-direction (which corresponds (more or less) to the grow direction of the vegetation) directly and an easier integration of additional observations within the simultaneous adjustment procedure of the surface pairs (cf. next sections). Thus, the choice depends on the individual application.

## 4.3   Robust Modelling

As stated at the beginning of the modelling aims the breaklines should be determined with the help of unclassified originally acquired ALS point clouds in order to exclude preprocessing errors and to use all available information. Therefore, the basic concept has to be extended in a way that the influence of off-terrain points (e.g. due to reflections of the laser beam on the vegetation or caused by measurement errors as a result of multipath reflection ("Long Ranges")) is reduced as much as possible.

The following extensions of the modelling concept are based on the robust interpolation techniques developed for the estimation of DTMs from ALS data presented by Kraus and Pfeifer

1998. In the following, these enhancements allow the modelling of breaklines in consideration of off-terrain points.

Robust interpolation was originally developed for the generation of DTMs from laser scanner data in wooded areas. For this purpose a solution was found, which integrates the elimination of gross errors resp. off-terrain points and the interpolation of the terrain in one process. The aim of this algorithm is to compute an individual weight for each point in the irregularly distributed point cloud in such a way that the modelled surface represents the terrain. Basically, it consists of the following steps (cf. (Kraus and Pfeifer 1998) and (Briese et al. 2002)):

1. The surface is determined under the consideration of individual weights for each point (at the beginning all points are equally weighted).

2. Calculation of the filter values (oriented distance from the surface to the measured point) for each point.

3. Determine a new weight for each point according to the filter value.

These steps are repeated until a stable situation is reached (all gross errors are eliminated) or a maximum number of iterations is reached. The results of this process are a surface model and furthermore, a classification of the points in terrain and off-terrain points in respect to their distance to the surface (under the consideration of their a priori known precision) can be performed.

The two most important entities of this algorithm are the functional model (step 1) and the weight model (step 3). For the determination of a DTM linear prediction (similar to kriging, cf. (Kraus 2000) and (Kraus 1998)) can be used. The elimination of the off-terrain points is performed with the help of a weight function, which assigns a low weight to points with a significant difference to the surface model (under the consideration of the measurement precesion) in order to reduce their influence subsequently in the following processing steps. For the weight function a bell curve (similar to the one used for robust error detection in bundle block adjustment) controlled by the half width value and its tangent slope at the half weight can be selected. Furthermore, it can be used in an asymmetric and shifted way in order to allow an adaptation to the distribution of the errors in respect to the "true" surface. The asymmetry means that the left and right branch are independent and the shift considers that the weight function is not centred at the zero point. Additionally, tolerance values can be used in order to exclude points with a certain distance to the computed surface totally from the determination process. These adaption allows to consider the typical data distribution of the ALS points in respect to the DTM surface. Finally, the classification into terrain and off-terrain points can be performed by the use of further tolerance values determined according to the measurement precision. Afterwards, the final surface model can be computed with the help of the classified terrain points with their a priori weights, in order to exclude the weight influence of the robust estimation (this is performed similarly to the robust estimation techniques within adjustment systems). A detailed description of this method can be found in (Kraus and Pfeifer, 1998).

So, in order to robustly estimate the surface patches of the breakline modelling procedure, the only thing that has to be adapted to the previous mentioned concept of DTM determination is the functional modelling part (first item in the previous mentioned processing). For the robust estimation of the surface patch pairs, which should describe the surface in the vicinity of the breaklines, it is just necessary to add the previous mentioned iterative robust determination
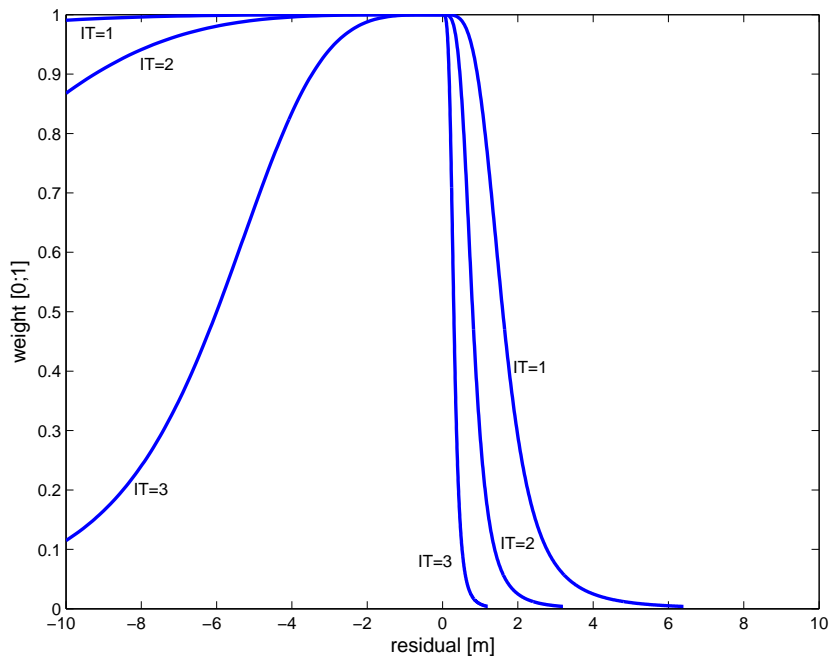
***Figure 4.7:*** *Example of automatically self adapting weight functions per robust iteration step (IT). The function adapts itself to the data considering to typical ALS characteristics and allows to decrease the weight of off-terrain points in ALS data. Positive residuals belong to points above the terrain, whereas points below the terrain have negative residuals. Especially the weight of off-terrain points above the terrain is reduced to a very high degree.*

concept. Practically, this means that a second weight function, next to the one, which is responsible for weighting in respect to the orthogonal distance to the breakline and a further iteration loop, next to the one, which iteratively refines the breakline, is necessary. These further steps have to be considered in the modelling procedure mentioned in section 4.2, whereas this extension only effects the adjustment procedure and secludes itself from the general workflow for breakline modelling.

Practically, the robust estimation of the patch pairs should be initiated automatically if off-terrain points are present. This automatic initialisation can be easily performed by an analysis of the residuals of the surface adjustment procedure. The presence of off-terrain points resp. gross errors can be determined if the normalised residuals exceed a certain value defined by a significance level. Furthermore, an automatic adaption of the weight function is essential in order to allow a fully automatic determination. This weight function has to adjust itself within a fully automatic procedure using an individual self-adapting weight function for every iteration step. In order to eliminate the off-terrain points step-by-step it is necessary to start with a broad weight function, which allows to eliminate extreme blunders (off-terrain points with a large distance to the determined surface model). Subsequently, the weight function can be set narrower iteratively to eliminate further off-terrain points. A practical example of such automatically adapted weight functions can be seen in figure 4.7. These functions especially reduce the weight of points above the terrain surface having in mind that, in general, the ALS points do not lie below the terrain surface (exceptions can be caused by multipath errors). Additionally, the shift of the origin is adapted step-by-step to assign the highest weight to points on the terrain surface.
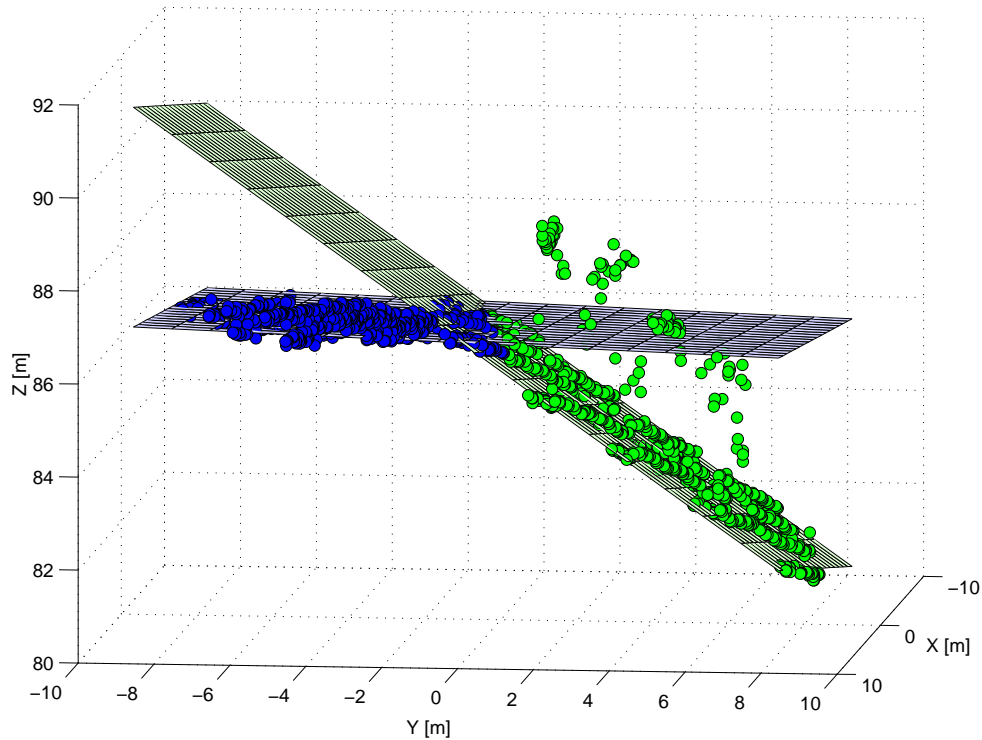
***Figure 4.8:*** *Practical example of a robust estimated plane patch pair (10m by 10m) on the basis of unclassified ALS data (circles). The elimination of off-terrain points allowed to reduce the sigma of the adjustment from previously 0.59m to 0.12m.*

Figure 4.8 presents a practical example of the determination of a plane pair by an automated robust estimation procedure. In the right part of the figure off-terrain resp. off-plane points can be recognised. The robust adjustment in this example allowed a reduction of the sigma of the adjustment from previously 0.59m to 0.12m. A comparison of the histograms of the residuals with and without robust estimation can be seen in figure 4.9. In both histograms the biggest gross errors can be recognised. Furthermore, it can be seen in the left part of the figure that the influence of the off-terrain points leads to an asymmetric and shifted distributed of the residuals about zero. By a look at the right part of the figure the significant enhancement of the distribution about zero due to robust estimation can be recognised. Based on this histogram a classification into terrain and off-terrain points can be performed.

At the end, the importance of robust estimation techniques for the determination of the patch pairs must be stressed (cf. the previous mentioned typical ALS example). Using original ALS data we always have to consider the presence of off-terrain points or measurement errors. Furthermore, it has to be mentioned that the usage of robust estimation is either possible with the previous mentioned 2.5D as well as with the 3D patch pair estimation procedure. However, one has to consider that the residuals of both adjustment procedures are measured in different directions, which has to be considered in the robust estimation procedure. Within the 2.5D concept the residuals are measured in z-direction (cf. subsection 4.2.2), whereas in the case of the 3D adjustment we have to deal with (algebraic) residuals measured in normal direction in respect to the adjusted plane cf. subsection 4.2.1). In order to convert the algebraic error measures into errors in certain co-ordinate directions a further computational afford is necessary
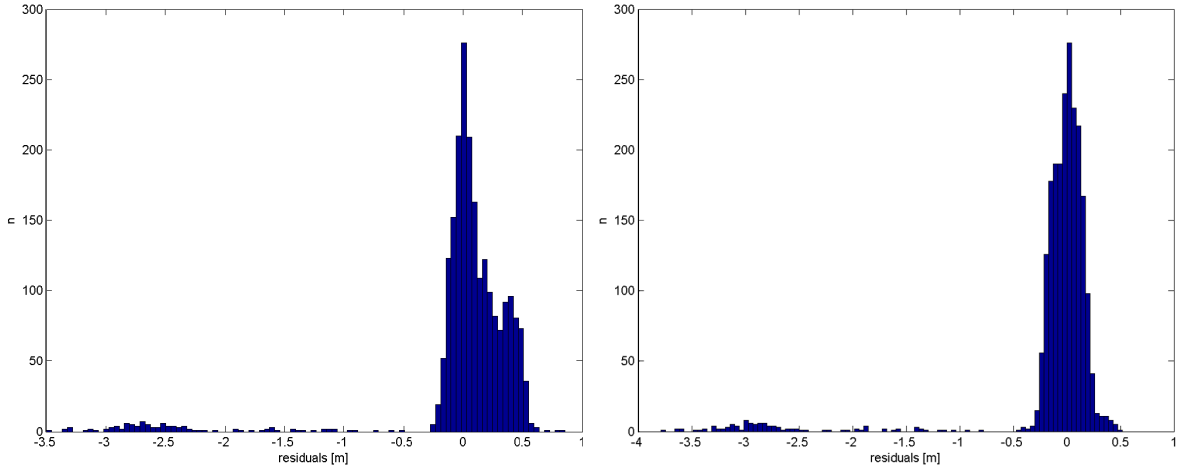
***Figure 4.9:*** *Histogram of the residuals of a patch pair adjustment of the ALS poins displayed in figure 4.8; Left: Histogram of the residuals of an adjustment with equal weighted ALS points; Right: Histogram of the residuals after an adjustment using robust estimation.*

(cf. (Kager 2000)).

## 4.4 Integration of Additional Observations

Nowadays, *sensor integration* is an often used term. A lot of research groups as well as companies try to overcome some limitations given by a certain sensor type by the help of further different sensors in order to use the advantages of both. This trend can also be seen in the case of ALS data acquisition. These days, a lot of ALS flights are carried out with a simultaneous registration of image data. Furthermore, one can consider to integrate available data within the modelling procedure.

In respect to the modelling of breaklines, one e.g. can think of integrating manually or automatically derived photogrammetric observations into the adjustment procedure. The benefit of the modelling framework presented within this chapter is that an integration of further observations can be performed easily. Next to observations, which help to determine the two surfaces by indirect observations of the breakline (in the vicinity of the breakline, like the ALS observations), direct observations of the breakline (e.g. in image data) can be considered.

Especially in the 2.5D modelling concept presented in subsection 4.2.2 this can be performed easily by adding the following two observation equations to the previously introduced ones 4.3:

$$
\begin{aligned}
r_{i,l} &= +\underline{a_l}X_{i,bl} \quad +\underline{b_l}Y_{i,bl} \quad +\underline{c_l} \quad -\underline{Z_{i,bl}} \\
r_{i,r} &= \qquad\qquad\qquad\qquad\qquad\qquad -\underline{Z_{i,bl}} \quad +\underline{a_r}X_{i,bl} \quad +\underline{b_r}Y_{i,bl} \quad +\underline{c_r}
\end{aligned}
\tag{4.4}
$$

where the point $P_{i,bl}(X_{i,bl}, Y_{i,bl}, Z_{i,bl})$ on the breakline (direct observation of the breakline) influences the run of the surface patch pair (the explanation of the further variables can be found at

the equation 4.3). This equation enforces an intersection (i.e. the same z-value of both planes) at the position of the observed point $P_{i,bl}$. Next to this functional extension of the adjustment system also the stochastical part of the adjustment has to be adapted, i.e. a further weight has to be considered and assigned to these additional observations considering their precision in respect to the ALS data. Furthermore, it has to be decided within the robust estimation if these observations should be considered to be free of gross errors or not. In the case of independently determined 3D plane pairs (cf. subsection 4.2.1), this additional observation with an individual weight can also be integrated. Though, the disadvantage compared to the 2.5D formulation of the equations 4.4 is that no simultaneity adjustment of the additional observations is performed.

It has to be stressed that this extension to the basic concept allows the integration of e.g. high quality 2D breakline information and high quality height information from ALS data within *one process*. Furthermore, it allows the consideration of the precision of the approximative breakline which also leads to a stabilisation of the adjustment process. The interdependence of the observations can be controlled easily by an additional weight factor that depends on the individual observation precision.

## 4.5 Determination of Jump Edges

As a special case in the modelling of breaklines the determination of jump edges has to be considered. Seen from a geometrically point of view, there is no difference between the modelling of these breaklines from the previous ones, because the breaklines (in this case two) can be determined by the intersection of two surface patches. However, a different treatment of this case is necessary due to the characteristics of the ALS data acquisition. As a result of the observation direction of ALS sensors, it is not possible do determine points on surfaces, which have a surface normal that is more or less orthogonal to the direction of the laser beam (e.g. there are usually no ALS points on vertical walls). Therefore, the ALS sensor delivers only a point cloud on the adjacent surfaces and usually no observations on these conjunctive (vertical) surfaces are available (cf. figure 4.10). The difference in modelling compared to the previous observed breaklines is that one of the patch pairs contains no resp. only a few ALS points (so that a determination of the surface along the whole line is not possible without further knowledge resp. assumptions).

The aim for the modelling of the jump edge is the determination of an upper and lower breakline in the observed surface. Having this in mind, the modelling of this special case can be (in a fist step) performed with the previous mentioned techniques with the use of the ALS points in the vicinity of this jump edge (caused by missing information of the conjunctive surface), whereas no intersection constraint of the two modelled surface patches is valid. The determination of the two surfaces described by the acquired ALS data can be performed by the use of robust estimation techniques. This leads to a description of the two surfaces in the vicinity of the jump edge. After the determination of the non-intersecting surface patches, the ALS data can be assigned to the individual surfaces (to the "Left" or "Right" surface). The position of the jump edge can be determined by the detection of (height) jumps between the assigned ALS data in normal direction to the approximative breakline. Both breaklines, which are necessary to model the "jump", can be determined with the help of an adjusting 2D line calculated on the basis of the previously detected jumps in between the two modelled surfaces and by a projection of the 2D breakline in either robustly estimated non-intersecting surfaces.
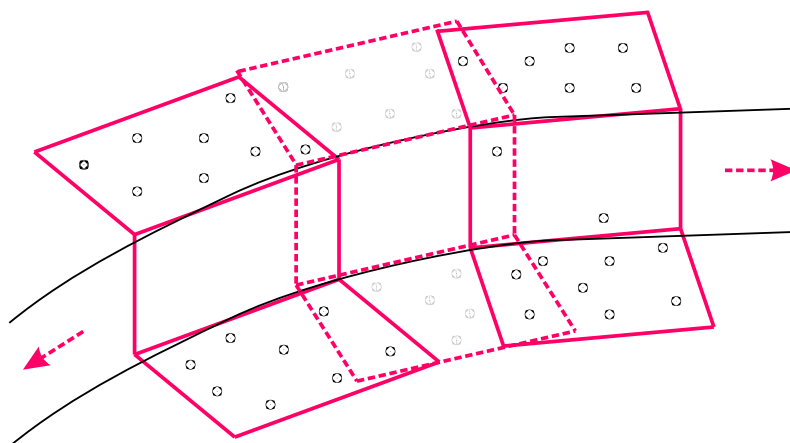
**Figure 4.10:** *Basic concept for the modelling of jump edges on the basis of ALS points.*

It has to be mentioned that the result of the jump edge modelling is just the 3D description of the upper and lower breakline. No information of the connecting surface due to the lack of observations is determined. Furthermore, the problem of echo overlay mentioned in chapter 3 has to be considered. Points very close to the jump edge might be affected by distance measurement errors caused by echo overlaying and will affect the modelling procedure. It has to be considered that the total separation of the echoes is only possible if the range difference of the two illuminated non-intersecting surfaces is bigger than the half of the pulse duration. If the range difference is smaller, points with a distance of the footprint diameter have to be excluded (with the help of a weight function) from the patch determination.

Additionally, it is very interesting that the occurrence of a jump edge can be automatically determined within the adjustment procedure. For this aim it is necessary to integrate the additional information of the approximate breakline as direct 2D observation into the adjustment procedure (cf. section 4.4). Subsequently, by an analysis of the discrepancy of these additional observations the appearance of a jump edge can be determined by a significant big residual error, indicating that the two surfaces do not intersect. The processing chain can adapt itself automatically to the different determination procedure, which is necessary for the modelling of jump edges.

## 4.6 Data reduction

This section shortly considers the data reduction of the determined breaklines. The result of the previous presented modelling framework is a very detailed description of the breakline with a very high point density and a lot of further information (e.g. tangent on the breakline points per patch, precision information, meta information (e.g. number of off-terrain points per patch), etc. ). Subsequently, software packages for the surface modelling cannot use all of this information. Furthermore, even when the input is reduced to a list of points describing the breakline, data reduction has to be considered in practical applications.

The general aim of data reduction is the generation of a further instance of an existing model (a second model), which approximates the given model with a certain approximation precision,
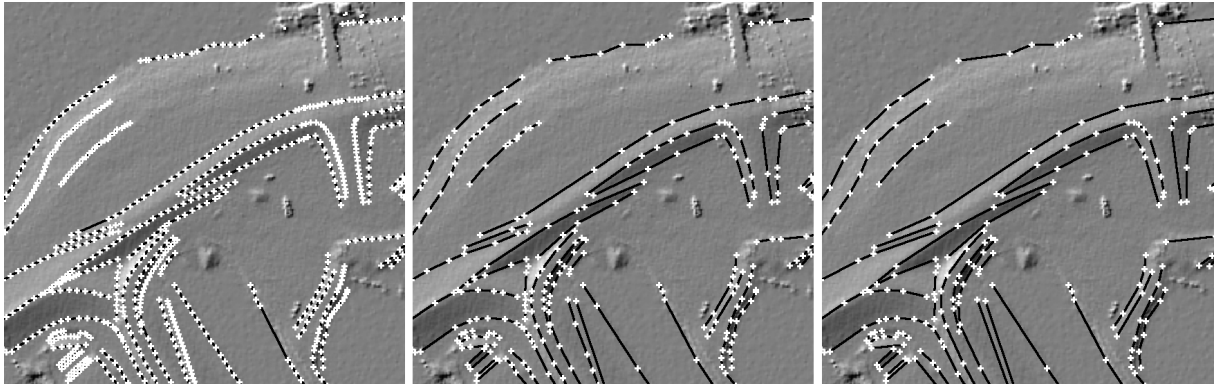
***Figure 4.11:*** *Data reduction of breaklines. Shading with vector breaklines (described by a sequence of 3D points (white crosses)) determined from ALS data. Left: Original representation of the breaklines; Middle: Breaklines with a maximal tolerance value of 0.25m (data reduction: 65%); Right: Breaklines with a maximal tolerance value of 0.5m (data reduction: 76%).*

and therefore allows a reduced amount of storage. For the data reduction of the breaklines one can think of a further adjustment procedure leading to a modelling of the breaklines with a reduced set of functional parameters (e.g. by the use of splines). However, it is often very difficult to exchange functional parameters from one software package to another. Therefore, a discretisation of the function is necessary. This leads to the fact that the storage advantage is usually lost.

In the following, an easy method is presented, which allows the reduction of the number of describing points of a breakline in respect to a user defined tolerance value (it can be adapted to the individual needs). This algorithm can either be applied to the originally determined breakline or to a discretised, functionally described version of the breakline. At the beginning, the algorithm initialises the reduced line with the start and end point of the breakline. Then, in an iterative process, the point with the maximum normal distance (3D) to the breakline is added to the rough description of the breakline (at the beginning consisting of only two points) until the maximum normal distance of the remaining points (which have not been added) is smaller than a certain user defined value. This simple, fast, and straight forward approach allows a data reduction of breaklines to the needs of a certain user, and is independent of the previous processing chains. An example of the data reduction of breaklines determined from ALS data based on this algorithm can be seen in figure 4.11.

## 4.7 Outlook: Further extensions of the method

A lot of further extensions of this method can be considered in order to improve its capability. Next to further developments in the weight model (e.g. no strict separation of "Left" and "Right" points at the beginning of the modelling) one can think of a combined adjustment of multiple patch pairs (cf. subsection 4.7.1). Furthermore, the usage of more complex surfaces has to be considered (cf. 4.7.2). These extensions are part of the future work. Nevertheless, the following subsections shortly describe some aspects.

### 4.7.1 Combined Adjustment of multiple Patches

The idea behind this extension is the simultaneous adjustment of multiple neighboured patch pairs. This means that the local approach presented in the previous sections within this chapter would be extended towards a more global one. On the one hand this should improve the capabilities of the breakline estimation in dense wooded areas with a lot of off-terrain points (bridging larger areas without terrain points), and on the other hand it should allow to add constraints between neighbouring surface patches. Due to the overlap of neighbouring patches, some ALS points would influence simultaneously the run of neighboured patches. In order to guarantee smoothness along the breakline, weighted constraints like parallel normal vectors of adjacent surfaces on either side of the breakline or other fictitious observations (as functions of the unknowns of the adjustment of the multiple patches) can be introduced.

In general, this extension would lead to a homogenisation of the results.

### 4.7.2 Modelling based on more Complex Surface Pairs

The aim of the basic breakline modelling concept is the description of the breakline with the help of two intersecting surfaces. Up to now, the modelling with small robustly estimated plane patch pairs was presented. However, having in mind the basic ideas, the process is not limited to a certain surface determination technique and to a certain patch size. With a rising complexity of the surface pairs, the size of the patches along the breaklines can increase, and, furthermore, more complex surface structures across the breakline direction can be considered within the modelling procedure.

So, the breakline modelling concept based on plane surface patches can be extended to general algebraic surfaces of order $n$, which is the set of all points $P_i(x, y, z)$ that fulfil the following equation:

$$F(x, y, z) \equiv \sum_{i+j+k \leq n} a_{ijk} x^i y^j z^k = 0 \tag{4.5}$$

However, one has to have in mind that this step to an increased complexity of the surface patches also leads to the need of more data within the adjustment procedure in order to determine all necessary parameters with a certain reliability. This necessitates bigger patch sizes. Furthermore, it must be considered that the increase of parameters for the surface determination also leads to an increase of the complexity of the intersection curve. The *theorem of Bézout* states that the intersection curve from two algebraic surfaces of the order $n_1$ and $n_2$ is an algebraic curve of order $n_c = n_1 n_2$. Having this in mind it should be considered that the order of the algebraic surfaces should not be too high for the surface description in the vicinity of the breaklines.

From the current point of view, thinking towards more complex surfaces, it can be assumed that algebraic patches of the order two (quadrics) allowing to describe the local surface curvature should be sufficient for the breakline modelling. However, there is a need of future research in order to estimate the necessary complexity, and to develop methods which automatically adapt the order of the surface to the given data.

# Chapter 5

# Automatisation

The modelling procedure presented in chapter 4 allows a semi-automatic modelling of breaklines with robustly estimated surface patch pairs on the basis of unclassified ALS data. The method relies on an initial 2D approximation of the breaklines. These values are on the one hand necessary to select the data in the vicinity of the breakline, and on the other hand they provide information for an initial grouping of the data into the surface classes "Left" and "Right" in respect to the initial line. However, there is a need to automate the process as much as possible for its practical application. Therefore, this chapter concentrates on methods, which help to automatise the process by the determination of the necessary initial values for the modelling procedure.

Basically, two different concepts in the area of automated breakline extraction can be distinguished. The aim of the main group of methods is the extraction (in general in 2D) of the whole breakline within one process (usually by grouping adjacent pixels classified as breakline pixels, cf. section 2.3). In contrast to these approaches, the following subchapters introduce algorithms based on a different automatisation strategy. The basic idea is a breakline growing scheme based on a step-by-step expansion of previously modelled breakline segments. These *3D breakline growing methods* based on point cloud data join the robust 3D modelling procedure with an iterative extraction technique, and allow therefore to overcome the must of the presented 3D modelling technique of an entire 2D approximation of the breakline.

The following subsection 5.1 presents next to the basic breakline growing concept a procedure based on one initial 2D start segment (resp. one point near the breakline and the approximative breakline direction). Subsequently, the method is extended to the use of just one initial point (cf. section 5.2). Small examples within the sections demonstrate the practical use. Furthermore, the final section 5.3 of this chapter gives an outlook on concepts allowing a fully automated determination of breaklines on the basis of ALS data.

## 5.1 Breakline growing on the basis of one Start-Segment

This section presents the 3D breakline growing scheme on the basis of a 2D start segment (e.g. manually digitised). Starting from this segment $S_0(L_0, R_0)$ the 3D breakline within this segment can be determined by robustly estimated surface patch pairs. Subsequently, the growing procedure can start into forward and backward direction on the basis of the refined breakline
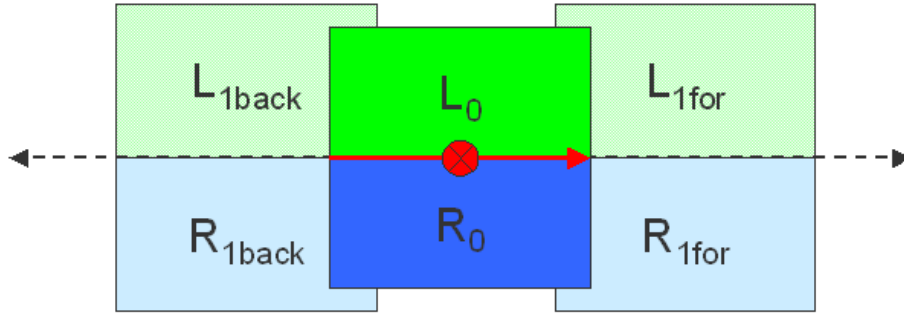
**Figure 5.1:** *Scheme for automated breakline growing by step-by-step expansion into forward ($S_{i,for}(L_{i,for}, R_{i,for})$) and backward ($S_{i,back}(L_{i,back}, R_{i,back})$) direction with the help of a start segment $S_0(L_0, R_0)$.*

within $S_0$ (cf. figure 5.1). For this growing scheme a fast access to the ALS point cloud within a certain extrapolated patch area (e.g. on the basis of a database) is necessary. The growing method proceeds in both breakline directions (one after another) in the following way:

1. Compute the breakline within the actual segment with the help of robust surface pairs. After an analysis of the results (precision, number of remaining terrain points, intersection angle, . . . ), store a list of representative points and the corresponding breakline directions if the determination was successful. If the adjustment was unsuccessful or a certain break off point (e.g. intersection angle) was reached, the growing procedure has to stop. At the beginning the start segment $S_0$ and in the following steps the extrapolated patch area $S_{i,for}$ resp. $S_{i,back}$ is used.

2. Extrapolate the breakline into the growing direction, and compute the boundary for the next patch pair.

3. Access the unclassified ALS data within the new patch boundary.

The growing sequence (from step 1 to 3) is continued until (in step 1) a certain break off point is reached or the breakline determination is unsuccessful. Within practical tests it turned out that the intersection angle between two patches is a very adequate criteria for the break off point.

This processing chain allows an expansion of the breakline until the surface discontinuity is not significant (e.g. defined by the intersection angle) or not determinable. Its practical application will be demonstrated in the following paragraph. However, it has to be mentioned that this technique of extrapolation and subsequently refined modelling can only be performed if the 2D extrapolation error in respect to the "true" breakline is not too big (in other words: if the initial extrapolated values are sufficient for the modelling). That means that the growing procedure will be successful as long as the 2D position of the breakline varies continuously ($C^1$ continuity). In the case of an abrupt change of the 2D breakline direction the algorithm will fail, if no further cases are considered (e.g. redetermination of the breakline direction with the help of another method (e.g. main curvature estimation, cf. section 5.2)). Furthermore, it has to be mentioned that at breakline crossings the algorithm enforces the growing into the direction of the previous segment, and that, without further considerations, the presence of crosses cannot be determined. Additionally, practical tests showed that the use of bigger patch sizes (compared to the one that is usually used for the breakline modelling (the size can be determined
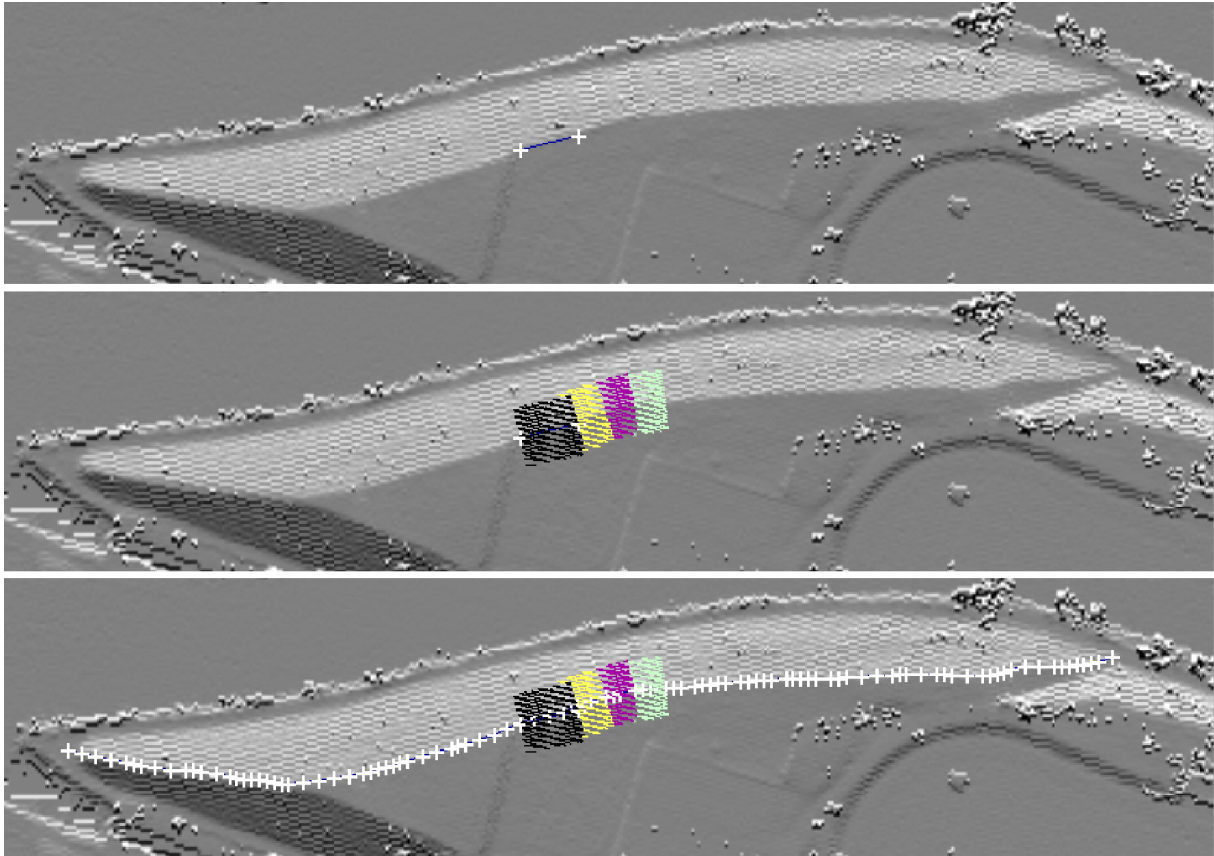
***Figure 5.2:*** *Breakline growing demonstrated within a practical example based on a manually digitised start segment; Top: Shading of a surface model and start segment; Middle: ALS points within the start patch $S_0$ (black) and within the three subsequently extrapolated patch areas in forward direction; Bottom: Result of the breakline growing procedure.*

on the basis of the sampling resolution (EIFOV, cf. section 3.2))) is preferable (the robustness and reliability increases). This bigger patches lead to a rougher description of the line (due to the fact that only one point on the intersection line is stored) and for the high quality determination a subsequently readjustment of the whole line with smaller patches on the basis of the growing result is necessary. Additionally, the simultaneous adjustment of multiple surface pairs (cf. subsection 4.7.1) will increase the reliability of breakline growing.

The following practical example[1] demonstrates the results of the previously introduced breakline growing procedure based on one start segment. At the bottom of this figure the final resulting breakline can be inspected. The break off point in this example was defined by an intersection angle bigger than 170 degrees. The patch size for the computation was 10m by 10m with an overlap of 50 percent between neighbouring patches. This results in a breakline description with a point distance of approximately 5m along the line. The patch size for this growing is along the breakline direction by a factor of two bigger than in the practical example of chapter 4.2 (cf. figure 4.4), where the work flow of the basic modelling concept was demonstrated with the help of the same breakline.

---

[1]This practical example was obtained within a test project initiated by the German Federal Agency for Hydrology ("Bundesanstalt für Gewässerkunde").
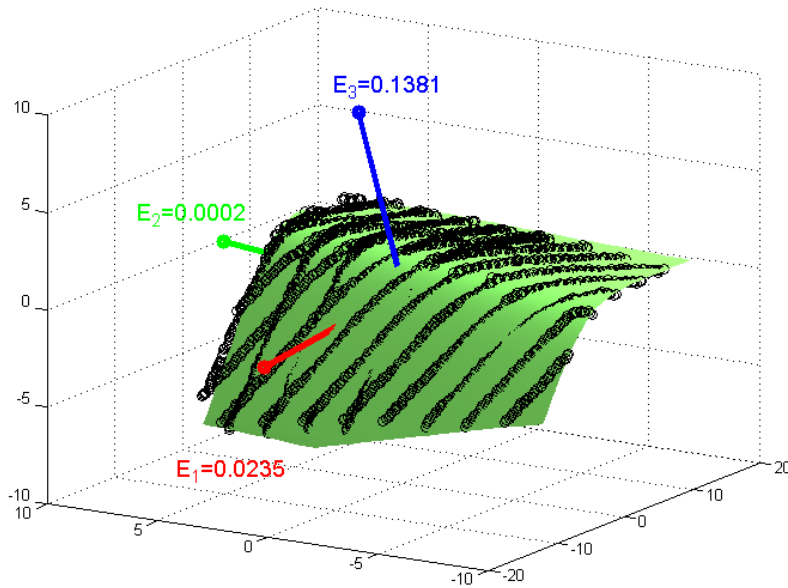
***Figure 5.3:*** *Automatic determination of the breakline direction with the help of a 3D quadric adjustment on the basis of the ALS point cloud. The eigenvector of the smallest eigenvalue (in this figure $E_2 = 0.0002$) points to the breakline direction in the case of a significant surface discontinuity.*

## 5.2 Breakline growing on the basis of one Start-Point

The growing procedure in the previous subsection relies on an initial start segment. However, in a similar way the growing based on just one initial 2D point next to the breakline can be performed. For this extension of the method it is necessary to determine the breakline direction in the vicinity of this start point in a first additionally step.

For the determination of the breakline direction different approaches can be considered. One possible solution is the determination of the direction of the main curvature of a small surface element around the initial start point by the use of differential geometry (cf. (Kraus et al. 2004)). A different solution is introduced in the following paragraph.

The following procedure is based on an analysis of locally adjusted small surface elements, and uses analytic surfaces of order two (quadrics) for the analysis of the local surface type with the help of the main axis transformation. This transformation determines a rotation of the co-ordinate system by the determination of the eigenvectors, which is the basis for the classification of the surface represented by the analytic description. Subsequently, the characterisation of the surface type is possible with the help of the corresponding eigenvalues. By the look at the list of surface types and by the corresponding attributes (eigenvalues) one can recognise that all types indicating a certain primely direction (e.g. surface type: two planes) like in the case of a surface discontinuity have an eigenvalue that is zero in this direction. Having this notice in mind, one can determine the breakline direction with the help of the main axis transformation of an adjusted 3D quadric. Then, the breakline direction is given by the eigenvector of the significant smallest (near by zero) absolute eigenvalue (due to the noise in the data and the not "ideal" surface shape some tolerance values for the classification have to be considered).

An example of such a breakline direction determination, which is very robust due to the high

redundancy of the data, can be seen in figure 5.3. However, it has to be considered that this process delivers very good initial values, but in the case of off-terrain points within the area around the initial 2D point the process might fail, if the number of terrain points is too low or if the 2D distribution of the terrain points in respect to the off-terrain points is bad. Therefore, a prior robust estimation step for the elimination of off-terrain points in the vicinity of the start point is essential before the analysis of the surface can be performed with the help of the main axis transformation.

## 5.3   Outlook: Full-Automatisation

The automatisation process presented in the previous two sections allows to overcome the need of a whole initial breakline for the 3D modelling, and can be seen as a step towards full automatisation. However, in order to fully automate the process a previous detection of 2D start points resp. start segments is necessary. Therefore, this section provides an outlook on automatisation techniques, which allow the determination of breaklines based on unclassified original data without or – on the basis of a more realistic view – with very few manual interaction. As mentioned in the section 2.3 different concepts for the solution of automated modelling techniques do exist. In the following, some aspects of future research are mentioned.

Up to now, we have a gap between the 2D extraction methods operating on an already filtered raster surface model and the 3D modelling concept presented in chapter 4. Though, one solution for the full-automatisation can be the combined use of both by the integration of one of the published 2D raster based methods (cf. section 2.3) with the basic concepts operating on the point cloud data presented within this thesis. The raster based method can deliver initial 2D breakline segments (by grouping of adjacent edge pixels), whereas for the subsequently modelling robust surface patch pairs determined on the basis of the unclassified ALS point cloud (in order to use all available information for the modelling) can be used. Furthermore, the breakline growing procedure presented in the previous subsections can be used to refine the 2D detection results by an expansion of the modelled breaklines allowing a modelling through areas were the 2D classification of edge pixels failed.

Another different detection concept is presented in the following. It is based on the analysis of the main axis transformation of locally fitted quadrics (cf. section 5.2). This allows to detect areas with an eigenvalue close by zero, which indicates a certain primely breakline direction. The surface fitting within a grid cell is performed on the basis of the unclassified ALS points. A preliminary result of the detection of these start segments can be seen in figure 5.4 (OEEPE (now EuroSDR) test data set Vaihingen). The subsequently determined breaklines by breakline growing are visualised in figure 5.5. It has to be mentioned that these are the first tests of the eigenvalue analysis, and a lot of further enhancements can be considered in order to improve the results.

Automatic breakline detection methods like the ones shortly presented in the previous paragraphs are not able to distinguish between breaklines on the terrain surface and on other object surfaces (e.g. building roofs). Therefore, a classification step using further object knowledge resp. also further available data (sensor integration, e.g. image data) is essential. Finally, it must be stressed that a lot of further research work for the practical application will be necessary to determine reliable results for the fully automated 3D modelling of breaklines.
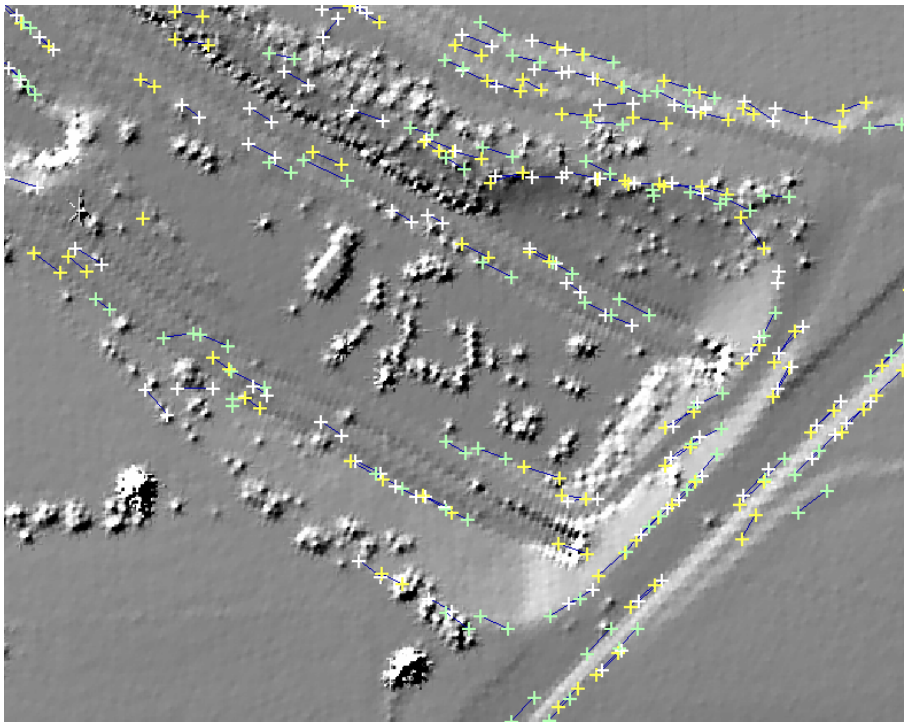
*Figure 5.4:* *Automatically detected start segments based on an analysis of locally fitted quadrics.*
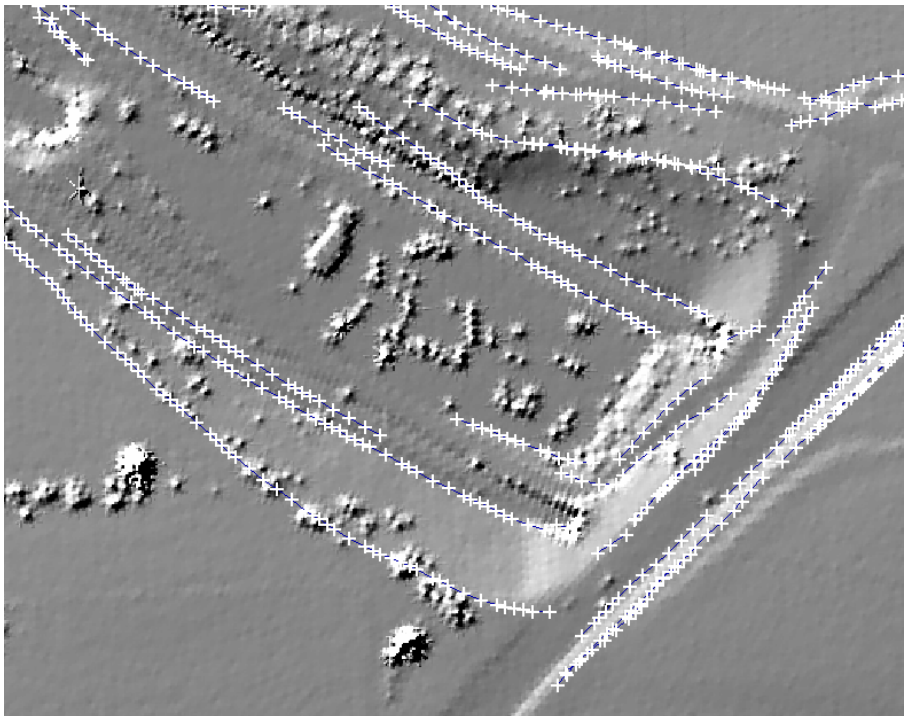


*Figure 5.5:* *Result of a fully-automatic breakline determination process.*

# Chapter 6

# Examples

This chapter presents some results of the introduced methods for breakline modelling using robustly estimated surface patch pairs. As stated in the introduction, the main issue of this thesis is the determination of breaklines from ALS. Therefore, the emphasis of this chapter lies in the presentation of results based on ALS data (cf. section 6.1). Next to the breakline modelling, a further subsection focuses on the integration of breaklines within the surface determination process. Moreover, a data reduction of the resulting models is considered.

Additionally, in order to demonstrate the general use of the presented concepts for breakline modelling, auxiliary sections consider the use of different data acquisition systems (cf. sections 6.2 (Image matching) and 6.3 (TLS)). Next to the results based on these data sources, the respective sections mention necessary adaptations of the breakline modelling procedure.

## 6.1 Airborne Laser Scanning (ALS)

This section presents the practical use of the introduced algorithms considering special ALS data characteristics. The following subsection 6.1.1 focuses on the breakline modelling, whereas the subsection 6.1.2 concentrates on the subsequent surface generation process with the consideration of the determined breaklines. Within the surface generation process the filtering resp. classification of the ALS data including breakline information and data reduction of the final models is treated.

One part of the practical examples of this section was obtained within the test projects "Lahn" and "Elbe" initiated by the German Federal Agency for Hydrology ("Bundesanstalt für Gewässerkunde", (BFG 2004)), whereas the data of the other part was taken from the pilot project "Hainburg" initiated by the Austrian Federal Agency for waterway transport "Österreichische Wasserstraßendirektion" (WSD 2004).

### 6.1.1 Breakline Modelling

A precondition for the breakline modelling is a fast access to the ALS point cloud within a buffer zone around the breakline. Therefore, considering large ALS projects (hundreds of

square kilometres), but even for smaller areas, a topographic database providing the georeferenced data is essential. Thus, the first step is the import of the data into a database resp. a software package that allows a fast access to the points within a 2D buffer zone around the initial breakline.

Subsequently, the next step within the breakline modelling process is the determination of the necessary initial values (cf. chapter 4 and 5). Depending on the available data different strategies can be considered. Next to manual digitisation of the approximate breaklines in image data or visualisations of the surface (e.g. a shading and/or contour lines), breakline growing (cf. section 5.1 resp. 5.2) can be considered. Additionally, automated detection results can be utilised with further user interaction in order to reduce the manual work. Practical tests with the subsequent breakline modelling software have shown that the approximation accuracy of the 2D position of the breakline should be $\pm1$m.

After the definition of the initial values, the automatic iterative refinement resp. expansion (breakline growing) of the breakline based on robust surface patch pairs works automatically based on few user input parameters. One set of parameters defines the buffer zone around the approximative breakline (cf. figure 4.4) and the patch size. However, in the future one can think of an automated determination of these parameters based on the sampling resolution (cf. section 3.2). Furthermore, the input of a priori information for the stochastic part in the adjustment is essential. This a priori precision information (on the one hand concerning the ALS points and on the other hand the additional observations) defines the weight model for the first adjustment. Additionally, if gross errors are detected (cf. section 4.3), this information is used for the iterative adaption of the weight functions for the elimination of off-terrain points within the robust determination of the surface pairs. Furthermore, the user has to set the weight functions, which describe the subsequent decrease of the weight of the points in respect to the normal distance (2D) to the breakline (cf. figure 4.3). Additionally, the breakline growing procedure (if used within the breakline modelling) necessitates the definition of the break off point (e.g. intersection angle between the surface patch pairs bigger than 170 degrees), which might be project dependent (cf. section 5.1) and allows to terminate the iterative growing procedure.
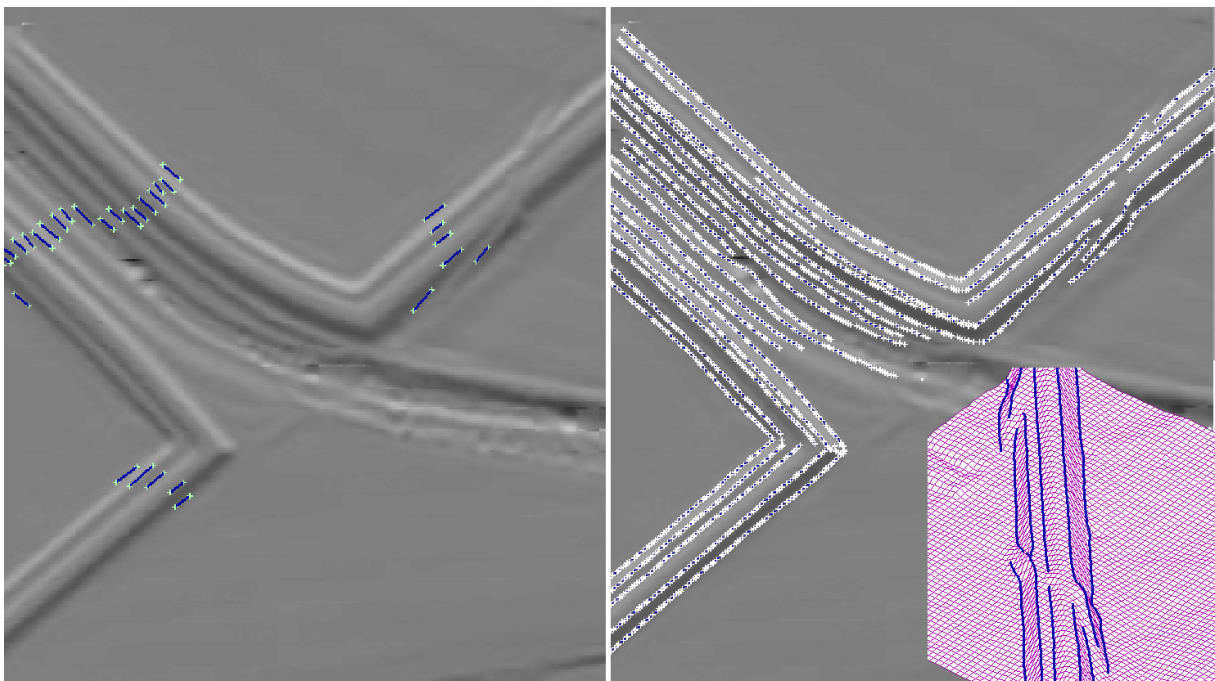
Figure 6.1 shows the results of the breakline modelling of a part of the project area Lahn. For the determination of the breaklines, manual digitised initial 2D lines were used. The data was acquired with a TopoSys airborne laser scanner, which has a significant different point density in vs. across the flight direction (cf. section 3.2). This inhomogeneity in the sampling pattern effected certainly the breakline modelling. With the help of visual inspection after the modelling procedure this loss in detail can be directly seen especially at breaklinesrunning more or less parallel to the flight direction (across the flight direction the modelling has to cope with fewer data).

As a second example, figure 6.2 presents a high amount of modelled breaklines in the area of a dike. For the determination initial 2D start segments (cf. left part of figure 6.2) were used. The 3D breaklines were calculated by the use of breakline growing with a patch pair size of 5m (along the line) by 10m (across the line). The growing was performed as long as the intersection angle between one surface pair was smaller than 170 degrees. The breakline modelling in this example enables a very high degree of automatisation. However, it has to be considered that a manual refinement of the results in areas of breakline intersections is still necessary.

The dikes in this example were mainly free of vegetation, but nevertheless in certain areas the elimination of off-terrain points was essential. Though, it must be mentioned that in areas were the breaklines are partly densely overgrown (nearly no terrain points) the breakline growing
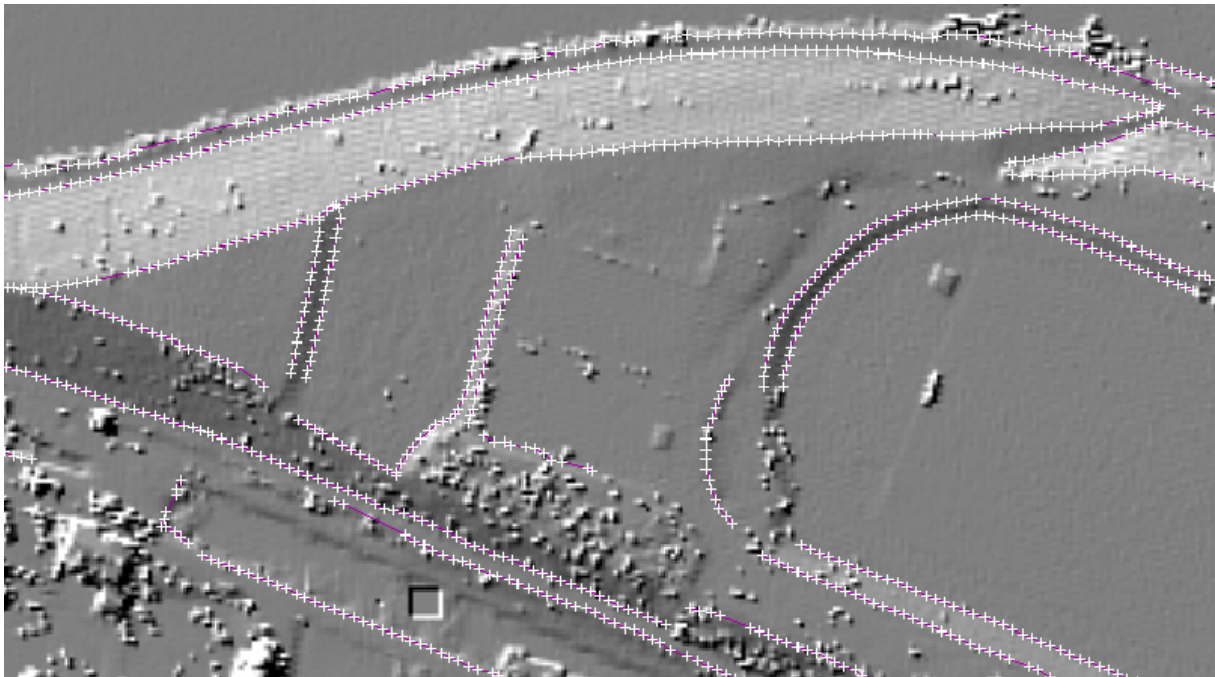
**Figure 6.1:** *Part of the breakline modelling result (superposed by a surface shading) of the project area Lahn. The initial values were set by manual digitisation.*



**Figure 6.2:** *Part of the breakline modelling result (superposed by a surface shading) of the project area Hainburg. Left: The initial start-segments were set by manual digitisation; Right: The resulting breaklines determined by breakline growing (cf. section 5.1). Down to the right of the figure a 3D view (parallel projection) of a part of the dike can be seen.*
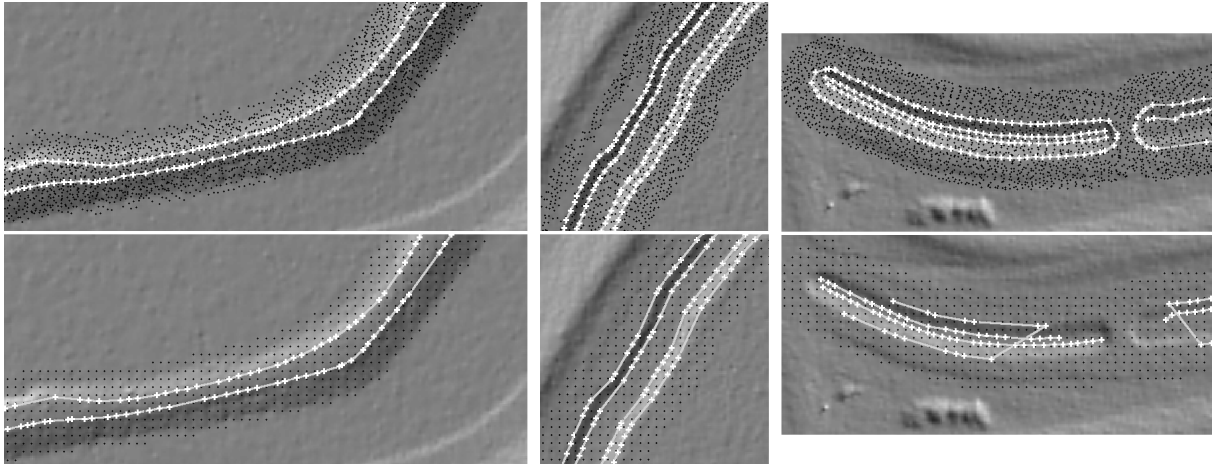
***Figure 6.3:*** *Surface shadings of the project area Elbe with breaklines determined on the original ALS point cloud (upper part) and a 2.5m raster DSM (lower part). White crosses/lines: connected points representing the breaklines; Black dots: respective point cloud in a buffer zone around the breaklines.*

might stop too early due to missing terrain points within one patch. For this case it might be useful to skip the determination in this patch and resize the patch area along and/or across the extrapolated breakline direction or skip and overleap the determination within this patch (jump over one patch) and perform a larger extrapolation. Though, the decision of how far these jumps are allowed is project and/or application dependent and needs a further user input. It is important that these jumps within the breakline growing are documented. This should allow a localisation of these jumps, which might be critical if such a jump is performed from one breakline to another separated one, by user interaction.

In order to test the breakline modelling performance for different ground sampling distances the original ALS point cloud was reduced to different resolutions for a number of tests. The results of the breakline modelling based on the original ALS data (Optech sensor, point distance approx. 1m) and in contrary on a 2.5m raster data set determined on the basis of the original ALS data are presented in figure 6.3. It can be seen in all three examples that the results based on the original ALS data allow a significantly more detailed description of the breaklines than the ones obtained on the 2.5m raster data. On the basis of the raster data source some patch pairs could not be adjusted successfully due to the reduced amount of information. This leads to a rougher representation leading to a lower amount of points describing the breakline (cf. figure 6.3, the amount of white crosses in the lower part of the figure (results based on the 2.5m raster data) is reduced strongly). However, as long as the run of the breaklines does not change too much, the representation is still valid. In the example of figure 6.3 the number of points describing the breaklines is reduced by 33% for the breaklines on the left (resp. 45% (breaklines in the middle) and 53% (right breaklines)). One can see that the 2.5m raster result in respect to the breaklines determined from the original ALS point cloud of the left example is still good, whereas the quality of the example in the middle of the figure is due to the smaller gap between the neighboured breaklines highly reduced. The result of the modelling of the breaklines based on the reduced raster data in the example displayed on the right is widely useless, because the determination of too many patch pairs failed. Additionally, it has to be considered that the results of the successfully determined patches have a lower quality due to the reduced information resp. redundancy within the adjustment procedure, which leads to a
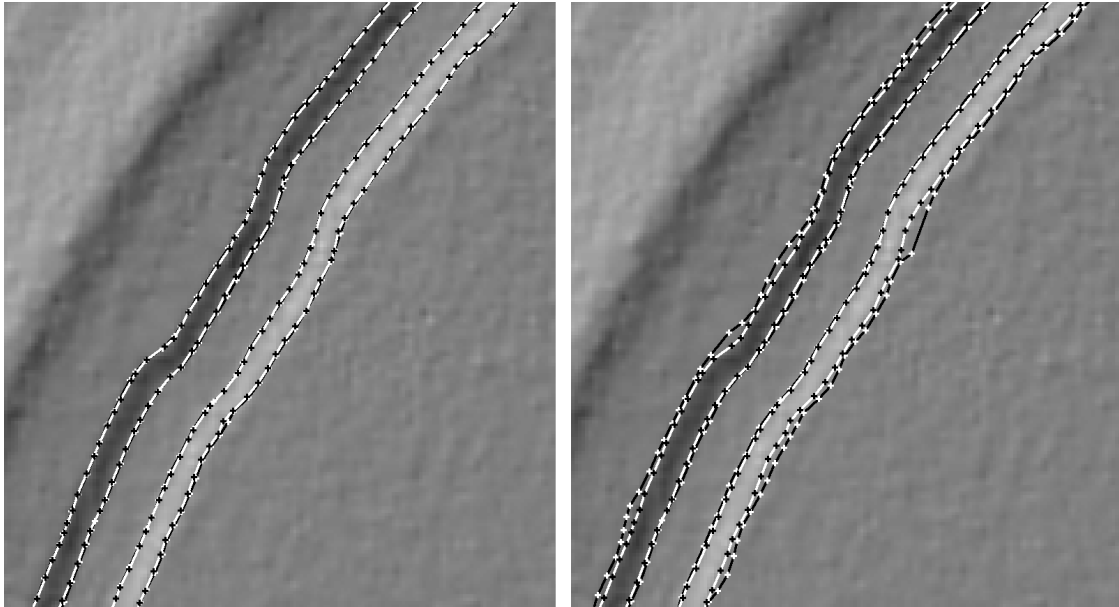
**Figure 6.4:** *Project area Elbe. Left: comparison of breaklines determined on the basis of originally unclassified ALS data (white crosses/lines) and 1m raster data (DSM, black crosses/lines); Right: comparison of breaklines determined on the basis of original unclassified ALS data (white crosses/lines) and filtered 1m raster data (DTM) determined without breakline information (black crosses/lines).*

worse quality of the breaklines.

Further practical tests showed that the use of original data in wooded areas is essential for the breakline modelling, because the higher degree of information allows a more stable and reliable determination of the surface patches by the robust elimination of off-terrain points. Additionally, it has to be considered that dealing with raster data implies certain preprocessing effects caused by the raster determination. Especially the filtering resp. the elimination of off-terrain information can cause unwanted smoothing effects in the resulting models. Such an example can be seen in figure 6.4 (project area Elbe). Whereas the determination of the breaklines based on the original ALS point cloud does not differ much from the result based on the 1m DSM (the 3D difference is smaller than 20cm), the difference compared to the breaklines determined on the basis of the filtered DTM is often bigger than 50cm (right part of figure 6.4). This example demonstrates that it is essential to exclude the negative influence of a priori preprocessing resp. filter steps.

In order to check the accuracy of the results of the breakline modelling procedure based on ALS data an analysis in respect to independently acquired control data is essential. Up to now no statistically relevant quantitative comparison describing the accuracy of the breaklines modelled with robust surface patches can be presented. Figure 6.5 just visualises two ALS breaklines together with tacheometric control data. It can be seen that the results fit overall very well, but partly some disagreements can be recognised. In certain areas it seems that the ALS lines are a little bit more detailed than the control data, but further analysis on a lot of different breaklines is necessary for reliable answers in the future. What has to be considered within this controls is that the definition of the breaklines varies strongly. Some of the lines can be easily accessed and are well defined, whereas the definition of breaklines in some areas (e.g. with low vegetation) is very difficult. To solve this problem the documentation of the control
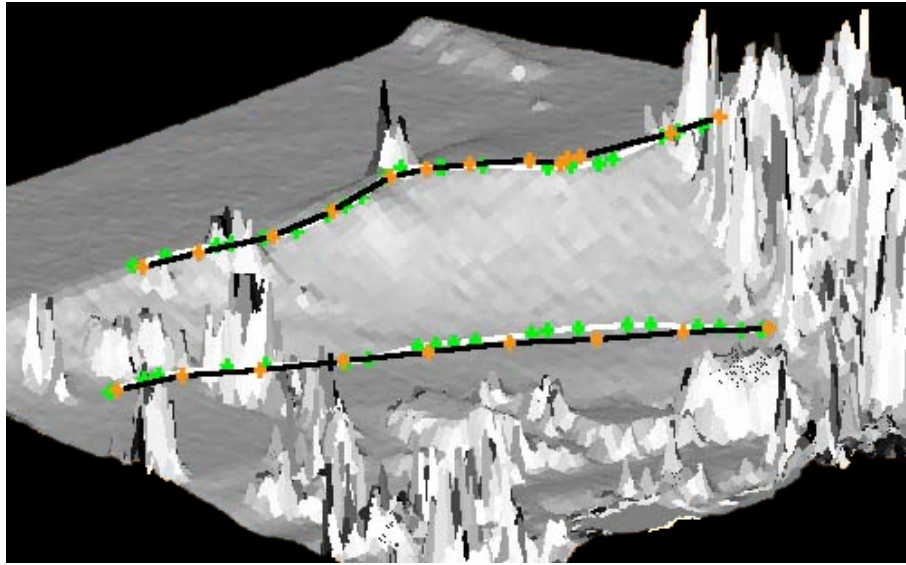
***Figure 6.5:*** *Accuracy check by comparison of ALS breaklines (light green) with tacheometric measured breaklines (orange). This comparison was performed within the ALS project Almtal of the provincial government "Oberöster-reich".*

data (e.g. by the acquisition of images demonstrating the measurement process and breakline identification in the nature during the tacheometric data acquisition) is essential.

Finally, the classification of the breaklines according to the intersection angle between the surface patch pairs should be mentioned. For the modelling the determination of the intersection of the surface patches is essential and the determination of the intersection angle between two surface pairs is an interesting byproduct, which allows a subsequent analysis. So, e.g. it is possible to sort the breaklines into different classes. Furthermore, the jump edges, which can automatically be recognised within the modelling procedure (cf. section 4.5), can get a separate attribute. However, a lot of further classifications of the lines or line segments (e.g. in respect to their precision or to the percentage of off-terrain points in the vicinity of the breakline) can be considered. Figure 6.6 visualises one results of a breakline classification in respect to the intersection angle, which was calculated for the project area Elbe.

### 6.1.2   Surface Modelling

This subsection considers the integration of the breaklines within the surface determination. As mentioned in section 2.2 the integration of breakline within the DTM modelling process is essential for high quality surface models. The way how the integration is performed depends on the surface modelling technique. In the case of TINs, breaklines are integrated as constraints within the determination of the absent topology, whereas within the functional modelling frame breaklines can be considered as intersection lines between two smooth functionally described surface patches (cf. section 2.2). So, the way breaklines are considered within the surface determination depends on the modelling technique, but after the modelling it is essential to store the breaklines within the resulting data structure. Furthermore, in the case of DTM generation from ALS data it is necessary to integrate the breakline knowledge into the filtering and classification process for the elimination of off-terrain points. An example of a
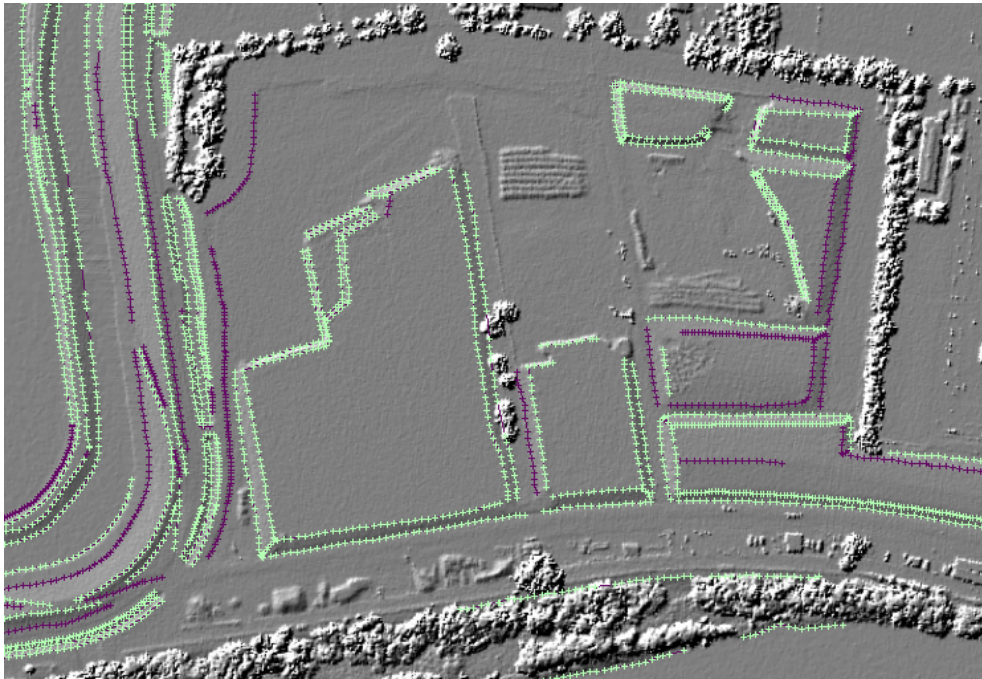
**Figure 6.6:** *Classification of breaklines according to the intersection angle (project area Elbe). Breaklines with a maximal intersection angle smaller than 160 degrees along the line are displayed in light green, whereas breaklines with a maximal intersection angle bigger than 160 degrees are visualised in dark magenta.*
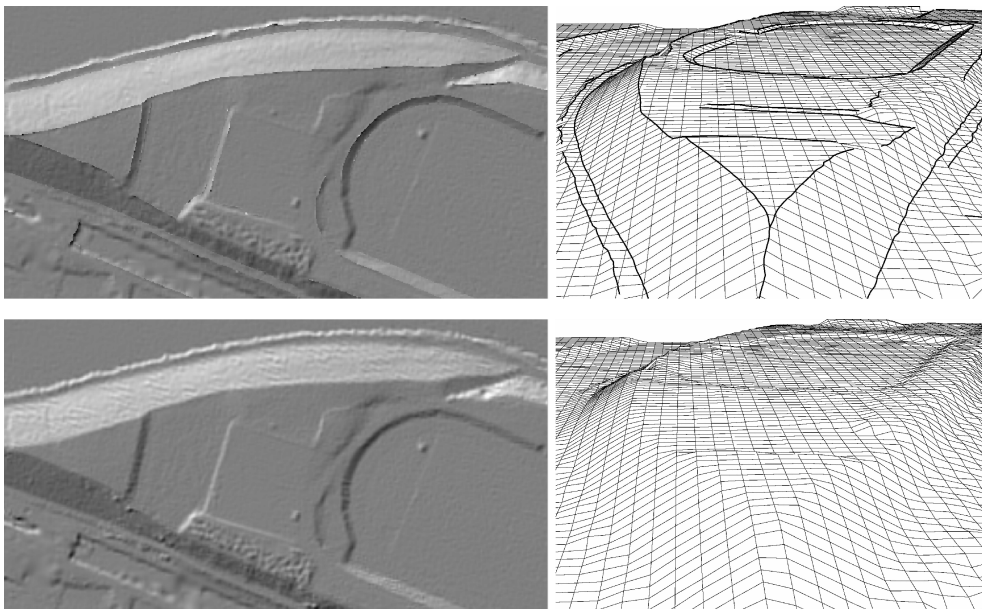


**Figure 6.7:** *Part of the DTM Lahn displayed in a shading and a perspective view with (upper part of the figure) and without (lower part of the figure) the use of breaklines.*
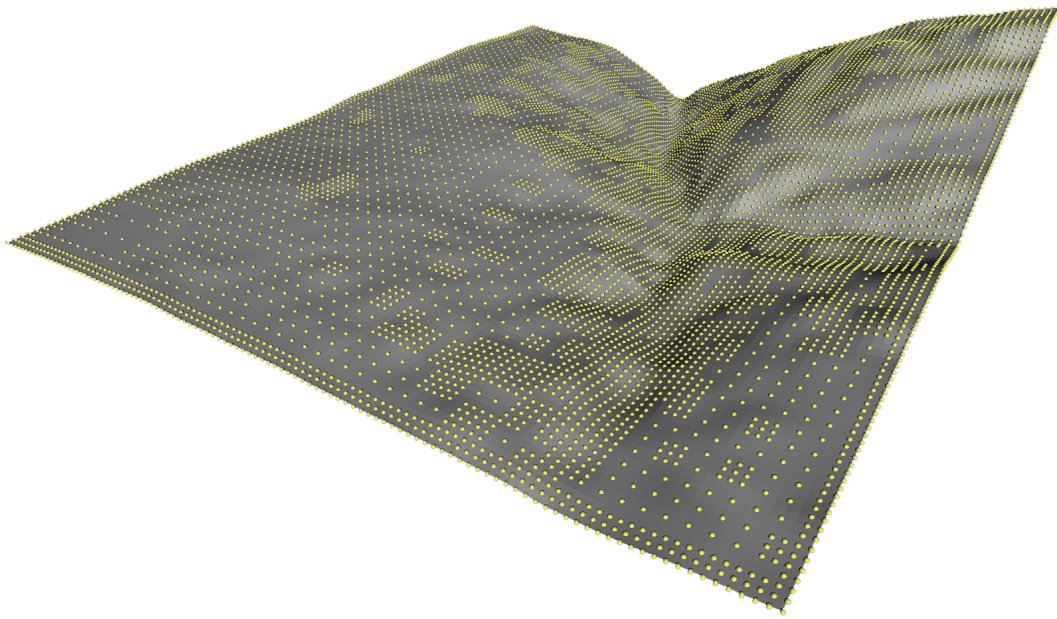
***Figure 6.8:*** *Surface shading with a reduced number of grid points describing the surface with a certain approximation precision. (Briese and Kraus 2003)*

DTM derived from ALS data with and without the consideration of breakline information in the filtering resp. classification and DTM determination procedure is visualised in figure 6.7. It can be seen in this example that the DTM with breaklines meshed into the data structure with relatively large grid cells allows in respect to the model without breaklines a big quality enhancement of the surface description in these discontinuity areas.

However, what can be seen furthermore comparing figure 6.7 with figure 2.2 is that in certain areas in between the breaklines the regular size of the large grid cells eliminate small surface structures that would be eventually interesting for the final DTM. In order to describe these structures a finer grid has to be chosen. In many practical applications this is not possible, because subsequent analysis methods often cannot handle the resulting high amount of data. Therefore, it is relevant to develop algorithms, which allow on the one hand a detailed surface description if it is necessary (in order to represent certain surface structures), but on the other hand allowing large grid sizes in areas without any relevant surface structure.

For the aim of data reduction a lot of different algorithms based on a TIN data structure exits (e.g. (Kobbelt et al. 1998)). In respect to these methods, Briese and Kraus 2003 present a method which allows the reduction of dense ALS surface models based on a grid data structure. This algorithm leaves ajar the *progressive sampling* method (Makarovic 1976) used in photogrammetry and enables a data reduction based on local curvature estimation. It allows to determine an irregular distributed point cloud, which approximates the dense surface model with a certain user defined approximation precision. A small example of such a data reduction can be seen in figure 6.8. In areas with high curvature the original grid spacing is used, whereas in flat areas a maximal user defined grid spacing is sufficient. This method was originally published for its application of grid models, however the consideration of breaklines within the data reduction method is a straight forward task. The only thing that has to be adapted for the data reduction of hybrid grid models (cf. (Kraus 2000)) is the curvature determination. Additionally, a data

55

***Figure 6.9:*** *Practical example (project area Elbe): Data reduction of a hybrid ALS DTM.*

reduction of the breaklines themselves can be interesting. For this aim the method introduced in section 4.6 can be integrated into the data reduction process of hybrid grid surface models.

An example of the result of data reduction of a hybrid ALS surface model is presented in figure 6.9. Within this example the smallest grid width is 1m, whereas in flat areas a maximal grid width of 8m was allowed. What is noticeable within this example is that in the left part of the figure 6.9 a small stripe with comparatively dense grid points (especially in the lower part) can be seen. Further analysis showed that this denser surface description is caused by ALS strip discrepancies and has nothing to do with a real surface structure.

## 6.2   Image matching

As already mentioned, the developed method for breakline modelling is not limited to the use of ALS data. In a quite similar way data from image matching can be the input for the breakline modelling procedure.
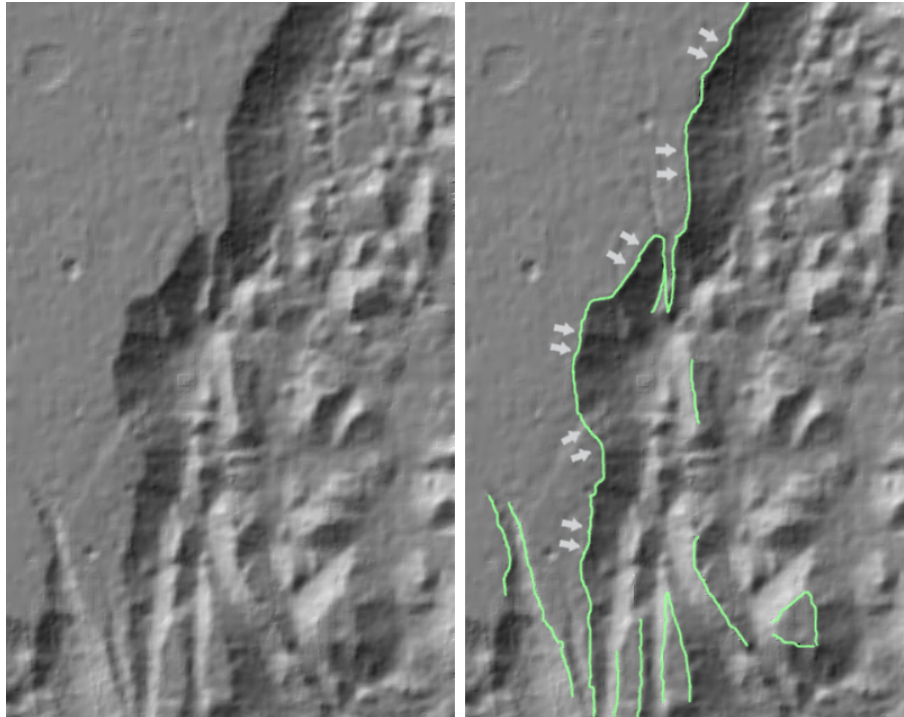
***Figure 6.10:*** *Practical example of breakline modelling based on image matching data from the Mars surface (cf. (Albertz et al. 2004)).*

However, due to the different data characteristics (e.g. point density on the surface) an adaption of the input parameters is necessary. For example the weight function, which decreases the influence of the points with a higher normal distance to the breakline, can be used in a similar way, whereas a reduction of the weight of points very close to the breakline - as it is useful with ALS data due to the laser footprint - is unessential with the use of image matching data. Whereas robust modelling is as essential using data of both acquisition methods. However, also for the determination of the off-terrain points the precision information, which is used for the automatic adaption of the robust weight function, has to be adapted.

The small practical example displayed in figure 6.10 presents a result of the breakline modelling from image matching data on the Mars surface (cf. (Albertz et al. 2004)). The image data was acquired within the European mission Mars Express (conducted by the European Space Agency (ESA, (ESA 2004))) by the digital line camera HRSC (High Resolution Stereo Camera). The image processing as well as the image matching were performed at the DLR ("Deutsches Zentrum für Luft- und Raumfahrt", (DLR 2004)). Further information about the data source can be found in the following publications: (Albertz et al. 2004), (Dorninger 2004), and (Scholten et al. 2005).

Overall it can be summarised that the process of breakline modelling based on image matching data is quite comparable to the one with ALS data. The main differences lie in the point density and point distribution, but they can be solved easily by an adaption of the input parameters (e.g. patch size). However, in order to study the reliability of the results based on image data further tests are necessary in the future.

## 6.3  Terrestrial Laser Scanning (TLS)

TLS is often used for the determination of local area surface models e.g. of waste dumps or quarries. For the breakline modelling based on these very inhomogeneous data sets (due to the usually low observation height the point density in the vicinity of the sensor is extremely high compared to the data in a farer distance) just a few parameters like the patch size have to be customised. However, this adaption might be necessary within one project area due to the previously mentioned inhomogeneity. Therefore, an automatic adaptable parameter determination – especially for these applications – is essential (e.g. locally adapting patch size within the breakline growing procedure).

In general, breakline modelling based on TLS data is quite similar to the one based on ALS data or image matching data, but a different treatment is necessary in areas where the TLS point cloud describes 3D surface structures. If the 2D data selection in the buffer zone around the breakline leads due to the 3D structure to a selection of the points on more than two surfaces. Subsequently, this leads to problems within the 3D surface pair determination. Therefore, a different data selection strategy for the data in the vicinity of the two intersecting surfaces has to be considered.

A solution for the data selection problem can be found by the definition of the buffer zone within the polar domain of a TLS position (cf. section 4.1). This allows to reduce the complex problem in Cartesian co-ordinates to a simple 2D problem in the angular domain. After the data selection, the polar co-ordinates of the TLS points in the 2D vicinity of the initial line, which has to be defined in the 2D space, can be converted into Cartesian co-ordinates. Afterwards, the modelling can be performed by the use of a 3D surface description of the intersecting patch pairs in a similar way as in the ALS case. However, in order to integrate further data from other TLS positions into the breakline modelling further considerations are essential.

The previous mentioned extension allows to model breaklines in the area of 3D terrain surface structures. For some applications this might be unnecessary (as long as 3D structures are not relevant for the surface modelling), but one can think of further application fields in the area of TLS. For example, seen from the surface modelling point of view, edges on a building facade can be treated in a similar way as breaklines on the terrain surface. Therefore, one can think of modelling building edges using the same concepts introduced for the modelling of breaklines of the terrain surface. This application can directly be performed using the previous mentioned extensions within the data selection process.

The first tests for the modelling of building edges based on robustly estimated surface patch pairs were already carried out. One example of determined breaklines on the building facade can be seen in figure 6.11 and 6.13. This test data set of a small part of the Viennese town hall was provided by the company Geodata (Geodata 2004). It can be seen in these figures that a very detailed modelling of the building edges is possible (cf. figure 6.12). It must be stressed that the breakline growing procedure presented for ALS data can be used in a similar way on the building facades.

Summarising the first results from the modelling of breaklines on the building facades, it has to be mentioned that for its practical application a lot of further extensions (e.g. the integration of more than one scanner position) and further research work is necessary. The results presented within this section just demonstrate that a modelling based on the basic concepts introduced in
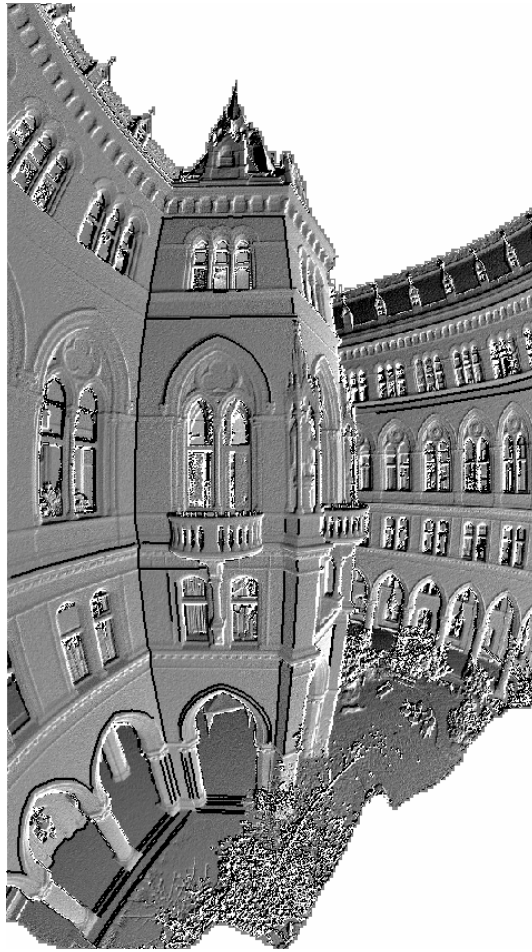
**Figure 6.11:** *Result of the breakline determination by robust 3D surface patches displayed on a surface shading in polar domain.*
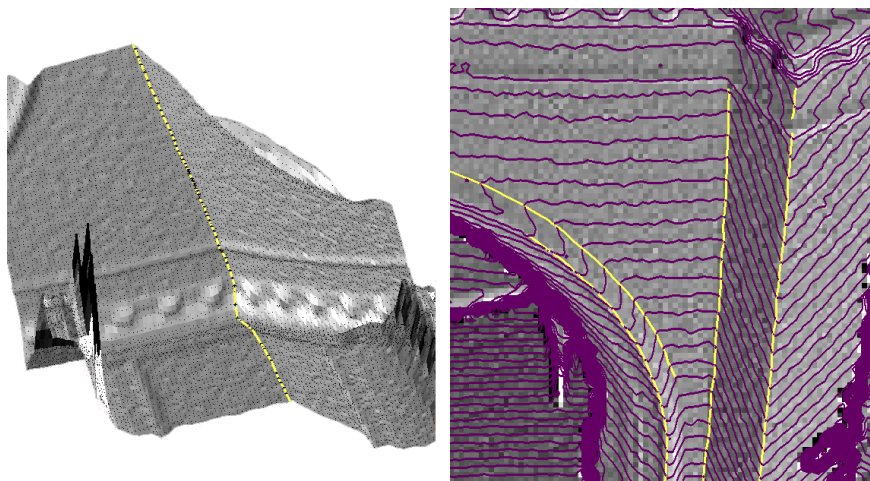


**Figure 6.12:** *Details of the breakline determination on the building facade (polar domain). Left: Shading of the surface model with TLS points (black dots) and determined breakline (yellow); Right: Shading of a surface model with isolines (dark magenta) and determined breaklines (yellow).*
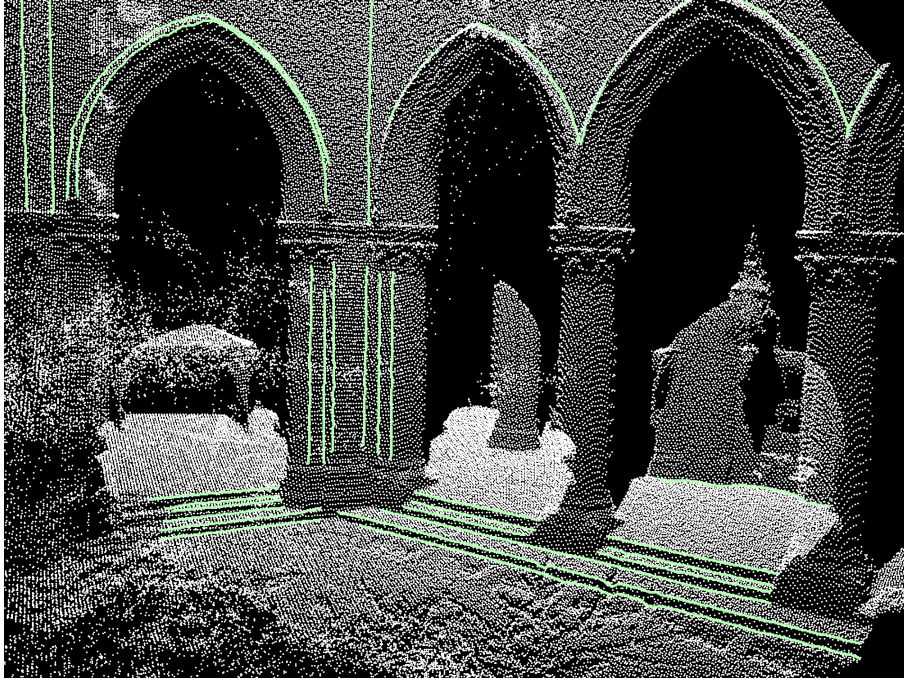
**Figure 6.13:** *3D view of a TLS point cloud of the Viennese town hall with determined 3D breaklines (light green).*

section 4.1 is visible. However, one should bear in mind that a lot of 2.5D applications of breakline modelling from TLS data (e.g. for hydrological applications), which works in principle in an identical way as with ALS data, does exist next to these complex 3D problems.

# Chapter 7

# Conclusion

This thesis presents a method for the explicit 2.5D resp. 3D modelling of breaklines based on irregularly distributed point cloud data. Furthermore, a special focus within the whole work is given to topographic surface modelling using ALS data.

Next to a summary of the current status of research related to the thesis (cf. chapter 2), chapter 3 provides a detailed look at some aspects of the ALS sampling process. On the basis of this knowledge, the basic modelling concept is extended step-by-step until it fulfils the needs for the practical application. The resulting modelling framework uses robustly estimated local surface patch pairs for the description of the breaklines on the basis of the originally unclassified ALS data in the vicinity of the breaklines (cf. chapter 4). Furthermore, the integration of direct breakline observations within the modelling process is presented. In general, the modelling starts from a 2D approximation of the breakline, which is refined within an iterative process. However, for the practical application there is a need to automate the process as much as possible. Therefore, the subsequent chapter 5 concentrates on methods, which can help to automate the whole process. For this aim the concept of breakline growing is introduced, which allows an iterative expansion of the modelled breaklines. Finally, the results of practical examples are presented in chapter 6. This practical part of the thesis mainly focuses on ALS data. Next to the breakline determination, the integration of the resulting breaklines into the surface modelling determination is presented. The importance of data reduction of the final models is stressed and demonstrated with the help of a practical example. However, in order to demonstrate the general use of the developed methods for breakline modelling, further examples using image matching and TLS data are presented. Additionally to the topographic applications, this chapter demonstrates the use of the method for the reconstruction of building edges.

The practical examples demonstrate that the modelling framework presented within this thesis can be successfully applied to unclassified ALS data. Some of the examples in chapter 6 demonstrate the advantage and quality enhancement with the use of the original point cloud within the breakline modelling procedure instead of a preprocessed raster surface model.

Nevertheless, one can think of a lot of further developments in order to enhance the capability of breakline modelling. Some of them are already mentioned in the respective chapters, but in the following the basic statements are summarised. Next to improvements in the weight model (e.g. no strict separation into the classes Left and Right) a combined adjustment of more than one patch pair can be considered (cf. subsection 4.7.1). This extension within the adjustment procedure would on the one hand improve the capabilities of the breakline estimation in dense

wooded areas by the bridging of larger areas with off-terrain points and on the other hand a more global approach would allow to use constraints between neighbouring patch pairs. These constraints provide a homogenisation of the resulting breaklines as long as there is no abrupt change in the run of the breakline. However, the algorithm should be able to detect such discontinuities of the breaklines, which would subsequently enable the reduction resp. elimination of these false assumptions introduced by fictitious observations. A second important extension in respect to the presented modelling framework is the use of more complex surface pairs (cf. subsection 4.7.2). This extension would provide a more flexible surface structure in the vicinity of the breaklines and therefore would allow to avoid errors caused by model deficits. However, this increase in the flexibility also produces some disadvantages. So, for example there will be a need of bigger patch sizes in order to determine all necessary parameters of the surface model and furthermore, the intersection of the surface pairs will be quite more complex. An additional problem is the question of the degree of flexibility. Therefore, a method, which allows to determine the necessary surface flexibility, is required. This task can be critical in the presence of off-terrain points. Especially low vegetation, which can hardly be distinguished from observations of the terrain surface, can have a negative effect for this procedure. In the future, next to the previous mentioned extensions, the development of techniques allowing to consider breakline intersections and other relations between neighbouring breaklines (e.g. parallelism) within the modelling concept, will be furthermore very important.

Still, the fully automated extraction of breaklines from point clouds is not visible. Therefore, next to the improvements within the modelling of the breaklines further research in the area of breakline extraction is necessary to allow a higher automatisation. Next to raster based methods algorithms operation on the point cloud data should be considered. Additionally, a classification of the extracted breaklines is necessary, which should offer to separate lines on the terrain surface from breaklines on other objects (e.g. building roofs).

Another issue within the area of topographic surface modelling is data reduction. Algorithms, which reduce the information of the dense and accurate surface models to the individual needs, are essential. For this aim methods, which guarantee a certain approximation precision in certain surface areas, are necessary. Next to the data reduction of the models, the reduction of the breaklines is also important. For the task of data reduction a lot of different solutions are already available (cf. section 4.6 and subsection 6.1.2), however there is a need to integrate these concepts into current available software packages.

It must be mentioned that a detailed quality analysis of the results of the presented 3D breakline modelling procedure is necessary in the future. These investigations can help to detect some deficits of the method and will allow to get an idea of the achievable accuracy of the breaklines in respect to independently acquired reference data.

Finally, the importance of breakline modelling and the extraction of other structure information must be stressed. Explicitly modelled breaklines allow a high quality improvement within the ALS classification (filtering) process for DTM generation and offer, next to a better morphological description of these surface discontinuity areas, a higher data reduction of the final surface models. Furthermore, breaklines can be considered as a very useful additional information within the georeferencing process of ALS strips (cf. chapter 4).

# References

Ackermann, F. (1999). Airborne laser scanning – present status and future expectations. *ISPRS Journal of Photogrammetry and Remote Sensing 54*, 64–67.

Ackermann, F. and K. Kraus (2004). Reader commentary: Grid based digital terrain models. *Geoinformatics 7, 6*.

Albertz, J., M. Attwenger, J. Barrett, S. Casley, P. Dorninger, E. Dorrer, H. Ebner, S. Gehrke, B. Giese, K. Gwinner, C. Heipke, E. Howington-Kraus, R. L.Kirk, H. Lehmann, H. Mayer, J.-P. Muller, J. Oberst, A. Ostrovskiy, J. Renter, S. Reznik, R. Schmidt, F. Scholten, M. Spiegel, U. Stilla, M. Wählisch, G. Neukum, and the HRSC CoI-Team (2004). HRSC on Mars Express – Photogrammetric and Cartographic Research. *Photogrammetric Engineering & Remote Sensing, in press*.

Axelsson, P. (2000). DEM generation from laser scanner data using adaptive TIN models. In *International Archives of Photogrammetry and Remote Sensing, Vol. XXXIII, B4*, Amsterdam, Netherlands, pp. 111–118.

BFG (2004, 10). http://www.bafg.de. Bundesanstalt für Gewässerkunde.

Blair, J., D. Rabine, and M. A. Hofton (1999). The laser vegetation imaging sensor: a medium-altitude, digitisation-only, airborne laser altimeter for mapping vegetation and topography. *ISPRS Journal of Photogrammetry & Remote Sensing 54*(3), 115–122.

Brenner, C. (2000). Towards fully automatic generation of city models. In *International Archives of Photogrammetry and Remote Sensing, Vol. XXXIII, B3*, Amsterdam, Netherlands, pp. 85–92.

Briese, C. (2000). Masterthesis: Digitale modelle aus Laser-Scanner-Daten in städtischen Gebieten, Vienna University of Technology, Institute of Photogrammetry and Remote Sensing.

Briese, C. (2004). Three-dimensional modelling of breaklines from airborne laser scanner data. In *International Archives of Photogrammetry and Remote Sensing, Vol.XXXV, B3*, Istanbul, Turky.

Briese, C., P. Belada, and N. Pfeifer (2001). Digitale Geländemodelle im Stadtgebiet aus Laser-Sanner-Daten. In E. Seyfert (Ed.), *21. Wissenschaftlich-Technische Jahrestagung der DGPF, Publikationen der Deutschen Gesellschaft für Photogrammetrie und Fernerkundung, Band 10*, Konstanz, Germany, pp. 165–172.

Briese, C., C. Eberhöfer, and N. Pfeifer (2004, 9). EuroSDR Distance Learning Course: Airborne Laserscanning and Interferometric SAR, Filtering and Classification of Laser Scanner Data. http://www.ipf.tuwien.ac.at/eurosdr/index.htm.

Briese, C. and K. Kraus (2003). Datenreduktion dichter laser-geländemodelle. *Zeitschrift für Geodäsie, Geoinformation und Landmanagement (zfv) 5*(128), 312–317.

Briese, C., K. Kraus, and N. Pfeifer (2002). Modellierung von dreidimensionalen Geländekanten in Laser-Scanner-Daten. In *Festschrift anlässlich des 65. Geburtstages von Herrn Prof. Dr.-Ing. habil. Siegfried Meier*, TU Dresden, Inst. für Planetare Geodäsie, Germany, pp. 47 – 52.

Briese, C., N. Pfeifer, and P. Dorninger (2002). Applications of the robust interpolation for DTM determination. In *International Archives of Photogrammetry and Remote Sensing, Vol. XXXIV, 3A*, Graz, Austria, pp. 55–61.

Brügelmann, R. (2000). Automatic breakline detection from airborne laser range data. In *International Archives of Photogrammetry and Remote Sensing, Vol. XXXIII, B3*, Amsterdam, Netherlands, pp. 109–115.

Brzank, A. (2001). Masterthesis: Automatische Ableitung von Bruchlinien aus Laserscannerdaten, Dresden University of Technology, Institute of Photogrammetry and Remote Sensing.

Dickerson, M., R. Drysdale, S. McElfresh, and E. Welzl (1997). Fast greedy triangulation algorithms. *Computational Geometry: Theory and Applications 8*, 67–86.

DLR (2004, 10). http://www.dlr.de/. Deutsches Zentrum für Luft- und Raumfahrt (DLR).

Dorninger, P. (2004). *A Topographic Mars Information System – Concepts for management, analysis and visualization of planet–wide data*. Ph. D. thesis, Vienna University of Technology.

ESA (2004, 10). http://www.esa.int/esacp/index.html. European Space Agency (ESA).

Filin, S. and G. Vosselman (2004). Adjustment of airborne laser altimetry strips. In *International Archives of Photogrammetry and Remote Sensing, Vol.XXXV, B3*, Istanbul, Turky.

Flood, M. (2001). Laser altimetry: From science to commercial lidar mapping. *Photogrammetric Engineering & Remote Sensing 67*(2), 1209–1217.

Förstner, W. (1998). Image processing for feature extraction in digital intensity, color and range images. In *Proceedings of the International Summer School on Data Analysis and Statistical Foundations of Geomatics*, Greece, Springer Lecture Notes on Earth Sciences.

Geodata (2004, 10). http://www.citygrid.at/. Geodata Ziviltechnikergesellschaft.

Gülch, E. (1994). *Erzeugung digitaler Geländemodelle durch automatische Bildzuordnung*. Ph. D. thesis, Institute of Photogrammetry, University of Stuttgart.

Gomes-Pereira, L. and L. Janssen (1999). Suitability of laser data for dtm generation: A case study in the context of road planning and design. *ISPRS Journal of Photogrammetry and Remote Sensing 54*, 244–253.

Gomes-Pereira, L. and R. Wicherson (1999). Suitability of laser data for deriving geographical information – a case study in the context of management of fluvial zones. *ISPRS Journal of Photogrammetry and Remote Sensing 54*, 105–114.

Heitzinger, D. (1999). *Wissensbasierte 3D-Oberflächenrekonstruktion*. Ph. D. thesis, Vienna University of Technology, Vienna, Austria.

Hoschek, J. and D. Lasser (1993). *Fundamentals of Computer Aided Geometric Design*. A K Peters Ltd.

Journel, A. G. and C. J. Huijbregts (1978). *Mining Geostatistics*. New York: Academic Press.

Jutzi, B. and U. Stilla (2004). Extraction of features from objects in urban areas using space-time analysis of recorded laser pulses. In *International Archives of Photogrammetry and Remote Sensing, Vol.XXXV, B2*, Istanbul, Turky.

Kager, H. (2000). Adjustment of algebraic surfaces by least squared distances. In *International Archives of Photogrammetry and Remote Sensing, Vol XXXIII, Part B3*, Amsterdam.

Kager, H. (2004). Discrepancies between overlapping laser scanner strips – simultaneous fitting of aerial laser scanner strips. In *International Archives of Photogrammetry and Remote Sensing, Vol.XXXV, B1*, Istanbul, Turky, pp. 472–479.

Katzenbeisser, R. (2003). About the Calibration of LiDAR Sensors. In *International Archives of Photogrammetry and Remote Sensing, Vol. XXXIV, 3/W13*, Dresden, Germany, pp. 59–64.

Katzenbeisser, R. (2004, 9). Technical note on echo detection. http://toposys.de/pdf-ext/Engl/echo-detec3.pdf.

Kerschner, M. (2003). *Snakes für Aufgaben der digitalen Photogrammetrie und Topographie*. Ph. D. thesis, Vienna University of Technology.

Kobbelt, L., S. Campagna, and H.-P. Seidel (1998). A general framework for mesh decimation. In *Graphics Interface '98 Proceedings*, pp. 43–50.

Kraus, K. (1998). Interpolation nach kleinsten Quadraten versus Krige-Schätzer. *Österreichische Zeitschrift für Vermessung & Geoinformation 1*.

Kraus, K. (2000). *Photogrammetrie, Band 3, Topographische Informationssysteme*. Dümmler. An english edition by Taylor and Francis (translator: H. Rüther) is in preparation.

Kraus, K. (2004). *Photogrammetrie, Band 1, Geometrische Informationen aus Photogrammetrie und Laserscanneraufnahmen* (7 ed.). Walter de Gruyter.

Kraus, K., C. Briese, M. Attwenger, and N. Pfeifer (2004). Quality measures for digital terrain models. In *International Archives of Photogrammetry and Remote Sensing, Vol.XXXV, B2*, Istanbul, Turky.

Kraus, K. and E. M. Mikhail (1972). Linear least-squares interpolation. *Photogrammetric Engineering 38*, 1016–1029.

Kraus, K. and N. Pfeifer (1998). Determination of terrain models in wooded areas with airborne laser scanner data. *ISPRS Journal of Photogrammetry and Remote Sensing 53*, 193–203.

Kraus, K. and N. Pfeifer (2001). Advanced DTM generation from LIDAR data. In *International Archives of Photogrammetry and Remote Sensing, Vol. XXXIV, 3/W4*, Annapolis, MD, USA, pp. 23–30.

Kraus, K. and W. Schneider (1988). *Fernerkundung, Band 1, Physikalische Grundlagen und Aufnahmetechniken* (1 ed.). Dümmler / Bonn.

Lancaster, P. and K. Salkauskas (1986). *Curve and surface fitting, An Introduction*. Academic Press.

Löffler, G. (2003). Aspects of raster dem data derived from laser measurements. In *International Archives of Photogrammetry and Remote Sensing, Vol. XXXIV, 3/W13*, Dresden, Germany.

Lichti, D. D. (2004). A resolution measure for terrestrial laser scanners. In *International Archives of Photogrammetry and Remote Sensing, Vol.XXXV, B5*, Istanbul, Turky.

Makarovic, B. (1976). Digital terrain model system. *ITC-Journal* (1), 57–83.

Melzer, T. and C. Briese (2004). Extraction and modeling of power lines from als point clouds. In *Proceedings of 28th Workshop of the Austrian Association for Pattern Recognition (ÖAGM)*, Hagenberg, Austria.

Merriam-Webster (2004, 9). Merriam-webster online dictionary. http://www.m-w.com.

Mikhail, E. (1976). *Observations And Least Squares*. New York: IEP-A Dun-Donnelley.

Optech (2004, 9). http://www.optech.on.ca/. Homepage of Optech.

Park, S. K., R. Schowengerdt, and M.-A. Kaczynski (1984). Modulation-transfer-function analysis for sampled image systems. In *Applied Optics. 23 (5)*.

Pfeifer, N. (2002). *3D Terrain Models on the Basis of a Triangulation*. Ph. D. thesis, Vienna University of Technology.

Pfeifer, N. (2004). Oberflächenmodelle aus laserdaten. *Österreichische Zeitschrift für Vermessung & Geoinformation 4*.

Pfeifer, N., B. Gorte, and G. Vosselman (2003). Laser altimetry and vegetation. Technical report, Report for the AGI (Adviesdienst Geoinformatie en ICT van Rijkswaterstaat, The Netherlands.

Pyysalo, U. and H. Hyyppä (2002). Reconstructing tree crowns from laser scanner data for feature extraction. In *International Archives of Photogrammetry and Remote Sensing, Vol. XXXIV, 3A*, Graz, Austria.

Rieger, W., M. Kerschner, T. Reiter, and F. Rottensteiner (1999). Roads and buildings from laser scanner data within a forest enterprise. In *International Archives of Photogrammetry and Remote Sensing, Vol. XXXII, 3/W14*, LaJolla, CA, USA, pp. 185 –191.

Riegl (2004a, 9). http://www.riegl.com/lms-q560/e_lms-q560_echo-digitization.htm. Echo Digitization of the RIEGL LMS-Q560.

Riegl (2004b, 9). www.riegl.com. Homepage of Riegl.

Rottensteiner, F. and C. Briese (2003). Automatic generation of building models from lidar data and the integration of aerial images. In *International Archives of Photogrammetry and Remote Sensing, Vol. XXXIV, 3/W13*, Dresden, Germany, pp. 174–180.

Schenk, T. (2001). Modeling and recovering systematic errors in airborne laser scanners. In *OEEPE Workshop on Airborne Laserscanning and Interferometric SAR for Detailed Terrain Models*, Stockholm, Schweden.

Scholten, F., K. Gwinner, T. Roatsch, K.-D. Matz, M. Wählisch, B. Giese, J. Oberst, R. Jaumann, , and G. Neukum (2005). Mars Express HRSC data processing – Methods and operational Aspects. *Photogrammetric Engineering & Remote Sensing, in press*.

Sithole, G. and G. Vosselman (2003). Comparison of filter algorithms. In *International Archives of Photogrammetry and Remote Sensing, Vol. XXXIV, 3/W13*, Dresden, Germany, pp. 71–78.

Sui, L. (2002). Processing of laser scanner data and automatic extraction of structure lines. In *Prodeedings of ISPRS Commission II Symposium, 20. – 23. August 2002, Xi´an, P.R. China*, Xi´an, P.R. China.

Thurston, J. (2003, August/September). Looking back and ahead: The triangulated irregular network (tin). *GEOInformatics 7*.

TopoSys (2004, 9). www.toposys.de. Homepage of TopoSys.

Vosselman, G. (2000). Slope based filtering of laser altimetry data. In *International Archives of Photogrammetry and Remote Sensing, Vol. XXXIII, B3*, Amsterdam, Netherlands, pp. 935–942.

Vosselman, G. and H.-G. Maas (2001). Adjustment and filtering of raw laser altimetry data. In *Proceedings of OEEPE Workshop on Airborne Laserscanning and Interferometric SAR for Detailed Digital Terrain Models*, Stockholm, Sweden.

Wack, R., M. Schardt, U. Lohr, L. Barrucho, and T. Oliveira (2003). Forest inventory for eucalyptus plantations based on airborne laser scanner data. In *International Archives of Photogrammetry and Remote Sensing, Vol. XXXIV, 3/W13*, Dresden, Germany, pp. 40–46.

Wagner, W. (2004). Robust filtering of airborne laser-scanner data for vegetation analysis. In *Laser-Scanners for Forest and Landscape Assessment - Instruments, Processing Methods and Applications*, Freiburg, Germany.

Wagner, W., A. Ullrich, T. Melzer, C. Briese, and K. Kraus (2004). From single-pulse to full-waveform airborne laser scanner: Potential and practical challenges. In *International Archives of Photogrammetry and Remote Sensing, Vol.XXXV, B3*, Istanbul, Turky.

Wehr, A. and U. Lohr (1999). Airborne laser scanning – an introduction and overview. *ISPRS Journal of Photogrammetry and Remote Sensing 54*, 68–82.

Weidner, U. (1994). Information-preserving surface restoration and feature extraction for digital elevation models. In *International Archives of Photogrammetry and Remote Sensing, Vol.XXX, B3/2*, Munich, Germany.

Wild, D. and P. Krzystek (1996). Automated breakline detection using an edge preserving filter. In *International Archives of Photogrammetry and Remote Sensing, Vol. XXXI, B3*, Vienna, Austria, pp. 946–952.

WSD (2004, 10). http://www.wsd.bmv.gv.at. Österreichische Wasserstraßendirektion.

# Curriculum vitae

**Personal Data**      Dipl.-Ing. Christian Briese

Born on 25/10/1975 in Eisenstadt, Burgenland, as child of Wolfgang Briese, official, and Hermine Briese (born as Dorfmeister), official

married with Mag. Eva Briese (born as Prenosil)

**Education**

1982 – 1986      Primary school in Siegendorf, Burgenland

1986 – 1995      Grammer school with emphasis on nature sciencies (Bundesrealgymnasium) in Eisenstadt, Burgenland

06/1995      School leaving exam (Matura)

**Studies**

1995 – 2000      Studies in Geodesy at Vienna University of Technology, in-depth studies in geo-information, photogrammetry and remote sensing

2000      Diploma thesis at the Institute of Photogrammetry and Remote Sensing: *„Digitale Modelle aus Laser-Scanner-Daten in städtischen Gebieten"* ("Digital models from laser-scanner-data in urban areas")

12/2000      Diploma eximination with excellence - graduated „Diplomingenieur"

2001      Start of PhD degree at the Faculty of Science and Engineering, Vienna University of Technology

09/2001 – 07/2002      Research associate at the research project P14083-MAT *"Three Dimensional Topographic Information System (3D TIS)"*, sponsored by the Austrian Science Fund (FWF)

08/2002 – 07/2004      Research associate at the research project P15789 *"Extraction of Structure Elements in Laser Scanner Data"*, sponsored by the Austrian Science Fund (FWF)

11/2003      Visiting Scientist at the Section of Photogrammetry and Remote Sensing Delft funded by the Spearhead Earth program (Reasearch Theme Earth) of the TU Delft

Vienna, 28. October 2004